

CRYSTAL CHEMISTRY OF FERRIC-RICH FAYALITES

by

MARTHA WILLIAMS SCHAEFER

S.B., Massachusetts Institute of Technology  
Physics (1979)

S.B., Massachusetts Institute of Technology  
Earth and Planetary Sciences (1979)

Submitted to the Department  
of Earth and Planetary Sciences  
in Partial Fulfillment of the  
Requirements of the  
Degree of

DOCTORATE IN PHILOSOPHY

in

PLANETARY SCIENCES

at the

MASSACHUSETTS INSTITUTE OF TECHNOLOGY

June 1983

© Massachusetts Institute of Technology 1983

Signature of Author: \_\_\_\_\_  
Department of Earth and Planetary Sciences, June 17, 1983

Certified by: \_\_\_\_\_  
Roger G. Burns, Thesis Supervisor

Accepted by: \_\_\_\_\_  
Theodore R. Madden, Chairman, Departmental Committee

**WITHDRAWN**  
MASSACHUSETTS INSTITUTE  
OF TECHNOLOGY  
NOV 30 1983  
**MIT LIBRARIES**  
LIBRARIES



Room 14-0551  
77 Massachusetts Avenue  
Cambridge, MA 02139  
Ph: 617.253.5668 Fax: 617.253.1690  
Email: docs@mit.edu  
<http://libraries.mit.edu/docs>

## **DISCLAIMER OF QUALITY**

Due to the condition of the original material, there are unavoidable flaws in this reproduction. We have made every effort possible to provide you with the best copy available. If you are dissatisfied with this product and find it unusable, please contact Document Services as soon as possible.

Thank you.

**Poor text reproduction on pgs. 30-31.**

"...when you have eliminated all which is impossible, then whatever remains, however improbable, must be the truth. It may well be that several explanations remain, in which case one tries test after test until one or the other of them has a convincing amount of support."

--Sherlock Holmes,

"The Adventure of the  
Blanched Soldier"

## CRYSTAL CHEMISTRY OF FERRIC-RICH FAYALITES

by

MARTHA WILLIAMS SCHAEFER

Submitted to the Department of Earth and Planetary Sciences  
on June 17, 1983 in partial fulfillment of the  
requirements for the Degree of Doctor of Philosophy in  
Planetary Science

## ABSTRACT

Samples of dark to black fayalite from ten localities around the world were examined by  $^{57}\text{Fe}$  Mössbauer spectroscopy to see if any contained significant proportions of ferric iron. Of these ten samples, four, including a sample of ferrifayalite from Qianan County, China, previously known to contain ferric iron, were found to contain large amounts of this cation. Ferric/ferrous ratios of these samples range from 0.19 to 1.38 (for ferrifayalite itself).

Low temperature (down to 4.2 K) Mössbauer spectra were also taken of the four ferric-rich fayalites. Two types of ferric-rich fayalite were found. The first type, the ferrifayalite type, was found in three samples. The second type, the St. Peter's Dome type, was found only in the sample from that locality. The three ferrifayalite type samples show Mossbauer spectra indicating a domain structure to the mineral, with domains of ferrous fayalite and domains of ferric-rich fayalite, in varying proportions. The St. Peter's Dome sample also shows a domain structure.

A structure for the ferric-rich domains is proposed, in which the ferric cations occupy the M2 site, and the ferrous cations occupy the M1 site. The occupancy of the M1 site alternates between ferrous cations and vacancies.

The ferric-rich fayalites appear to comprise a new series in the olivine group, probably a solid solution. One end member of the series is ferrous fayalite, and the other end member is extremely ferric-rich fayalite, with a  $3+/2+$  cation ratio of 2. A new nomenclature for this system is proposed, in which the ferric-rich end member is known as laihunite, and the series between this end member and fayalite is known as ferrifayalite.

Thesis Supervisor: Dr. Roger G. Burns

Title: Professor of Geochemistry

Dedication

First of all, to my parents, and last of all, to Brad.

Acknowledgements

Thanks go to Prof. David Kohlstedt for his TEM work on my samples, to Prof. Jim Besançon for his assistance with X-ray diffraction measurements and interpretation, and to Prof. Gene Simmons for suggesting and carrying out an SEM survey of my samples. Thanks also go to Georgia Papaefthymiou and Dr. Richard Frankel for allowing me the use of their low-temperature Mössbauer apparatus, and again to Dr. Frankel for his helpful discussions. Special thanks go to Darby Dyar, for her time and effort in maintaining the computer system on which much of my data were analyzed.

Without the assistance of David J. Birnbaum, Eliza Xu, and Christof Stork as translators, much of my work would have been impossible. Thanks also go to Joan Harris for her discussions of Mexican Fe-deficient fayalite and Berkeley synthetic fayalite, as well as to Prof. Adolf Pabst and Prof. Ian Carmichael for the use of unpublished data.

Samples of fayalites for study were provided by the Harvard Mineralogical Museum, Carl Francis, Curator, by the British Museum of Natural History, and by Dr. Ruyuan Zhang, to whom I would like to express my particular thanks.

Thanks also go to Prof. Frank Spear and Prof. Tim Grove for their helpful discussions, and most especially to my thesis advisor, Prof. Roger Burns, who offered a helping hand at every step along the way.

This work was supported in part by NSF grant EAR-8016163, and in part by funds supplied through the Department of Earth and Planetary Sciences' Student Research Fund.

Particular thanks also go to my husband, Brad Schaefer, for his helpful discussions and his constant support.

Table of Contents

Title Page.....	1
Epigraph.....	2
Abstract.....	3
Dedication.....	4
Acknowledgements.....	5
Table of Contents.....	6
List of Tables.....	8
List of Figures.....	9
Chapter 1 - Purpose.....	11
Chapter 2 - Olivine .....	16
Chapter 3 - Previously Known Ferric-Rich Fayalites.....	27
Talasskite.....	27
Russian Ferrifayalite.....	28
Laihunite and Chinese Ferrifayalite.....	33
Others.....	37
Chapter 4 - Geological Settings of My Samples and a Few Other Recent Discoveries.....	38
Pantelleria.....	38
Mourne Mountains.....	42
St. Peter's Dome.....	46
Sierra La Primavera.....	49
Berkeley Synthetic.....	52
Chapter 5 - Experimental Procedure.....	56
Chapter 6 - Mössbauer Spectra.....	71
Room Temperature Spectra.....	71

Low Temperature Spectra.....	74
Chapter 7 - Other Determinative Methods.....	85
Chapter 8 - Discussion.....	90
Chapter 9 - Summary and Suggestions for Further Study.....	115
Summary.....	115
Suggestions for Further Study.....	116
Appendix.....	119
References.....	122

List of Tables

Table 1 - X-ray powder diffraction spectra of previously known ferric-rich fayalites.....	29
Table 2 - Chemical analyses of previously known ferric-rich fayalites..	30
Table 3 - Summary of physical properties of ordinary fayalite and previously known ferric-rich fayalites.....	31
Table 4 - Soellner's chemical analyses of Pantelleria fayalite.....	43
Table 5 - Microprobe analyses of my ferric-rich fayalites and Rockport fayalite.....	44
Table 6 - Hidden and Mackintosh's chemical analysis of St.Peter's Dome fayalite.....	50
Table 7 - Carmichael's analyses of Fe-deficient fayalites from Mexico.....	53
Table 8 - Harris' microprobe analysis of Berkeley synthetic.....	54
Table 9 - Samples examined in this study, their localities and sources.....	57
Table 10 - X-ray powder diffraction spectra of my ferric-rich fayalites and Rockport fayalite.....	68
Table 11 - Cell parameters of my ferric-rich fayalites and Rockport fayalite.....	69
Table 12 - Ferric/ferrous ratios of samples, based on Mössbauer peak areas.....	72
Table 13 - Room temperature center shifts and quadrupole splittings of all samples.....	73

List of Figures

Figure 1a - Room temperature Mössbauer spectrum of Mourne Mountains fayalite.....	13
Figure 1b - Room temperature Mössbauer spectrum of Rockport fayalite.....	13
Figure 2a - Ideal olivine structure.....	19
Figure 2b - Actual forsterite structure.....	19
Figure 3 - Nomenclature of olivines.....	22
Figure 4 - Low temperature spectrum of Rockport fayalite.....	25
Figure 5a-c - Observed crystal habits of Pantelleria fayalite.....	41
Figure 6a - Room temperature Mössbauer spectrum of Pantelleria fayalite.....	60
Figure 6b - Room temperature Mössbauer spectrum of St. Peter's Dome fayalite....	60
Figure 6c - Room temperature Mössbauer spectrum of North Tunaberg fayalite.....	61
Figure 6d - Room temperature Mössbauer spectrum of artificial fayalite.	61
Figure 6e - Room temperature Mössbauer spectrum of Hilläng fayalite....	62
Figure 6f - Room temperature Mössbauer spectrum of Värmland fayalite...	62
Figure 6g - Room temperature Mössbauer spectrum of Qianan County ferrifayalite.....	63
Figure 6h - Room temperature Mössbauer spectrum of Palmer Peninsula fayalite....	63
Figure 7a - 125 K Mössbauer spectrum of Rockport fayalite.....	65
Figure 7b - 125 K Mössbauer spectrum of Mourne Mountains fayalite.....	65
Figure 7c - 125 K Mössbauer spectrum of Pantelleria fayalite.....	66
Figure 7d - 125 K Mössbauer spectrum of St. Peter's Dome fayalite.....	66
Figure 7e - 125 K Mössbauer spectrum of Qianan County ferrifayalite....	67
Figure 8 - Change in Qianan County ferrifayalite Mössbauer spectra with temperature.....	76

Figure 9 - Mössbauer spectra of ferric-rich fayalites at 100 K.....	79
Figure 10 - Mössbauer spectra of ferric-rich fayalites and Rockport fayalite at 55 K.....	81
Figure 11 - Mössbauer spectra of ferric-rich fayalites and Rockport fayalite at 20 K.....	83
Figure 12 - SEM photographs of Mourne Mts. fayalite.....	89
Figure 13 - Weight percent Fe <sub>2</sub> O <sub>3</sub> vs. FeO for ferric-rich fayalites.....	94
Figure 14 - Mass per unit cell vs. 3+/2+ cation ratio for ferric-rich fayalites and Rockport fayalite.....	97
Figure 15 - Infrared spectra of some ferric-rich fayalites and Rockport fayalite.....	100
Figure 16a - Average metal-oxygen distance vs. cation radius for the M1 site in olivine.....	103
Figure 16b - Average metal-oxygen distance vs. cation radius for the M2 site in olivine.....	103
Figure 17a - Average oxygen-oxygen distance vs. cation radius for the M1 site in olivine.....	105
Figure 17b - Average oxygen-oxygen distance vs. cation radius for the M2 site in olivine.....	105
Figure 18a - Average oxygen-oxygen distance vs. average metal-oxygen distance for the M1 site in olivine..	107
Figure 18b - Average oxygen-oxygen distance vs. average metal-oxygen distance for the M2 site in olivine..	107
Figure 19 - A possible structure for ferrifayalite.....	110

Chapter 1Purpose

This study was begun largely because of a serendipitous discovery of significant quantities of ferric iron in a fayalite previously thought to be ordinary. A Mössbauer spectrum was taken of fayalite from the Mourne Mountains, in Ireland, at room temperature (Figure 1a), and found to contain two doublets (one ferrous and one ferric), instead of the simple two peak spectrum expected for fayalite (Figure 1b).

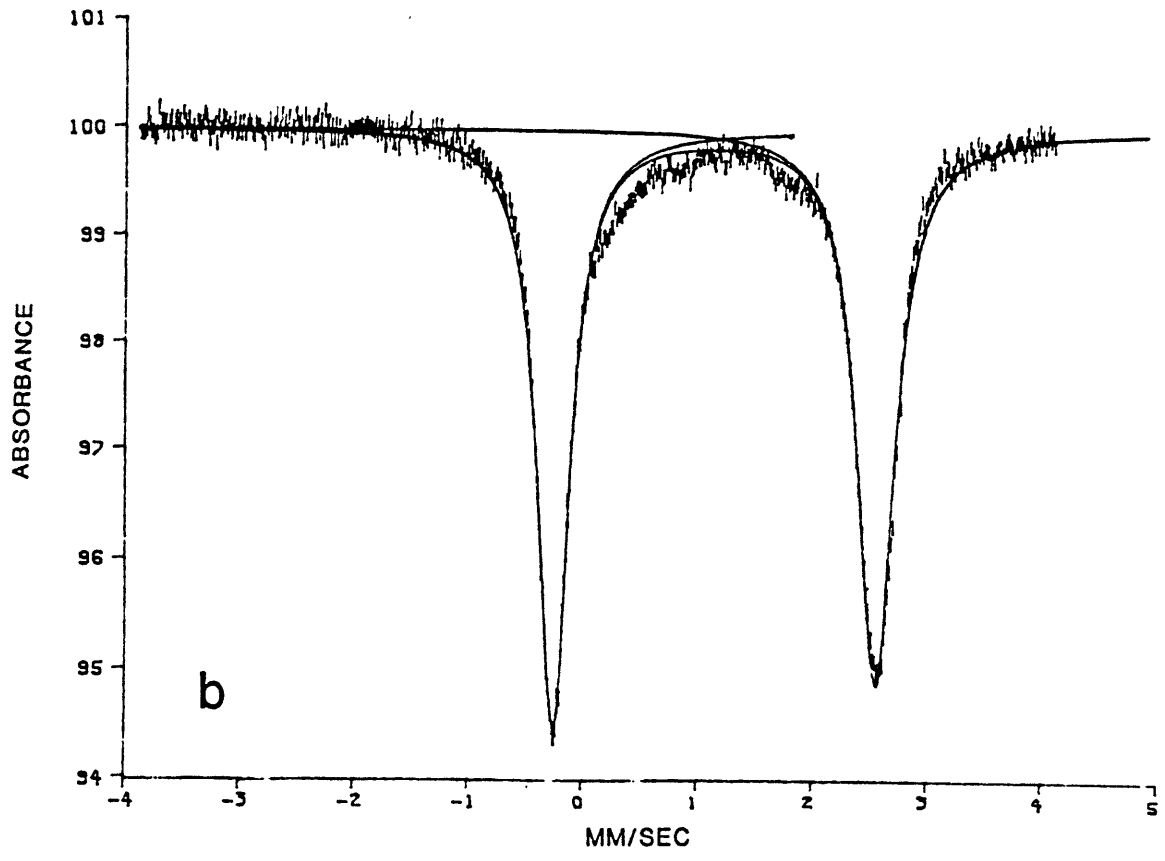
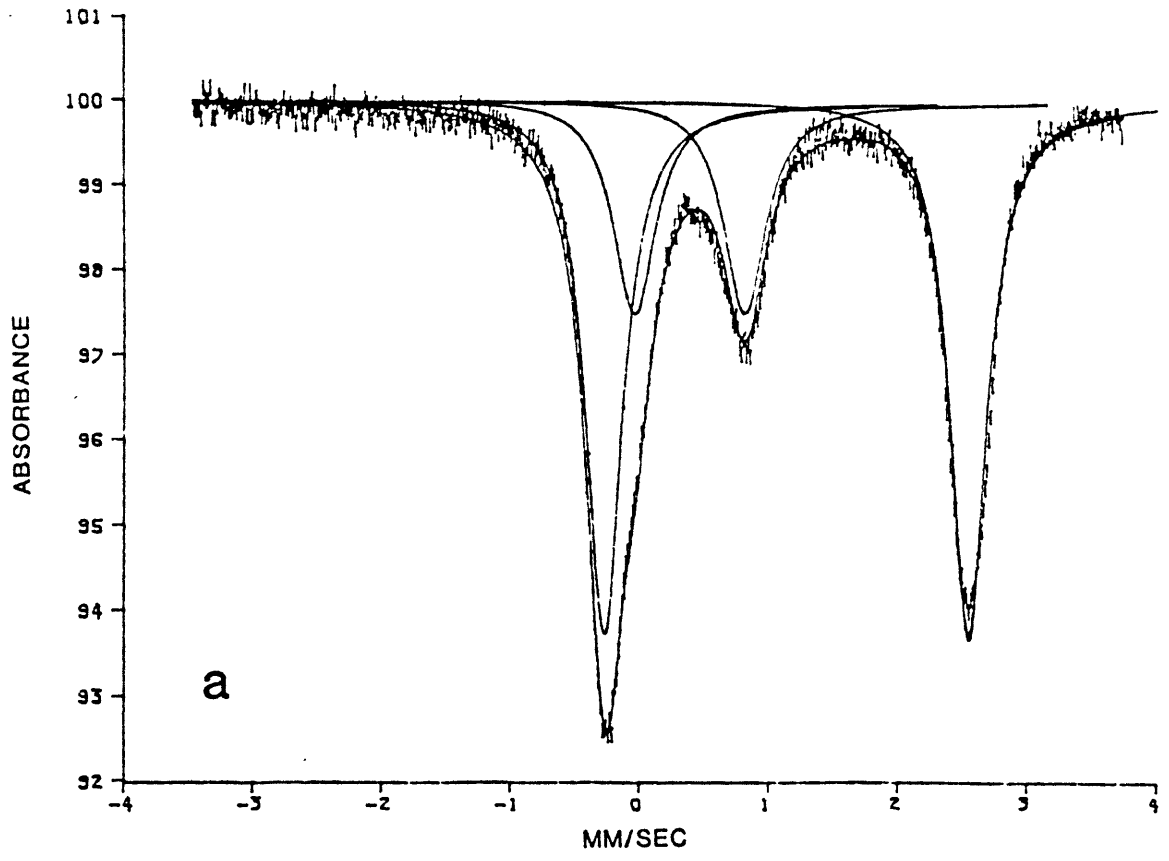
The recent discoveries of Chinese ferric-rich olivines (ferrifayalite and/or laihunite) provided a possible explanation for what could be 'wrong' with the Mourne Mountains fayalite. If it was misidentified as fayalite, and was actually a sample of ferrifayalite, the presence of ferric iron in its spectrum would be explained. Since the Mourne Mountains fayalite was also extremely dark in color for a fayalite (black in hand specimen and dark olive green in thin section or powder), somewhat similar in appearance to the descriptions of ferrifayalite in the Chinese literature, the premise that it was also ferrifayalite or a related mineral was strengthened. It was not found to contain as large a proportion of ferric iron as the Chinese sample, however.

The discovery of one ferric-rich olivine, "hidden" in a museum collection, sparked a search for others. Surely if one ferric-rich olivine had escaped discovery years after its locality was first described, some others had also. Requests were made to many museums for samples of dark-colored to black fayalites, including the British Museum of Natural History, the Harvard Mineralogical Museum, and the Smithsonian

Figure 1a - Room temperature Mössbauer spectrum of Mourne Mountains fayalite.

Figure 1b - Room temperature Mössbauer spectrum of Rockport fayalite.

These spectra were fit with the program described by Stone et al. (1971).



Institution. Of the ten samples eventually examined by Mössbauer spectroscopy, four were found to contain large amounts ( $\text{Fe}^{3+}/\text{Fe}^{2+}$  ranged between 0.19 and 1.38 ) of ferric iron. In addition, one sample was found to have an entirely anomalous Mössbauer spectrum, and will be mentioned further in Chapter 6.

At the same time as requests were sent to museums for fayalites, inquiries were sent to China and the Soviet Union as to the availability of any of their ferric-rich fayalites. Although regrettably no response was heard from the Soviet Union, a sample of ferrifayalite for study was obtained from Dr. Ruyuan Zhang of the Academia Sinica, Beijing.

Since ferric-rich fayalites apparently comprise a new, unstudied subgroup of the olivine group, I considered the study of their crystal chemistry and relationship to the other members of the olivine group, particularly ferrous fayalite, to be of great interest. The chief instrument of study which I used was the Mössbauer spectrometer (more accurately, two different Mössbauer spectrometers). Mössbauer spectrometry can be particularly useful in measuring ferric/ferrous ratios, determining coordination symmetry about iron cations and site distortions from octahedral or tetrahedral symmetry, and assigning individual cations to structurally distinct cation positions (Bancroft, 1973).

I hope to determine in a qualitative way the structure differences between ferric-rich fayalites and ferrous fayalites. I wish to determine the crystallographic distribution of ferric iron and the assumed cation vacancies, and indeed if cation vacancies are necessary to explain the crystal structure. I also wish to determine how the existence of a ferric-and vacancy-rich component might affect the low-temperature

Mössbauer spectrum of fayalite.

Chapter 2Olivine

The minerals of the olivine group all possess a structure consisting of independent  $[\text{SiO}_4]^{4-}$  tetrahedra linked by cations (usually divalent) in distorted octahedral coordination. The oxygen atoms are arranged in approximate hexagonal closest-packing and lie in sheets parallel to the (100) plane. The  $[\text{SiO}_4]^{4-}$  tetrahedra point alternately either way in both the  $x$  and  $y$  directions, in accordance with full orthorhombic symmetry. The spinel structure is the cubic closest-packed analogue of olivine, and is the structure to which minerals of olivine composition revert at high pressure.

The major structural factor in olivine is the chain of edge-sharing distorted octahedra parallel to the  $z$  axis; this chain is serrated or zig-zag in form. The presence of these chains in olivine explains the two observed cleavages (parallel to (100) and to (010)) and the dominance of  $\{hk0\}$  crystal faces. The chains of occupied octahedra in a  $yz$  layer are separated from like chains above and below by the displacement  $a/z$ . They are related to each other by a  $b$  glide plane.

In the olivine structure the distribution of the cations within the hexagonal closest-packed array of oxygen atoms reduces the space group symmetry of the crystal from  $P6_3/mcc$  (hexagonal) to  $Pbnm$  (orthorhombic). Only one-eighth of the available tetrahedral interstices are occupied by Si atoms, and half the available octahedral interstices are filled by other cations, such as Mg, Fe, Mn, or Ca. Half of the octahedrally coordinated cations are located at centers of symmetry and half on

reflection planes, with the former having as nearest neighbors two oxygens from two adjacent tetrahedra and the latter, two oxygens from one adjacent tetrahedron.

The octahedral sites at centers of symmetry are denoted as M1 sites. The M1 octahedron shares six of its twelve edges with other polyhedra: two with other M1 octahedra, two with M2 octahedra, and two with tetrahedra. The octahedral site located on a reflection plane is the M2 site. The M2 octahedron shares only three edges: two with M1 octahedra and one with a tetrahedron.

Pauling's third rule predicts that shared polyhedral edges in olivine will be shorter than unshared edges. The resulting polyhedral distortions are significant: the point group of the M1 octahedron is reduced from  $O_h$  to  $C_1$  and the point group of the M2 octahedron is reduced from  $O_h$  to  $C_s$ . The point group of the  $SiO_4$  tetrahedron is reduced from  $T_d$  to  $C_s$  as well. However, for the purpose of infrared and optical spectral analysis, the point groups of the M1 and M2 octahedra have been approximated as  $D_{4h}$  and  $C_{3v}$ , respectively (Burns, 1970). Ideal and actual olivine structures (Brown, 1970) are seen in Figures 2a and 2b.

Cations found in the octahedral sites of olivine commonly include magnesium and iron, with less common manganese and calcium. Although any cation composition for  $(Mg, Fe, Mn)_2SiO_4$  would appear to be permitted, it is commonly found that two of these cations will constitute over 95% of the total cation content of the olivine. For this reason, specimens are usually described as belonging to one of three binary series based on the principal two cations found in the particular olivine. These series are:

$Mg_2SiO_4$  -  $(Mg, Fe)_2SiO_4$  -  $Fe_2SiO_4$       forsterite - fayalite series

Figure 2a - Ideal olivine structure (from Brown, 1970).

Figure 2b - Actual forsterite structure (from Brown, 1970).



$\text{Fe}_2\text{SiO}_4 - (\text{Fe},\text{Mn})_2\text{SiO}_4 - \text{Mn}_2\text{SiO}_4$  fayalite - tephroite series

$\text{Mg}_2\text{SiO}_4 - (\text{Mg},\text{Mn})_2\text{SiO}_4 - \text{Mn}_2\text{SiO}_4$  forsterite - tephroite series

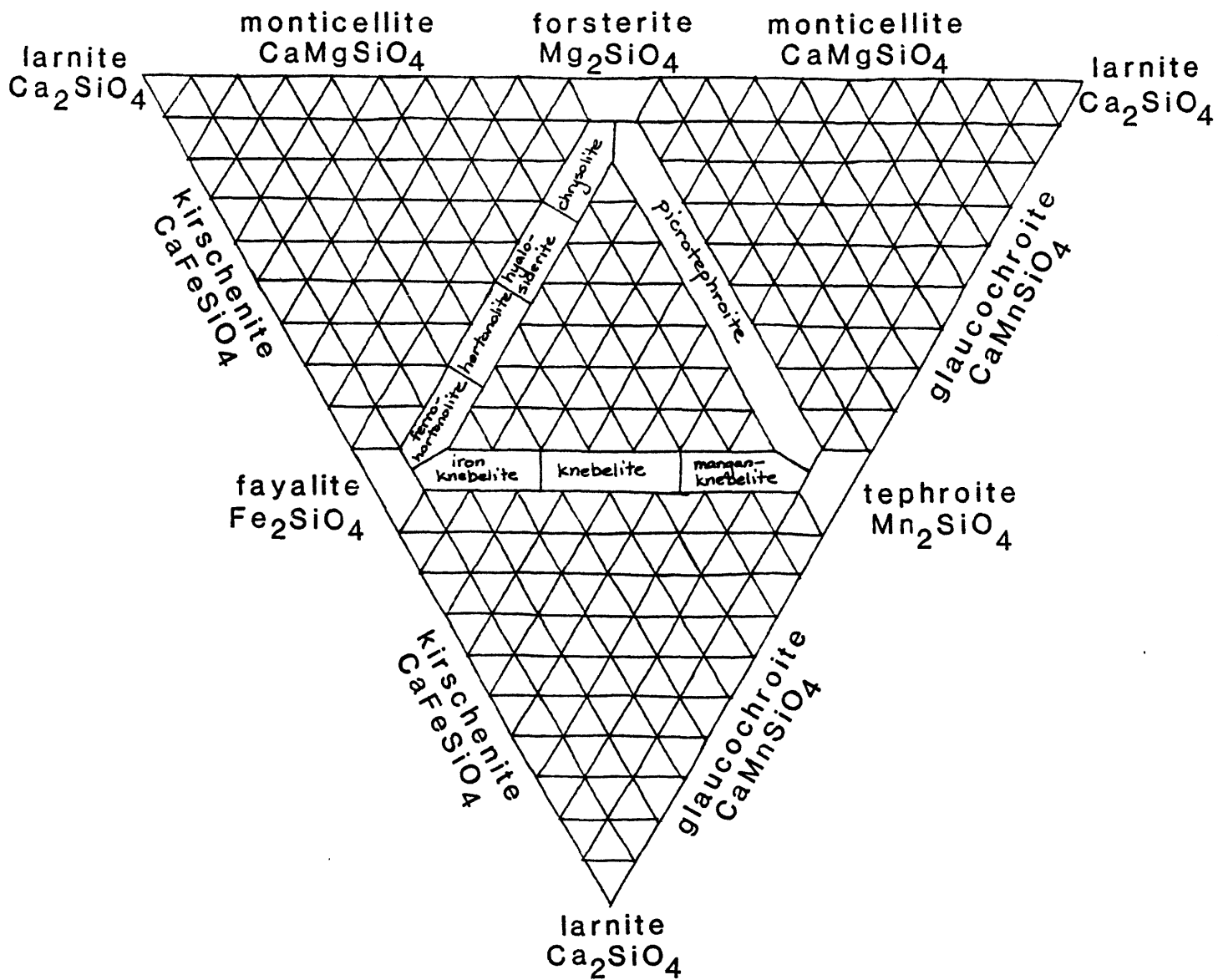
There is only limited solid solution over the series between  $\text{Ca}_2\text{SiO}_4$  and  $\text{Mg}_2\text{SiO}_4$ , but the midpoint of that series,  $\text{CaMgSiO}_4$ , is occasionally seen and is known as monticellite. A diagram showing commonly accepted nomenclature of olivine is shown in Figure 3.

Fayalite is found in small amounts in many acid and alkaline volcanic rocks, particularly those in which sodium is present in greater amount than potassium. It has been reported with tridymite in liparite, in lithophysae in obsidian, and in dacite as a reaction rim around porphyritic orthopyroxene. Fayalite occurs in acid and alkaline plutonic rocks, and is a relatively common constituent of quartz syenites, in which it is often associated with hedenbergite and arfvedsonite. It is a less frequent constituent of acid plutonic rocks, and its occurrence in granite is usually restricted to pegmatitic segregations. Fayalite also occurs in metamorphosed iron-rich sediments; in eulysites and collobrierite it is associated with hedenbergite, grunerite, almandine, and iron-rich orthopyroxenes.

Except for traces of  $\text{Ti}^{4+}$ ,  $\text{Cr}^{3+}$ , and  $\text{Fe}^{3+}$ , there has been no strong evidence previous to the Chinese ferrifayalite/laihunite discovery and the present work that indicates that cations of different formal vacancies mix on a given octahedral site in olivine. Ferrous ions in silicates frequently prefer octahedrally coordinated sites with a distinct local distortion, such as the olivine M1 site. The M1 site, as well as being more distorted, is also slightly smaller than the M2 site, on account of its larger number of shared edges.

If cation size and valences are alike, the more electronegative

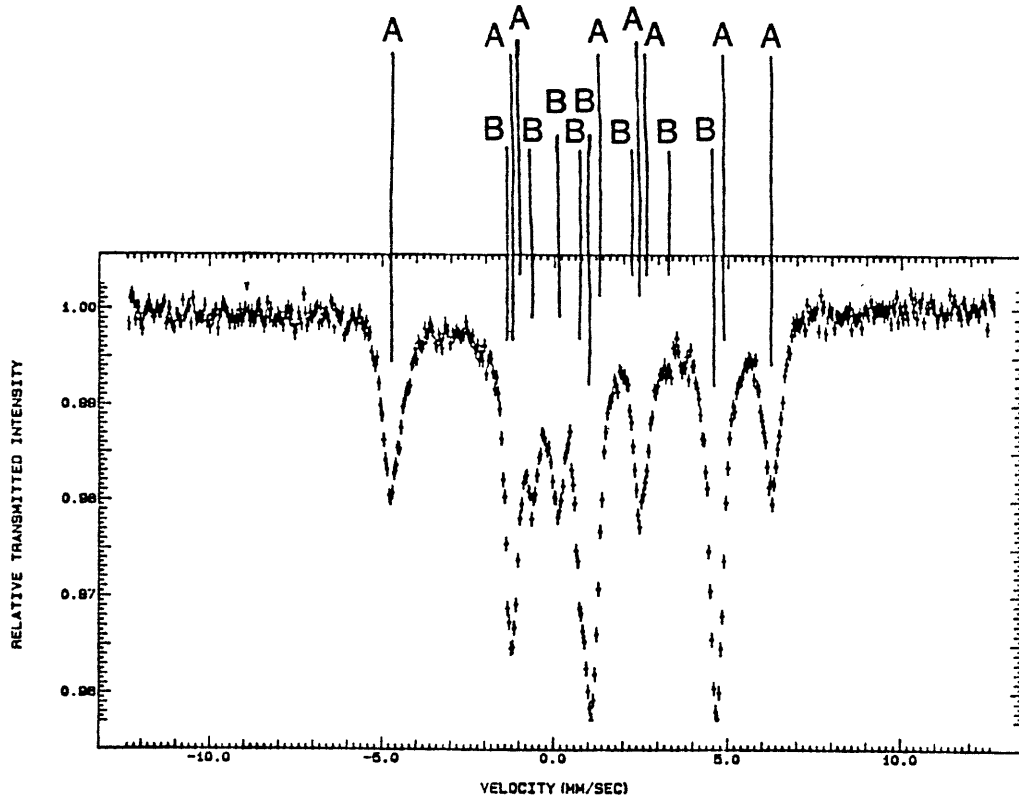
Figure 3 - Nomenclature of olivines (from Mossman and Pawson, 1976).



element will generally prefer M1 because it permits more covalent bonding. In this case,  $\text{Fe}^{2+}$ ,  $\text{Co}^{2+}$ , and  $\text{Ni}^{2+}$  will prefer M1 because they may gain greater crystal field stabilization energy (CFSE) in relation to M2 (Lumpkin and Ribbe, 1983). In forsterite-fayalite series olivines, there is a close to random distribution of iron and magnesium cations with respect to the M1 and M2 sites, with a slight preference of iron for the M1 site (Huggins, in Ghose et al., 1976). In fayalite-tephroite series olivines, on the other hand, there is a distinct site preference of  $\text{Mn}^{2+}$  for the M2 site and of  $\text{Fe}^{2+}$  for the M1 site (Burns, 1970; Huggins, 1973).

The Mössbauer spectrum of ordinary fayalite, while exceedingly simple at room temperature (it apparently consists of one ferrous doublet) is much more complex at low temperatures (less than  $\sim 65$  K). At 66 K a magnetically ordered Mössbauer spectrum begins to appear. This transition is fairly sharp, and involves the splitting of the higher temperature two peak spectrum into a spectrum which appears to have eight lines. These eight lines may be resolved into a sixteen peak spectrum, with eight lines each from the two iron sites, although it has not yet been determined which eight line pattern is from which site (Kundig et al., 1967). The existence of an eight-peak pattern as the magnetically split spectrum for a cation site may at first seem odd, since generally hyperfine splitting in the Mössbauer spectra (with zero external field) of geological materials produces a six-peak pattern. The extra two peaks here are produced by spin-forbidden ( $\Delta m = \pm 2$ ) transitions, which become allowed if the orientation of the nuclear magnetic moment is not parallel to that of the magnetic field of the nucleus. This spectrum is seen in Figure 4, with the resolved lines labeled A and B, to indicate the two eight-peak sub-spectra.

Figure 4 - Low temperature spectrum of Rockport fayalite, with peak assignments from Kundig et al. (1967). Of the sites, it is not known which of the A or B sites corresponds to M1 or M2.



Magnetization curves taken at 4.2 K, 25 K, and 300 K indicated that between 60 K and 20 K fayalite is a weak ferromagnet, possibly of the Morin-Dzyaloshinsky type (Kundig et al., 1967). Both fayalite and tephroite show an unusual magnetic susceptibility dependence on temperature. Three regions may be observed: above 66 K, the minerals are paramagnetic; below 23 K, they are canted antiferromagnetic; and in the region between 23 K and 65 K, they are collinear antiferromagnetic (Santoro et al., 1966). Specific heat measurements of fayalite indicate a pronounced  $\lambda$  point at 65 K, another indication of a sharp transition at this temperature. The magnetic reflections (from neutron diffraction analysis) of fayalite and tephroite can be indexed using X-ray diffraction lattice parameters, indicating that the magnetic and chemical unit cell are identical in size (Santoro et al., 1966).

Two models of the electronic spin structure of fayalite have been proposed (Santoro et al., 1966). In both models the M2 site spins (with mirror symmetry) are in identical modes collinear to  $\underline{b}$  and the canted M1 site spins (with inversion symmetry) possess components along all three crystallographic axes. The two models differ in that in one model the M1 site spins are invariant under spin reversal with the symmetry operations of the crystallographic group and in the other model they are not.

Chapter 3Talasskite

The first recorded discovery of a ferric iron bearing fayalite was by V. D. Nikitin in 1934 (Nikitin, 1934), in the Talassa valley of the Kirghiz ASSR. This mineral, called talasskite, was found in pegmatite veins of the granite massif of intrusive rocks forming the central part of the Kirghiz Range. The crystals of talasskite, up to 4 or 5 centimeters in size, were found sparsely scattered, primarily in the central parts of the veins. They were usually surrounded by biotite leaflets.

These granites are coarse-grained, in marginal zones porphyritic, and rich in pegmatite veins. Primary minerals found include microcline-perthite, quartz, some orthoclase and albite, biotite, hornblende, sphene, magnetite, allanite  $((\text{Ce}, \text{Ca}, \text{Y})_2(\text{Al}, \text{Fe}^{3+})_3(\text{SiO}_4)_3(\text{OH}))$ , apatite, rutile, zircon, and rarely almandine. Secondary minerals include muscovite, chlorite, sausserite (a mineral aggregate produced by the alteration of calcic plagioclase), sericite (fine-grained mica), and kaolinite.

Talasskite is described as being of a brownish color, with adamantine luster on the cleavage surfaces but tarry in fractures, which are uneven. Its streak is light yellowish. It has a Mohs hardness of 5.5 -6, a specific gravity of 4.1, and a melting point of  $1250^\circ \pm 10^\circ\text{C}$ . It is weakly pleochroic, and almost colorless in thin section, with a 2V of  $-49^\circ$ . The crystals were found to have perfect cleavage at (010), distinct at (100), and quite perfect at (001). From the chemical analysis the formula was determined to be  $20\text{FeO} \cdot 2\text{MgO} \cdot 2\text{Fe}_2\text{O}_3 \cdot 13\text{SiO}_2$ , which was

simplified to  $(\text{Fe,Mg})_5\text{Fe}^{3+}(\text{SiO}_4)_3$ . The X-ray powder diffraction spectrum is given in Table 1 and the chemical analysis in Table 2. A comparison of talasskite with other ferric-rich fayalites is given in Table 3.

When a mixture of 20% talasskite, 40% microcline, 30% quartz, and 10% NaF (a composition close to that of the pegmatites) was heated in a furnace in a sealed porcelain crucible to 1300<sup>o</sup>-1400<sup>o</sup>C and then cooled, in the general vitreous mass were found minute columnar crystals believed by Nikitin to be talasskite.

#### Russian Ferrifayalite

The next appearance of a ferric bearing fayalite is also seen in the Russian literature. In 1962, I. V. Ginzburg et al. found a mineral they called ferrifayalite in the Charkasarskii granite massif of the Kuraminskii Range, Central Asia (Ginzburg et al., 1962). They believed this mineral to be an intermediate phase in the alteration of Mn-rich fayalite, midway between the appearances of magnetite, quartz, and gedrite, and the appearance of hematite.

Under a microscope the transformation from Mn-rich fayalite to ferrifayalite could be traced completely: The change usually begins along small cleavage cracks and other cracks, gradually covering greater surfaces to eventually spread over the entire crystal. This alteration is a low temperature supergene process, which takes place in a system open to the atmosphere. The form of the ferrifayalite crystals exactly repeats the form of the Mn-fayalite crystals, but the cleavage is different. Together with the perfect (001) cleavage in the original Mn-fayalite crystal, two other cleavages arranged at a 60<sup>o</sup> angle to each other and

Table 1. X-ray Powder Diffraction Spectra of Previously Known Ferric-rich Fayalites

Talasskite <sup>1</sup>		Russian ferrifayalite <sup>2</sup>		Laihunite <sup>3</sup>			Chinese ferrifayalite <sup>4</sup>			Chinese ferrifayalite (cont.)		
*distance (mm)	I	d	I	d	I	hkl	d	I	hkl	d	I	hkl
26	1	3.81	5	5.80	3	100	5.820	2	001	1.407	6	331,302
31	1	3.49	9	5.21	1	002	5.090	3	020	1.391,1.387	4,1	170,312;260
37.5	2	3.05	1	3.78	6	102	4.350	5	110	1.354	5	322,340,171
39.5	4	2.80	10	3.47	9	111	3.824	3	021	1.341	1	124
41.3	1	2.53	10	2.90	3	200	3.488	10	111,120	1.321	1	341
43.5	1	2.42	6	2.78	8	013	2.993	1	121	1.298	2	332,243
46	1	2.26	4	2.528	10	202,113	2.911	3	002	1.292	1	134
48.6	1	2.18	2	2.405	6	020,211	2.774	9	130	1.262	3	350
52.2	1	2.04	1	2.350	1	104	2.521	10	022,131,040	1.254	1	172,262
54.3	5	1.946	1	2.260	5	014	2.486	2	102	1.245	1	204,270
57.5	1	1.761	10	2.180	2	022,121	2.425	4	112	1.226	1	313,342,180
61.5	1	1.686	1	2.055	1	122	2.405	7	200	1.202	4	400,323,181
64.8	4	1.645	1	1.870	1	123	2.339	5	210,041	1.165	3	360,082,411
70	2	1.483	2	1.750	7	024,222	2.246	7	140,122	1.158,1.153	3	352,154
75	1	1.451	1	1.675	1	124,303	2.219	2	201	1.146,1.143	1	421;272,361
80	1	1.410	4	1.635	2	106,223	2.175	6	211,220	1.127,1.123	2	263,115;280
		1.367	2	1.595	1	215	2.094	1	141	1.116,1.113	2	244;402,343
		1.203	1	1.555	1	304,025	2.037	2	221	1.105	2	412,281
		1.153	1	1.475	3	206,314	1.845	3	202	1.084,1.080	2,4	422,440;362,191
		1.094	1	1.440	4	401,332	1.785	1	151			
		1.043	1	1.410	3	133,230	1.775	4	113,142	1.076	3	370,135
				1.395	2	017,305,216	1.745	8	240,222	1.065	1	083,441
							1.678,1.667	2,4	241	1.036	3	450
				1.355	3	126,117	1.634	5	060,232	1.030	2	192
				1.200	2	040,118	1.601	1	160	1.023,1.107	2	0.10.0,451
				1.084	3	242,416	1.584	3	310,133	0.996	2	380,1.10.0,363
				1.035	2	045,219,318	1.576	2	152			
							1.555	1	250	0.971,0.966	2	283,006;461,292,245
							1.543	1	301,161			
							1.528	3	311,320	0.949,0.945	4	501,443;520,511,274
							1.508	1	203			
							1.501	1	251	0.936	1	2.10.0
							1.495	2	213,242	0.930,0.927,	3	470,404;530,
							1.477,1.468	5	321,062	0.925		390,2.10.1
							1.456,1.449	6	004;330,223			

\*Since the wavelength at which these data were taken (presumably by powder camera) was not given, these data are useless for comparison, but are included here for completeness.

<sup>1</sup>Nikitin, 1934

<sup>2</sup>Ginzburg et al., 1962

<sup>3</sup>Laihunite Research Group, 1976,1982

<sup>4</sup>Ferrifayalite Research Group, 1976

Table 2. Chemical analyses of previously known ferric-rich favalites

	<u>Talasskite<sup>1</sup></u>		<u>Russian ferrifayalite<sup>2</sup></u>						<u>Lainunite<sup>3</sup></u>						<u>Chinese ferrifayalite<sup>4</sup></u>					
			<u>1</u>		<u>2</u>		<u>3</u>		<u>1</u>		<u>2</u>		<u>3</u>		<u>1</u>		<u>2</u>		<u>3</u>	
	wt. %	formula	wt. %	formula	wt. %	formula	wt. %	formula	wt. %	formula	wt. %	formula	wt. %	formula	wt. %	formula	wt. %	formula	wt. %	formula
SiO <sub>2</sub>	29.87	0.963	30.48	0.950	29.02	0.901	30.18	0.920	31.00	0.938	31.07	0.933	31.85	0.947	31.94	0.957	31.96	0.533	31.67	0.951
TiO <sub>2</sub>	0.08	0.002	0.07	0.002	0.06	0.002	---	---	---	---	---	---	---	---	---	---	0.01	0.000	0.05	0.002
Al <sub>2</sub> O <sub>3</sub>	---	---	0.37	0.015	---	---	0.74	0.026	0.00	0.00	0.00	0.000	0.065	0.004	---	---	0.79	0.008	0.58	0.022
Fe <sub>2</sub> O <sub>3</sub>	12.07	0.294	32.19	0.752	47.18	1.098	45.74	1.047	43.57	0.987	44.24	0.998	45.07	1.006	45.10	1.015	35.31	0.221	36.14	0.816
FeO	54.88	1.478	26.77	0.696	12.53	0.324	15.14	0.384	25.50	0.643	23.64	0.591	22.52	0.558	22.62	0.565	29.59	0.411	28.08	0.704
H <sub>2</sub> O	2.54	0.124	0.10	0.006	0.70	0.033	0.20	0.013	0.00	0.00	0.87	0.040	0.47	0.021	---	---	1.43	0.034	1.64	0.074
MnO	0.02	0.000	7.96	0.210	7.55	0.197	5.49	0.141	---	---	---	---	---	---	---	---	0.02	0.000	0.12	0.004
CaO	0.20	0.006	0.82	0.028	0.77	0.026	0.40	0.013	0.00	0.00	0.21	0.007	0.47	0.014	---	---	0.75	0.013	0.82	0.027
Na <sub>2</sub> O	0.71	0.043	0.14	0.007	---	---	---	---	---	---	---	---	---	---	---	---	0.21	0.003	0.09	0.054
K <sub>2</sub> O	0.08	0.000	0.08	0.004	---	---	---	---	---	---	---	---	---	---	---	---	---	---	0.09	0.004
Sum	100.45		98.98		97.81		97.97		100.07		100.03		100.45		99.66		100.07		99.23	

<sup>1</sup>Nikitin, 1934

<sup>2</sup>Ginzburg et al., 1962

<sup>3</sup>Laihunite Research Group, 1976, 1982

<sup>4</sup>Ferrifayalite Research Group, 1976

Table 3. Summary of physical properties of ordinary fayalite and previously known ferric-rich fayalites

	Fayalite <sup>1</sup>	Talasskite <sup>2</sup>	ferrifayalite <sup>3</sup>	Lihunite <sup>4</sup>	ferrifayalite <sup>5</sup>	ferrifayalite <sup>6</sup>
Locality	-----	Talassa Valley, Kirghiz ASSR	Kuraminski Range, Central Asia (USSR)	Laine Village, NE China	Liaoning Province, China	Wuqi Mt., Western Guizhou, Eastern Hubei Province, China
Geologic Setting	found in small quantities in some acid and alkaline plutonic and volcanic rocks, also as a product of regional metamorphism in iron rich sediments	granite pegmatite	granite, as alteration product of Mn-fayalite	metamorphic iron deposit, Archaean Anshan group	Anshan-like magnetite province	eulysite in Early Archaean lower Qianxi group
Formula	Fe <sub>2</sub> SiO <sub>4</sub> (all Fe is Fe <sup>2+</sup> )	(Fe,Mg) <sub>2</sub> Fe <sup>3+</sup> (SiO <sub>4</sub> ) <sub>2</sub>	Fe <sup>3+</sup> 0.89Fe <sup>2+</sup> 0.87Mn <sup>2+</sup> 0.25CaO.3SiO <sub>4</sub>	Fe <sup>2+</sup> 1.01Fe <sup>3+</sup> 0.56Mn <sup>2+</sup> 0.03CaO.9SiO <sub>4</sub>	Fe <sup>2+</sup> Fe <sup>3+</sup> (SiO <sub>4</sub> ) <sub>2</sub>	(Fe <sup>2+</sup> ,Fe <sup>3+</sup> ) <sub>2</sub> SiO <sub>4</sub>
Crystal Structure	orthorhombic, Pbnm	related to rhombic system	orthorhombic	monoclinic, C <sub>2h</sub> - P2 <sub>1</sub> /c	monoclinic, C <sub>2h</sub> - P2 <sub>1</sub> /b	P2 <sub>1</sub> /b
Cell Parameters	a=4.817Å, b=10.477Å, c=6.105Å, V=308.11Å <sup>3</sup>	not determined	a=4.71Å, b=10.5Å, c=6.1Å, V=301.68Å <sup>3</sup>	a=5.813Å, b=4.812Å, c=10.211Å, V=285.62Å <sup>3</sup>	a=4.808Å, b=10.171Å, c=5.824Å, V=284.81Å <sup>3</sup>	a=4.816Å, b=10.270Å, c=5.860Å, V=290.23Å <sup>3</sup>
Density	4.392	4.1	4.90	3.92	3.967	4.92
Hardness	6.5	not determined	microhardness 572-744 kg/mm <sup>2</sup> , Mohs hardness 5.1-5.8	microhardness 890 kg/mm <sup>2</sup> , Mohs hardness 6.1	5.5 - 6.5	microhardness 883 kg/mm <sup>2</sup> , Mohs hardness 6.2
Streak	colorless	light, yellowish, almost colorless	brown	light brown	blackish-brown	not determined
Diaphaneity	(010) moderate, (100) weak	(010) perfect, (100) clear, (001) quite perfect	(001) perfect, two sets arranged at 60° to each other and at -90° to (001)	(001) perfect, (010) perfect, (100) imperfect	(100) distinct, (010) indistinct	two sets of good cleavage
Description	color: greenish-yellow, yellow-amber, pale yellow in thin section, vitreous luster; 2v=134°	brownish, adamantine luster, almost colorless in thin section, weakly pleochroic	dark gray to black, metallic luster, less reflective than magnetite, opaque, black, dark-brownish in thin section, no signs of pleochroism or birefringence, sometimes weakly anisotropic, sometimes isotropic, paramagnetic; somewhat diffuse X-ray pattern	thick tabular, short prismatic, opaque, black, metallic to sub-metallic luster, brown-red in very thin section, parallel extinction, indistinct double-reflection, weakly anisotropic, nonhomogeneous extinction, weak-medium magnetism (attracts steel needles), X-ray pattern similar to Russian ferrifayalite	xenomorphic granular, blackish, luster submetallic, opaque, grey in reflected light, anisotropic, distinct birefringence, nonmagnetic, moderately electromagnetic	black, opaque, glossy to semi-metallic luster, light grey in reflected light, weak magnetism (steel needles attracted by a hand magnet)
References	<sup>1</sup> Lover et al., 1962 <sup>2</sup> Walcott, 1934 <sup>3</sup> Wainburg et al., 1962	<sup>4</sup> Lihunite Research Group, 1976, 1982 <sup>5</sup> Ferrifayalite Research Group, 1976 <sup>6</sup> Zhang et al., 1981				

almost normal to the (001) cleavage can be observed in ferrifayalite.

In grains ferrifayalite is described as dark gray to black, with a metallic luster. It is opaque and only in very thin section does a brownish color show through. It has a brown streak. Its microhardness varies between 572 and 744 kg/mm<sup>2</sup>, corresponding to a Mohs hardness of 5.1 - 5.8, and its specific gravity is 3.90. It is paramagnetic. There are no signs of pleochroism or birefringence. It was observed to be sometimes isotropic, sometimes weakly anisotropic.

From chemical analysis, a formula for ferrifayalite was deduced:  $(\text{Fe}^{3+}_{0.89}\text{Fe}^{2+}_{0.83}\text{Mn}^{2+}_{0.25}\text{Ca}_{0.03})\text{SiO}_4$ . Since this is not charge-balanced, Ginzburg et al. came to the conclusion that ferrifayalite is not a single mineral, but a mixture of Mn-fayalite, magnetite, and silica. They were unable to confirm this hypothesis, however. Ferrifayalite gave an inadequately clear X-ray diffraction pattern with somewhat diffuse images, but appears as a single mineral for which cell parameters were determined:  $a = 4.71 \text{ \AA}$ ,  $b = 10.5 \text{ \AA}$ ,  $c = 5.94 \text{ \AA}$ ,  $V = 299.5 \text{ \AA}^3$ .

The infrared absorption spectra of forsterite, Mn-fayalite, Mn-fayalite heated to 200° and 400°, ferrifayalite, and ferrifayalite produced by heating Mn-fayalite to 600°C, turned out to be in general quite similar. In the regions showing lines characteristic of vibrations of the  $[\text{SiO}_4]^{4-}$  tetrahedra there were greater differences between the spectra of Mn-fayalite and forsterite than between the spectra of Mn-fayalite and ferrifayalite. Exchanging  $\text{Fe}^{2+}$  and  $\text{Mg}^{2+}$  deforms the  $[\text{SiO}_4]^{4-}$  tetrahedron more than exchanging  $\text{Fe}^{2+}$  and  $\text{Fe}^{3+}$ , based on ionic radii considerations. Neither hematite nor silica absorption bands were found in the ferrifayalite spectrum, in contradiction of the authors' belief that this was a mixture containing these minerals. The absence of

signs of the multiphasal character of ferrifayalite in Laue diffraction patterns and Debye powder patterns led Ginzberg et al. to suggest that the hematite and silica particles are so small (on the order of a few unit cells) that they are not perceived by either method.

Under the electron microscope ferrifayalite appears grainy, while fayalite is smooth. There appear to be rounded grains (of Mn-fayalite?),  $\sim 0.05\text{--}0.2\ \mu$  in size, with material between them (an aggregate of  $\text{SiO}_2$  and  $\text{Fe}_2\text{O}_3$ ?). Signs of the disintegration of the crystalline structure of ferrifayalite in comparison with Mn-fayalite were considered indirect experimental evidence for the possible three phase composition of ferrifayalite. These signs include its opacity, the diffuseness of the X-ray diffraction images, and the graininess observed under the electron microscope.

References are made in the Russian literature (Mineraly Uzbekistana, 1975-77) to ferrifayalites found elsewhere in the Soviet Union as well. Two occurrences, one discovered by I. E. Smorchkov in the Ashtskii granite massif of the Kuraminskii Range, and the other by N. N. Kriskevich in the Tuiukskii granite massif in the central part of the Chatkalskii range, are mentioned, but I have been unable to trace more detailed references to either.

#### Laihunite and Chinese Ferrifayalite

In 1976 a new iron silicate mineral was discovered by Geological Team No. 101 of Liaoning Metallurgical and Geological Prospecting Company near Little Laihe Village, in northeastern China (Laihunite Research Group, 1976, 1982). It was named laihunite after the locality of its discovery.

It was found in a metamorphic iron deposit in the metamorphic complex and migmatite (a composite rock composed of igneous or igneous-looking and/or metamorphic materials which are generally distinguishable megascopically; its formation may involve solid-state reconstruction in the presence of fluids) of the Archean Anshan group, associated with fayalite, hypersthene, quartz, and magnetite. The ores occur chiefly in hornblende-pyroxene-magnetite quartzites (i.e., hypersthene granulite facies), and subordinately in striped magnetite quartzites. They have three structures: compact massive, striped, and disseminated. The principal ore mineral is magnetite, with some limonite, minor pyrrhotite, and minor chalcopyrite. Gangue minerals consist mainly of hornblende, iron-rich pyroxene, chlorite, and quartz, with a minor amount of laihunite and trace apatite. Laihunite is found in the striped portion of the ore mainly in the upper portion of the ore body in quartz-hypersthene granulite or hypersthene granulite, in content of up to 1 to 4 percent. It is generally less common or absent in the lower part of the ore body, or beyond its limits. It is frequently associated with quartz, hypersthene, and magnetite.

The formula of laihunite, deduced from chemical analysis (Laihunite Research Group, 1976,1982), is  $\text{Fe}^{3+}_{1.00}\text{Fe}^{2+}_{0.58}\text{Mg}^{2+}_{0.03}\text{Si}_{0.96}\text{O}_4$ . The mineral is black, with metallic to submetallic luster. It shows a distinctive infrared spectrum. It is monoclinic, with space group  $\text{C}_{2h}^5\text{-P}2_1/\text{c}$ . The unit cell, calculated from X-ray diffraction data, is:  $a = 5.813 \text{ \AA} \pm 0.005$ ,  $b = 4.812 \text{ \AA} \pm 0.005$ ,  $c = 10.211 \text{ \AA} \pm 0.005$ ,  $\beta = 90.87^\circ$ . The crystals are thick tabular and short prismatic, 0.3 -0.65 mm in size, with a few up to 1.0 mm in length. Perfect cleavages along (001) and (010) are seen, as well as an imperfect cleavage along (100). Its streak

is light brown. Its microhardness is 890 kg/mm<sup>2</sup>, and Mohs hardness is 6.1, with specific gravity of 3.92. It has weak to medium magnetism which can attract steel needles. It is opaque in transmitted light, with some grains marginally brown-red. In ultrathin section (several microns thick) it is translucent brown-red, with parallel extinction. In reflected light, it is grey and shows indistinct double-reflection. It is weakly anisotropic and shows nonhomogeneous extinction, with inhomogeneity visible inside individual grains. Its X-ray diffraction lines are obscure and fewer in number than those of fayalite, indicating (to the Laihunite Research Group) a lower degree of crystallinity. The X-ray diffraction spectrum of laihunite appears similar to that of Russian ferrifayalite. Electron microprobe analysis suggests laihunite to be homogeneous with Fe and Si uniformly distributed.

There is a good deal of confusion in the Chinese literature concerning the naming of the mineral referred to above as laihunite. As well as the locality near Little Laihe Village, two other localities have been discovered. At these localities, the mineral in question is referred to as ferrifayalite, but appears to be essentially identical to laihunite. In the Anshan-like magnetite region of Liaoning Province, a discovery of ferrifayalite was made also in 1976 (Ferrifayalite Research Group, 1976). This mineral was named ferrifayalite by its discoverers because they believed it to be identical to the Russian ferrifayalite. Another locality for ferrifayalite is mentioned also, that at Louzi Mountain, Qianan County, eastern Hebei Province (Zhang et al., 1981), which occurs in the Lower Qianxi Group. It is from this locality that the sample I obtained for study comes.

The minerals laihunite and ferrifayalite from the three different

localities mentioned here have slightly different characteristics. I have already described laihunite from Little Laihe Village. Let me now describe the two ferrifayalite occurrences.

Ferrifayalite is found in the Anshan-like magnetite zone of Liaoning Province, distributed unevenly or commonly aggregated as bands. Its percentage in the rock is usually lower than that of magnetite, occasionally reaching 10%. The crystals are xenomorphic granular, individually 0.25 - 0.7 mm in diameter, sometimes as large as 1.0 mm. Their color is blackish, with a submetallic luster and a blackish-brown streak. Distinct cleavage is observed along (100), and indistinct cleavage along (010). The crystals are nonmagnetic but moderately electromagnetic. Its Mohs hardness is 5.5 - 6.6, with a specific gravity of 3.967. It is opaque. Under a reflecting polarizing microscope the crystals are grey, anisotropic, and with distinct bireflection (reflection-pleochroism). It is monoclinic, with space group  $C^5_{2h}-P2_1/b$ . The unit cell parameters are:  $a = 4.808 \text{ \AA}$ ,  $b = 10.171 \text{ \AA}$ ,  $c = 5.824 \text{ \AA}$ ,  $\alpha = 90^\circ$ . Its formula is given as  $Fe^{2+}Fe^{3+}_2(SiO_4)_2$ .

Ferrifayalite is also found in the Early Archaean Lower Qianxi group at Louzi Mountain, Qianan County, eastern Hebei Province. It occurs in a banded eulysite (granular pyroxene peridotite), which contains also eulite (orthopyroxene  $Fs_{70-90}$ ), almandine, quartz, and locally magnetite, ferroaugite, biotite, graphite, and apatite, with relict plagioclase surrounded by reaction rims of fine-grained garnets. Ferrifayalite is concentrated in bands composed of eulite and garnet, with minor quartz. It is distributed along intercrystalline boundaries, particularly along the boundaries, cracks, and cleavages of the eulite, as a result of replacement.

Sometimes the replacement is so extensive that only relict eulite is preserved. Ferrifayalite is crossed by magnetite, which is closely associated with it. The ferrifayalite-bearing eulysites are composed of over 90 weight percent iron and silica, and it may be assumed that their parent rock was an iron-rich sediment.

Ferrifayalite is described as being black, with glassy to semi-metallic luster, and opaque in thin section. Its microhardness is 883 kg/mm<sup>2</sup>, and Mohs hardness is 6.2. Its specific gravity is 3.95. There are two sets of good cleavages. It is weakly magnetic: small grains can be attracted by a hand magnet. It is light grey in reflected light. The unit cell parameters are:  $a = 4.816 \text{ \AA}$ ,  $b = 10.270 \text{ \AA}$ ,  $c = 5.868 \text{ \AA}$ ,  $\beta = 90^\circ$ . Its space group is  $P2_1/b$ .

### Others

Lastly, ferric iron has been detected by Shinno in three natural volcanic olivines of unspecified localities (Shinno, 1981). These olivines ranged in composition from  $Fa_{14}$  to  $Fa_{99}$ , with  $Fe^{3+}/Fe^{2+}$  ratios, uncorrelated, from 0.04 to 0.42. Shinno determined that the ferric iron was preferentially occupying the M2 site.

Chapter 4

In this chapter brief descriptions are given of the geological settings in which the three new ferric-rich fayalites I discovered are found. Also included is a description of the geological setting of a ferric-rich fayalite recently discovered by Mahood (1980) and Harris (1983), and the synthesis of a possible artificial ferric-rich fayalite at Berkeley (Stebbins, 1983).

Pantelleria

The fayalite from Pantelleria, Italy, comes from a volcanic cone (Cuddia Mida) on the island of Pantelleria. Pantelleria probably formed according to the following plan (Washington, 1913): First, submarine volcanic eruptions produced large amounts of pantelleritic trachyte and comendite (white pantellerite). Eventually these reached the surface of the sea to begin the formation of the island mass. Later than these, but issuing from the same volcanic center, came flows of green pantellerite (green to black alkalic rhyolite). The second phase of eruptions began also with trachyte (extrusive equivalent of syenite) flows, and later with pumicious lapilli (from Cuddia Mida). Following this, small parasitic cones produced flows of black pantellerite. The third phase of eruptions came after the cessation of these flows, but we do not know how long after. This phase consisted of basaltic eruptions and intrusions of basaltic dykes. The submarine eruption of 1891, four kilometers west of the island, is the last eruptive activity mentioned by Washington. Fumaroles and hot springs exist at present on Pantelleria.

Fayalite is found in the crater of Cuddia Mida, in euhedral crystals associated with cossyrite (aenigmatite), bipyramidal quartz, and feldspar (Soellner, 1911). It is found primarily in a dark and light sand on the rim of the crater. This sand was either formed from disintegrated pantellerites or erupted in this form. The light portion of the sand is formed from quartz and feldspar, while the dark portion is formed mainly of aenigmatite ( $\text{Na}_2\text{Fe}^{2+}_5\text{TiSi}_6\text{O}_{20}$ ), containing about one percent fayalite. Fayalite is also found on the island well distributed in pantellerite and augite andesite, and forsterite is found in trachydolerite basalt (an alkalic basalt).

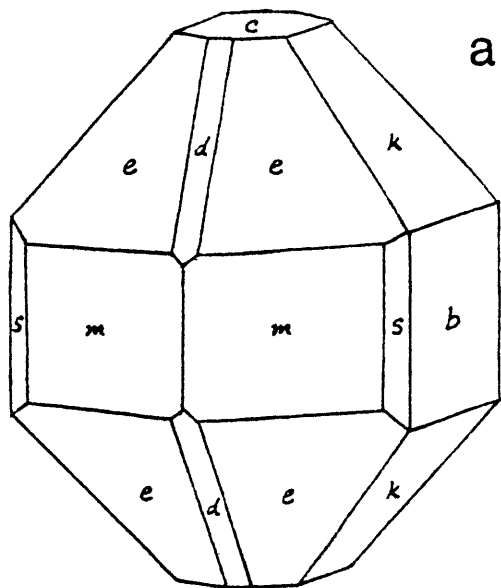
The crystal habit of fayalite found on Pantelleria is variable (Soellner, 1911). There are three forms seen. The first (Figure 5a) is short columnar along the c-axis, with a nearly pseudo-hexagonal habit. It forms a bipyramid with four prisms and two pinacoids.

The second habit (Figure 5b) is evidently columnar along the c-axis, but somewhat tabular along  $\{010\}$ . This habit is identical to the standard habit shown in Deer, Howie, and Zussman (1962) for fayalite.

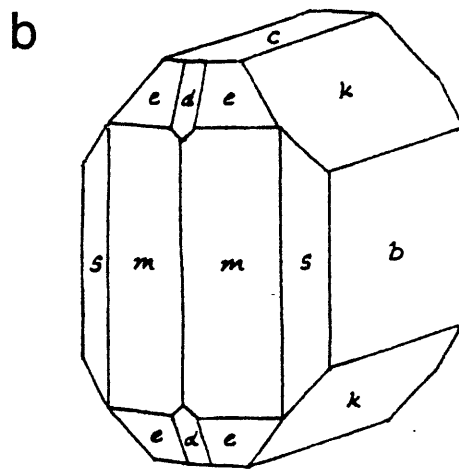
The third habit (Figure 5c) is tabular along  $\{010\}$  and stretched along the a-axis. No fayalites from Pantelleria are found with faces parallel to  $\{100\}$ ; it is totally absent as a crystal surface.

The size along the c-axis of types 1 and 2 is less than or equal to 1.25 mm, and along the a and b axes is 1.1 mm. Somewhat larger crystals are also seen, of sizes up to 2.15 by 2.00 mm. The largest crystals are those of the third habit, which have lengths up to 2.6 mm along the a-axis, 1.0 mm along the c-axis, and 0.7 mm along the b-axis. The cleavage is good along b  $\{010\}$ , and less good along c  $\{001\}$ . The hardness is 6.5 -7. The density is 4.24. It belongs to the rhombic crystal

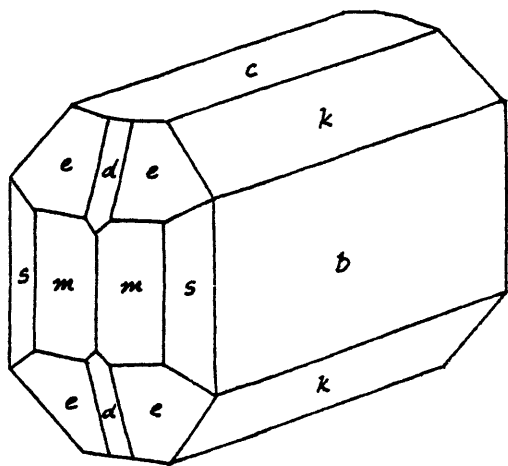
Figure 5a - c - Observed crystal habits of *Pantelleria fayalite* (from Soellner, 1911).



a



b



c

system, with unit cell dimensions in the ratio  $a : b : c = 0.4600 : 1 : 0.58112$ . The mineral is pleochroic.

Fresh crystals are wine-yellow or green-yellow, translucent, and glassy on their crystal faces. Many crystals are black and opaque, but when broken are similar to fresh crystals in appearance. Soellner suggested that this black color was caused by the oxidation of a thin film of iron on the surface during weathering. It could be a limonitic replacement product, containing  $H_2O$  and having the formula:  $Fe_2O_3 \cdot H_2O$ . This explained to Soellner's satisfaction the presence of  $Fe_2O_3$  and  $H_2O$  in the chemical analysis (Table 4a) in approximately those proportions. When alkalis and water were removed from the analysis, and  $Fe_2O_3$  converted to the iron molar equivalent of  $FeO$ , the revised analysis was listed (Table 4b). This analysis, though seemingly worse because of the low oxide totals produced, was used by Soellner in his later calculations concerning this fayalite.

My electron microprobe analysis of this sample (Table 5) agrees quite well with Soellner's original analysis of his samples from the same locality. The crystals I examined were also quite black on the outside, and very well formed, but in contrast to Soellner's crystals, appeared also black on the inside. No evidence of iron oxide contamination was found.

### Mourne Mountains

Fayalite is found in the Mourne Mountains in small detached masses at Slieve Corragh (a mountain peak) and as large euhedral crystals in the fine-grained margin of the Quartzose Granite next to the Felspathic

Table 4.Soellner's chemical analyses of Pantelleria fayalite

a.	<u>wt. %</u>	b.	<u>wt. %</u>
SiO <sub>2</sub>	28.89	SiO <sub>2</sub>	28.89
TiO <sub>2</sub>	1.19	TiO <sub>2</sub>	1.19
Fe <sub>2</sub> O <sub>3</sub>	5.08	Fe <sub>2</sub> O <sub>3</sub> +FeO	4.57
FeO	56.05	FeO	56.05
MnO	3.39	MnO	3.39
MgO	3.11	MgO	3.11
CaO	0.74	CaO	0.74
alkali	0.42		
H <sub>2</sub> O	1.07		
	<hr/>	Sum	<hr/>
Sum	99.94		97.94

Table 5. Microprobe analyses of my ferric-rich fayalites and Rockport fayalite

	<u>Rockport</u>		<u>Qianan County</u>		<u>Mourne Mountains</u>		<u>Pantelleria</u>		<u>St. Peter's Dome</u>	
	<u>weight %</u>	<u>formula</u>	<u>weight %</u>	<u>formula</u>	<u>weight %</u>	<u>formula</u>	<u>weight %</u>	<u>formula</u>	<u>weight %</u>	<u>formula</u>
SiO <sub>2</sub>	29.06 ± 0.15	1.018	30.97 ± 0.67	0.961	30.43 ± 0.19	0.981	29.72 ± 0.21	0.969	29.15 ± 0.39	0.901
TiO <sub>2</sub>	0.01 ± 0.00	0	0.00 ± 0.00	0	0.01 ± 0.01	0	0.00 ± 0.02	0	0.00 ± 0.03	0
Al <sub>2</sub> O <sub>3</sub>	0.00 ± 0.00	0	0.00 ± 0.00	0	0.01 ± 0.01	0	0.00 ± 0.00	0	0.00 ± 0.00	0
Fe <sub>2</sub> O <sub>3</sub> <sup>*</sup>	0.00	0	38.64 ± 0.38	0.905	22.36 ± 0.36	0.542	11.18 ± 0.21	0.27 <sup>h</sup>	33.53 ± 0.27	0.778
FeO	67.28 ± 0.33	1.964	24.99	0.650	41.67	1.120	53.18	1.444	35.92	0.925
H <sub>2</sub> O	0.08 ± 0.03	0.004	1.45 ± 0.03	0.067	0.38 ± 0.02	0.019	1.60 ± 0.04	0.078	0.00 ± 0.03	0
MnO	2.28 ± 0.07	0.067	0.08 ± 0.04	0.002	3.14 ± 0.09	0.085	4.08 ± 0.09	0.112	4.09 ± 0.13	0.107
CaO	0.00 ± 0.00	0	0.00 ± 0.00	0	0.06 ± 0.02	0.002	0.51 ± 0.08	0.018	0.00 ± 0.00	0
K <sub>2</sub> O	0.00 ± 0.00	0	0.00 ± 0.00	0	0.00 ± 0.00	0	0.00 ± 0.00	0	0.00 ± 0.00	0
Sum	98.71		96.13		98.06		100.27		102.69	

\*Values of Fe<sub>2</sub>O<sub>3</sub> and FeO were not determined directly by microprobe. The total iron content was analyzed as FeO, then the ferric/ferrous ratio was determined by Mössbauer spectroscopy. The standard deviation given is for the microprobe analysis of the total iron as FeO.

Granite of Eagle Rock, Slieve Donard (Richey, 1927). The Tertiary granite massif of the Mourne Mountains, which is intrusive into folded Silurian sediments, has been divided into four or five distinct intrusions composed of slightly different rock varieties (Nockolds and Richey, 1927). The varieties are closely alike mineralogically. They consist of somewhat sparse crystals of greenish or brown biotite, with the addition of hornblende (in two of the intrusions), euhedral quartz, a small amount of albite-oligoclase, and alkali feldspar, mainly microperthite. All the granite masse are traversed here and there by replacement veins which belong, in general, to the greisen (a granitic rock composed chiefly of quartz, mica, and topaz) class, the prevalent variety being dark green in color.

Both Slieve Corragh and Slieve Donard are formed of the inner Felspathic Granite, the oldest intrusive body in the range. In the Felspathic Granite, orthoclase is conspicuously in excess of quartz. Where it is porphyritic, the orthoclase phenocrysts measure rather more than 1 cm across. Early quartz grains measure about 2 mm across and are not conspicuously dark. In the ground mass, orthoclase and quartz are often found in micrographic intergrowth. Ragged brownish-green hornblende is usually present in addition to biotite, and helps to distinguish this granite from others of the district. The porphyritic habit is sometimes present right up to the margins against the Silurian shales, but in other places a marginal belt of non-porphyritic granite of finer texture is developed, which may be as much as 400 yards in width.

The Quartzose Granite, which is the next-to-oldest intrusive body in the range, contains very abundant quartz, a large proportion of which is so dark as to give the rock itself a characteristic appearance. The

porphyritic aspect of the orthoclase, where developed, is as a rule not as striking as in the Felspathic Granite, and the size of the phenocrysts is slightly under 1 cm. The early quartz grains are about 2 mm across. The Quartzose Granite tends to be non-porphyritic and is fine-textured for a considerable distance from its intrusive margins on the northern side. As in the Felspathic Granite, there is a complete gradation from the non-porphyritic into the porphyritic type.

#### St. Peter's Dome

St. Peter's Dome is located in the Mount Rosa area of Colorado, in the southeastern part of the Precambrian Pikes Peak batholith, less than seven miles from its eastern contact with Paleozoic sediments. The geology of the Mount Rosa area is described by Gross and Heinrich (1965, 1966). The major petrologic units (all of Precambrian age) within this area are: the Pikes Peak granite and its fine-grained variants; the porphyritic granite; granitic dikes and aplites; the fayalitic granite; the Mount Rosa alkalic granite and its fine-grained equivalent dike phase; and the Windy Point granite, which occurs several miles to the northwest, but appears to be genetically related to the other alkalic granites (Gross and Heinrich, 1965).

These units were probably deposited in the following sequence: first, the Pikes Peak granite and the porphyritic granite, followed by the fayalite granite. Later, granitic, aplitic, and pegmatitic dikes of Pikes Peak derivation were emplaced. Then, the Windy Point granite, followed by the Mount Rosa granite. The youngest units appear to be the Mount Rosa-type pegmatites.

The dark, greenish-gray, medium-grained fayalite granite occurs primarily in the Pikes Peak granite, in ellipsoidal bodies ranging in size from a few feet in diameter to large lenticular bodies, 1000 feet wide and 2700 feet long. Most bodies are less than 100 feet wide and several hundred feet long. The total amount of fayalite granite is probably not more than one percent of the total volume of the Pikes Peak granite in the Mount Rosa area.

The fayalite granite shows a gradational contact with the Pikes Peak granite. At one contact zone the change from typical granite to fayalite granite takes place within less than a foot. As the proportion of quartz and microcline-perthite decreases from the Pikes Peak granite to the fayalite granite, the proportion of mafic minerals increases. Fayalite itself occurs only in specimens low in quartz.

Numerous small bodies of fayalite granite occur in the pegmatite swarm area of the St. Peter's Dome district. A large body and two smaller ones are associated with the Mount Rosa granite two miles northeast of Mount Rosa. These three bodies show brecciation in part and extensive hematite alteration along a fault zone. Contact relations between the fayalite granite and the Mount Rosa granite are obscured here because of the alteration, but where Mount Rosa-type pegmatites cut the fayalite granite, a 3 to 6 inch wide aplitic border zone composed of quartz, microcline, zircon, and abundant astrophyllite is commonly present.

The fayalite granite is a medium-grained, dark olive-green granite composed of essential quartz, antiperthite, microcline-perthite, plagioclase, biotite, and fayalite. Accessory minerals include allanite, zircon, apatite, hornblende, epidote, and fluorite. Chlorite, calcite, hematite, and antigorite are found as alteration products. The grain size

of the minerals ranges from 0.4 mm to 4.0 mm. Dark brown biotite, the chief mafic mineral, usually includes allanite and zircon, both with radioactive haloes. Other species in biotite are fayalite, apatite, and magnetite. Much of the biotite occurs in mafic clusters associated with fayalite and accessory minerals. Locally, a green hornblende is associated with biotite.

Fayalite, in subhedral to anhedral fractured grains, displays varying stages of alteration to hematite, antigorite, and calcite, and locally chlorite and magnetite. Uncommonly, a reaction rim bordering fayalite includes a pale-green sodic pyroxene, a blue sodic amphibole (riebeckite), and where adjacent to microcline-perthite, a red-brown biotite. The composition of the fayalite was estimated at  $Fo_{14.68}$ , by the method of Yoder and Sahama (1957). This estimate implies a quite different value of  $d_{130}$  than the one I observed (Table 10).

Two small swarms of pegmatite dikes occur in the Pikes Peak granite and its variants within the Mount Rosa area. These pegmatites belong to two principal types, the Pikes Peak-type, a calc-alkaline granitic type, and the Mount Rosa-type, an alkaline granitic type. The Mount Rosa-type pegmatites contain no fayalite (Gross and Heinrich, 1966).

Minerals occurring in the Pikes Peak-type pegmatites include quartz, microcline, albite (including cleavelandite), biotite, fluorite, allanite, fayalite, topaz, cassiterite ( $SnO_2$ ), zircon, yttriotantalite ( $(Y,U,Fe^{2+})(Ta,Nb)O_4$ ), phenacite ( $Be_2SiO_4$ ), chlorite, siderite, and hematite. Most of the pegmatitic rock is stained brown by hematitic and limonitic alteration. The presence of fayalite as a late mineral in these pegmatites is an important piece of evidence that links the Pikes Peak granite to the fayalite granite and strongly supports the idea that the

fayalite granite is a late-fractionated derivative of the Pikes Peak granite (Gross and Heinrich, 1966).

In the USGS Bulletin on the minerals of Colorado (Eckel, 1961), it is stated that a fayalite locality described by Hidden (1885) and Hidden and Mackintosh (1891) which they reported to be located on Cheyenne Mountain (not far from the Mount Rosa area), may in fact be from pegmatites located in the St. Peter's Dome area. Fayalite from this area is described (Hidden, 1885) as formed in large, anhedral masses, with color dark brownish-black. There is slight evidence of cleavage in two directions at right angles. The specific gravity is 4.35. It is found in quartz and granite in vugs, and is quite abundant. Masses of many pounds weight occur at one locality. The chemical analysis (Hidden and Mackintosh, 1891) is given in Table 6a. Hidden and Mackintosh state that iron may be present in both the ferrous and ferric states, but that this point was not determined, nor the reason for the low oxide total in the analysis. If their value for FeO is converted into Fe<sub>2</sub>O<sub>3</sub> and FeO, using the ferric/ferrous ratio calculated from Mössbauer peak areas, the oxide total may be brought up to a much higher value (Table 6b).

#### Sierra La Primavera

An extremely ferric-rich olivine has been found in several volcanic domes in the Sierra La Primavera, in Mexico (Mahood, 1980). This mineral has been determined to have a ferric/ferrous ratio of 2.07 (Carmichael, 1982), even higher than that of Chinese ferrifayalite or laihunite. Mahood referred to this mineral as Fe-deficient fayalite (as opposed to normal fayalite, which is also present), since microprobe analyses of this

Table 6.Hidden and Mackintosh's analysis of St. Peter's Dome (?) fayalite

a.	<u>wt. %</u>	b.	<u>wt. %</u>
SiO <sub>2</sub>	27.66	SiO <sub>2</sub>	27.66
FeO	65.794	Fe <sub>2</sub> O <sub>3</sub>	33.60
MnO	4.17	FeO	35.57
CaO	0.47	MnO	4.17
		CaO	0.47
Sum	<u>98.24*</u>	Sum	<u>101.47</u>

\*Hidden and Mackintosh's published total. Should be 98.09.

mineral, in which iron was calculated as FeO, were consistently found to have low oxide totals (93% to 96%), due to a ~7% decrease in FeO and ~0.4% decrease in MnO, only partially offset by a 2% increase in SiO<sub>2</sub> and a 0.1% increase in Al<sub>2</sub>O<sub>3</sub>.

The Fe-deficient fayalites, as collected from the Rio Salado dome, the Canon de Las Flores flow, the Mesa El Burro dome, and Mesa El Leon, are found in mildly peralkaline, high-silica rhyolites (comendites), which are aphyric or contain up to 15% phenocrysts. These phenocrysts are more than 97% -99% quartz and sodic sanidine. Usually ferrohedenbergite is the most abundant mafic phenocryst, with fayalite and ilmenite making up less than 0.1% of the rock. Ferrohedenbergite, fayalite, and ilmenite are typically found in the proportions 50:10:1. Minute quantities of titanomagnetite, zircon, apatite, and/or astrophyllite are found in only a few units.

Fayalite occurs as small, round, honey-colored grains, few larger than 0.2 mm in diameter. Most grains contain ilmenite inclusions and are rimmed by opaque alteration products. Also, most samples show fayalite of two populations, one normal and the other Fe-deficient. The Fe-deficient fayalite occurs both as rims on normal fayalite and as small separate grains. Intermediate compositions between normal and Fe-deficient fayalites are rare, and gradational zoning from one to the other is absent. Oxygen analyses, while not quantitative, show significant increases in the Fe-deficient rims, suggesting either the presence of ferric iron and/or hydration products.

In a sample from the Rio Salado dome, replacement of normal, honey-colored fayalite by decomposition products has led to nearly opaque grains which can be mistaken for ilmenite. All the fayalite from this dome, as well as that from Mesa El Leon, is the Fe-deficient type. This

suggests that the Fe-deficient fayalite is an oxidation product of normal fayalite, produced when conditions moved from the fayalite stability field (below the FMQ buffer) to a region where quartz and magnetite are stable due to an increase in oxygen fugacity and/or a decrease in temperature. Both conditions are likely as a lava moves towards the surface just prior to an eruption. Various geothermometers and barometers indicated a formation temperature for the observed mineral assemblage of between 655° and 977°C, and a  $\log f_{O_2}$  of -13.8.

Analyses of Fe-deficient fayalites are given in Table 7.

#### Berkeley synthetic

Recently, a possible artificially produced ferric-rich fayalite sample was produced in a drop calorimetry experiment performed at the Lawrence Berkeley Laboratory by Stebbins (Stebbins, 1983). The starting material consisted of about 1.5 grams of synthetic fayalite obtained from Bohlen at UCLA. The sample was sealed in a Pt-10%Rh crucible, isolated from the atmosphere. The final quench of the capsule was from 1615 K to room temperature.

Although there was no net gain or loss of weight in the sample, 8-9% Fe<sub>2</sub>O<sub>3</sub> was present in the sample at the end of the experiment. Stebbins (Stebbins, 1983) suggests that this ferric iron may have been produced in part by the absorption of iron by the crucible, which was found to contain iron at the end of the experiment.

The crushed sample from the capsule appears entirely black. In thin section the product was seen to contain fayalite, thin bladed grains of magnetite, and brownish patches which gave low oxide totals under

Table 7.Carmichael's chemical analyses of Fe-deficient fayalites from Mexico

<u>wt.%</u>	<u>1</u>	<u>2</u>	<u>3</u>
SiO <sub>2</sub>	31.52	31.37	31.93
TiO <sub>2</sub>	0.02	0.01	0
Al <sub>2</sub> O <sub>3</sub>	0.11	0.08	0.13
FeO	59.05	59.87	58.44
MnO	2.83	2.9	2.86
MgO	0.26	0.13	0.14
CaO	0.28	0.20	0.19
Na <sub>2</sub> O	0	0	0
	<hr/>	<hr/>	<hr/>
Sum	94.07	94.56	94.69
%FeO (as opposed to Fe <sub>2</sub> O <sub>3</sub> )	19.2	15.6	14.5

Table 8.Harris' microprobe analysis of Berkeley synthetic

FeO	61.24
SiO <sub>2</sub>	34.19
	<hr/>
Sum	95.43

microprobe analysis (Table 8) and seem to have the composition of laihunite, if the deficit in the oxide total is assumed to be the amount of  $\text{Fe}_2\text{O}_3$  reported as  $\text{FeO}$ . The total  $\text{Fe}_2\text{O}_3$  in the sample cannot be accounted for by the amount of magnetite present. One crystal was found which, when X-rayed, showed the cell parameters and double spots of laihunite. Therefore, it appears quite likely that laihunite is present, but it is not absolutely certain (Stebbins, 1983).

Chapter 5Experimental Procedure

After the initial discovery of ferric iron in the sample of fayalite from the Mourne Mountains, a search for other similar samples was begun. A sample of ferrifayalite was requested (and later received) from Dr. Ruyuan Zhang, of the Academia Sinica, Beijing. At the same time, requests were sent to several well-known museums for samples of dark to black fayalites. A total of ten samples were eventually examined in this study. These samples, and their sources, are listed in Table 9.

All samples were ground, examined under a microscope, and hand-picked where necessary. Magnetite was separated out with a hand magnet. Samples to be examined by Mössbauer spectrometry were then mixed with sugar and ground under acetone to prevent oxidation during grinding. Samples of fayalite were weighed before mixing with the sugar such that all samples contained approximately  $8 \text{ mg/cm}^2$  of iron.

Mössbauer spectra at room temperature were taken on an Austin Sciences Associates spectrometer. The gamma ray source consisted of  $^{57}\text{Co}$  diffused into either Pd or Rh foils having activities of 50 - 100 mc. In general, baseline counts exceed one million. Spectra were calibrated against metallic Fe foil standards. Mössbauer parameters were determined by computer analysis with the program developed by Stone et al. (1971).

All samples were checked at a wide velocity range for the presence of magnetite or other magnetic phases which would produce a hyperfine sextet spectrum, and in all cases such evidence was not observed in room temperature spectra. This indicates that the fayalite samples did not

Table 9.

Samples examined, localities, and museum sources

<u>Sample</u>	<u>Locality</u>	<u>Source</u>
fayalite	Babson farm quarry, Rockport, Essex Co. MA (Palache, 1950)	Harvard Mineralogical Museum
ferrifayalite	Qianan County, China (Laihunite Research Group, 1976)	Dr. Ruyuan Zhang, Academica Sinica
fayalite	Mourne Mountains, Ireland (Richey, 1927; Nockolds and Richey, 1939)	Prof. Roger Burns, MIT
fayalite	Cuddia Mida, Pantelleria, Italy (Soellner, 1911; Washington, 1913)	Harvard Mineralogical Museum
fayalite	St. Peter's Dome, CO (Gross and Heinrich, 1965,1966; Hidden and Mackintosh, 1891)	Harvard Mineralogical Museum
fayalite(?)	Utteawig, North Tunaberg, Sweden	Harvard Mineralogical Museum
fayalite	artificial (from slag)	Harvard Mineralogical Museum
fayalite	Hilläng, Ludvika, Dalarne, Sweden	British Museum of Natural History
fayalite	Schisshyttan, Värmland, Sweden	British Museum of Natural History
fayalite	Red Rock Ridge, Nevy Fiord, Marguerite Bay, Palmer Peninsula, Antarctica	Harvard Mineralogical Museum

contain magnetite impurities in amounts of a percent or more, unless those impurities were of ultrafine grain size. In this case a superparamagnetic doublet spectrum would be produced, instead of the hyperfine sextet.

Spectra of all samples were then run at room temperature and at lower temperature ( $\sim 125$  K). The room temperature spectra, shown in Figure 1 and Figure 6a-h, indicate clearly the presence of ferric iron in four cases: Mourne Mountains fayalite, Qianan Co. ferrifayalite, and St. Peter's Dome and Pantelleria fayalites. The 125 K spectra were produced using the same system, with the sample cooled by exposing it to a cold finger inserted into a dewar of liquid nitrogen (77 K). The estimate of 125 K as the temperature is approximate, based partly on observations of magnetite spectra taken at this temperature, which do not appear to have passed below the Verwey transition at  $\sim 119$  K. Spectra of the ferric-rich fayalites at 125 K are shown in Figure 7a-e.

The ferric-rich fayalites were then studied in greater detail, the normal ferrous fayalites being excluded from further measurements (with the exception of Rockport fayalite, used as a standard throughout). X-ray powder diffraction spectra were taken of the ferric-rich fayalites and Rockport fayalite. These spectra were taken on the GE Diano No. 1 and No. 2 diffractometers belonging to the Department of Materials Science and Engineering at M.I.T. All samples were mixed with fluorite as an internal standard and mounted on glass slides. Chromium  $K\alpha$  radiation was used. Cell parameters and unit cell volumes were calculated from X-ray Diffraction spectra by means of a computer program modified from the one written by Burnham (1962). Tabulated spectra are listed in Table 10, and cell parameters are listed in Table 11.

Rockport fayalite and the four ferric-rich fayalites were also

Figure 6a - Room temperature Mössbauer spectrum of Pantelleria fayalite.

Figure 6b - Room temperature Mössbauer spectrum of St. Peter's Dome  
fayalite.

Figure 6c - Room temperature Mössbauer spectrum of North Tunaberg  
fayalite.

Figure 6d - Room temperature Mössbauer spectrum of artificial fayalite.

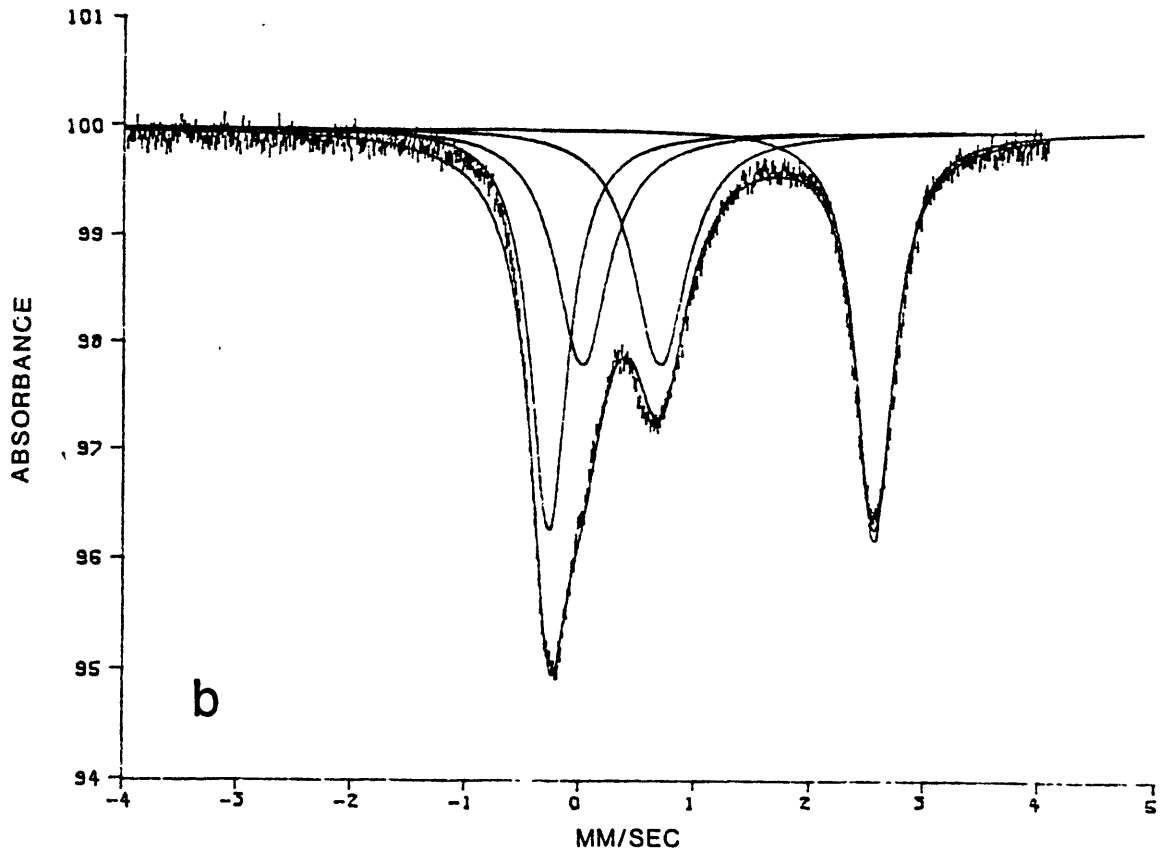
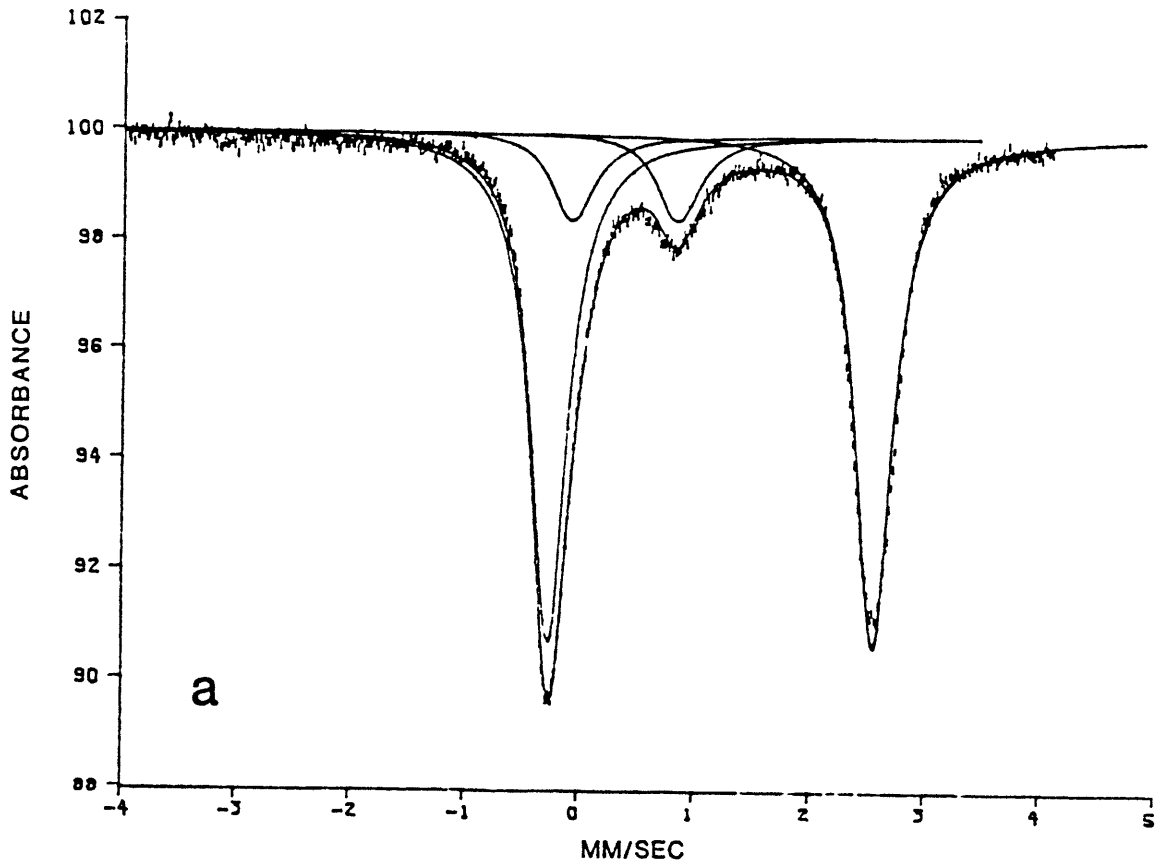
Figure 6e - Room temperature Mössbauer spectrum of Hilläng fayalite.

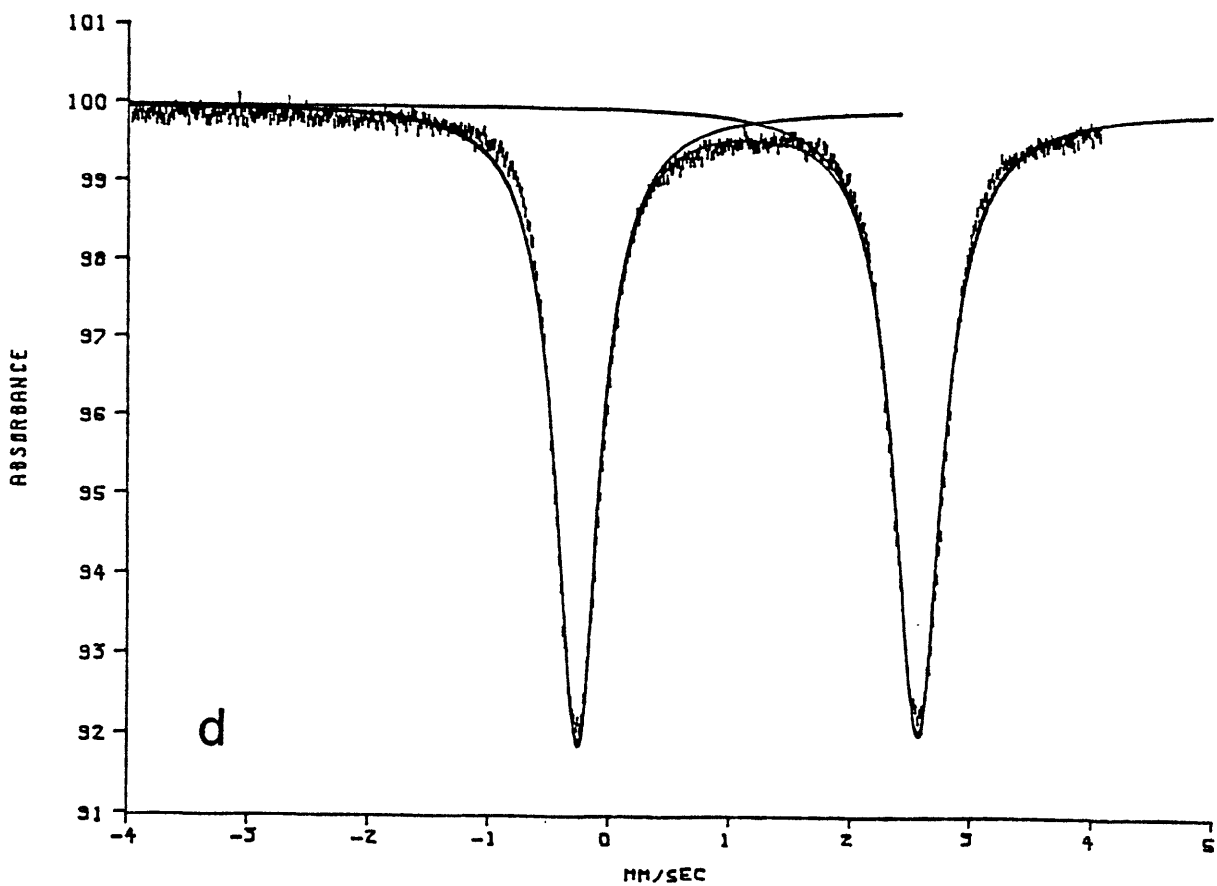
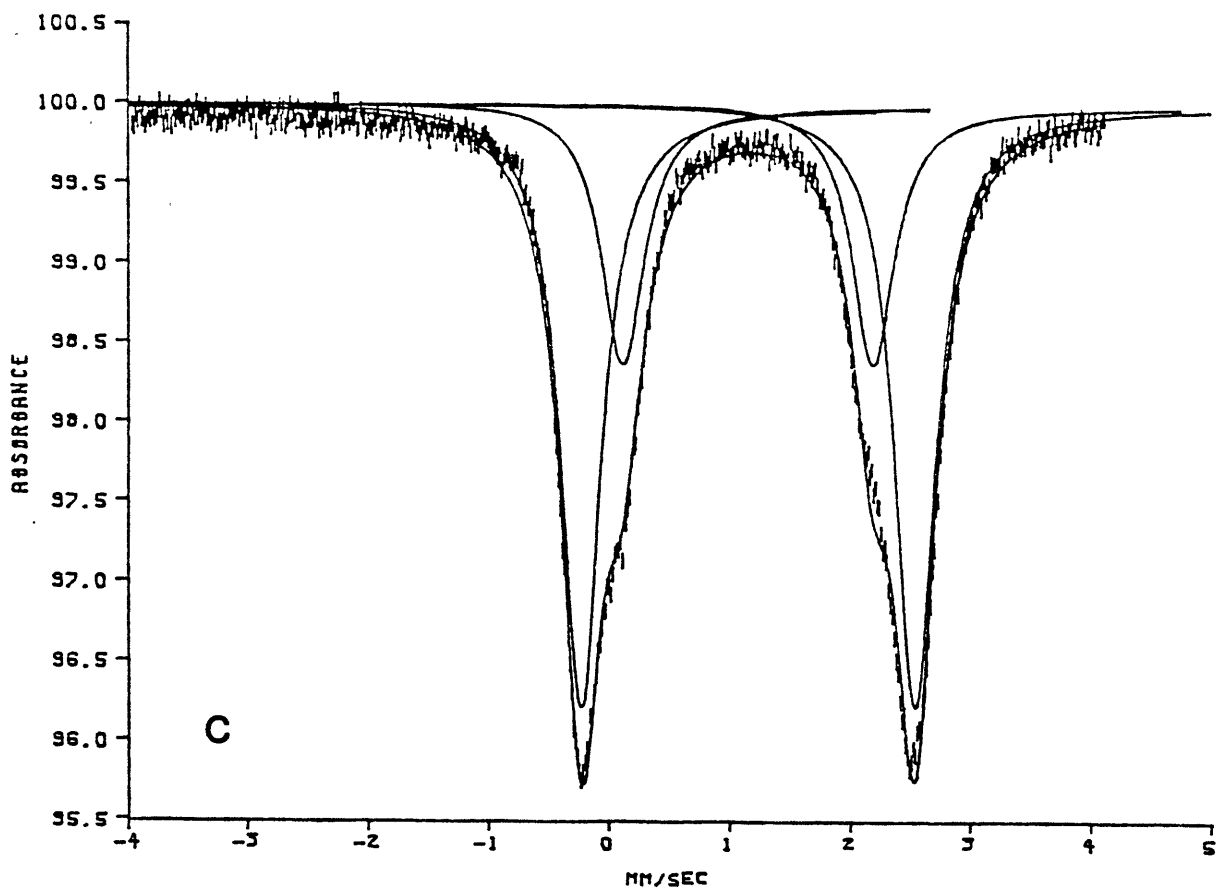
Figure 6f - Room temperature Mössbauer spectrum of Värmland fayalite.

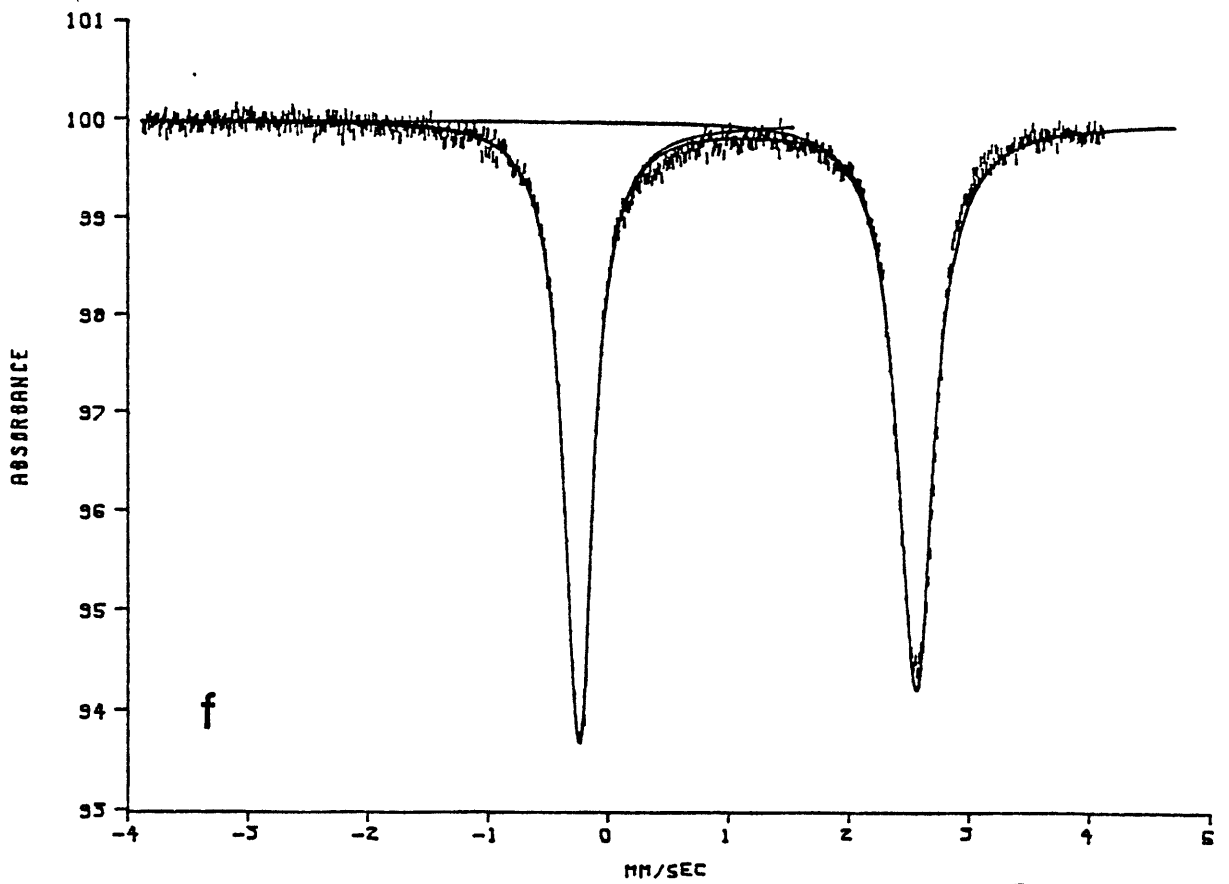
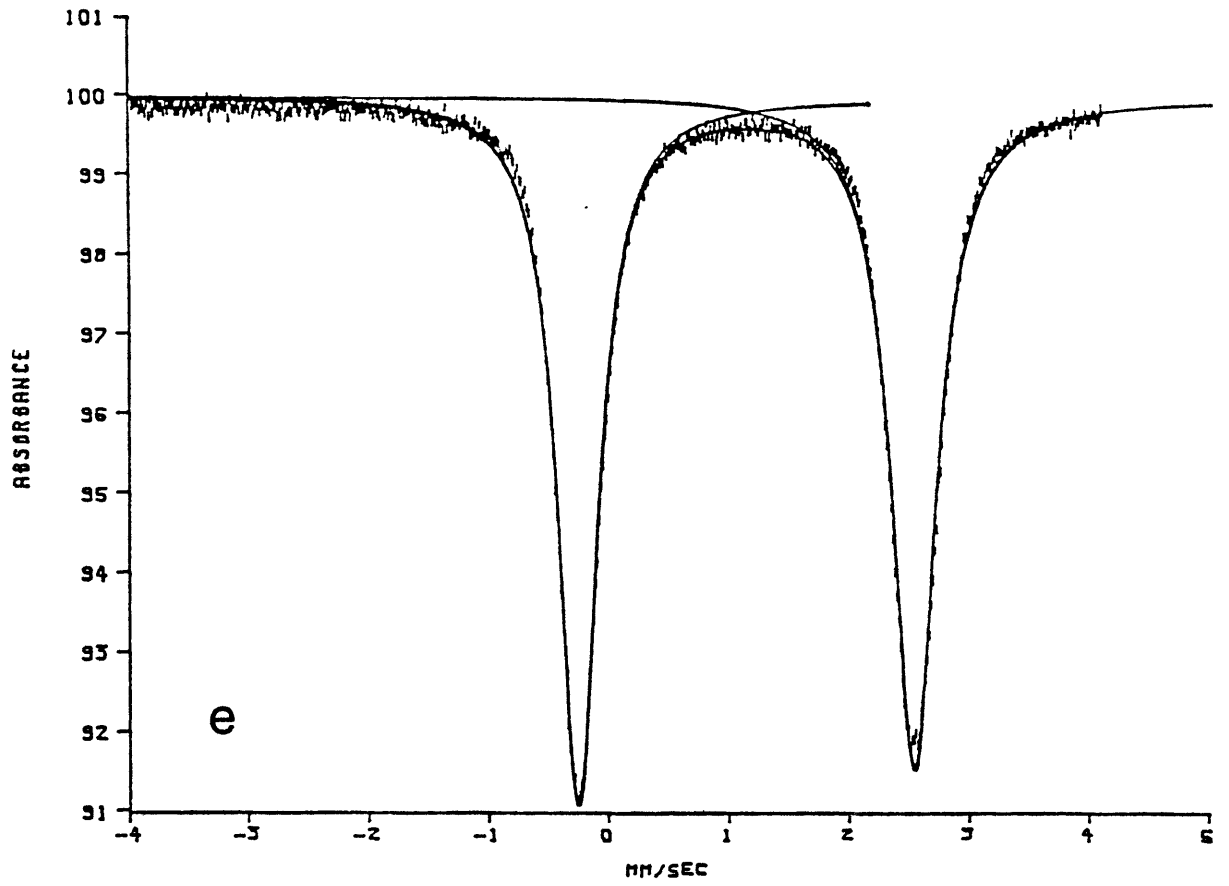
Figure 6g - Room temperature Mössbauer spectrum of Qianan County  
ferrifayalite.

Figure 6h - Room temperature Mössbauer spectrum of Palmer Peninsula  
fayalite.

These spectra were fit with the program described by Stone et  
al. (1971).







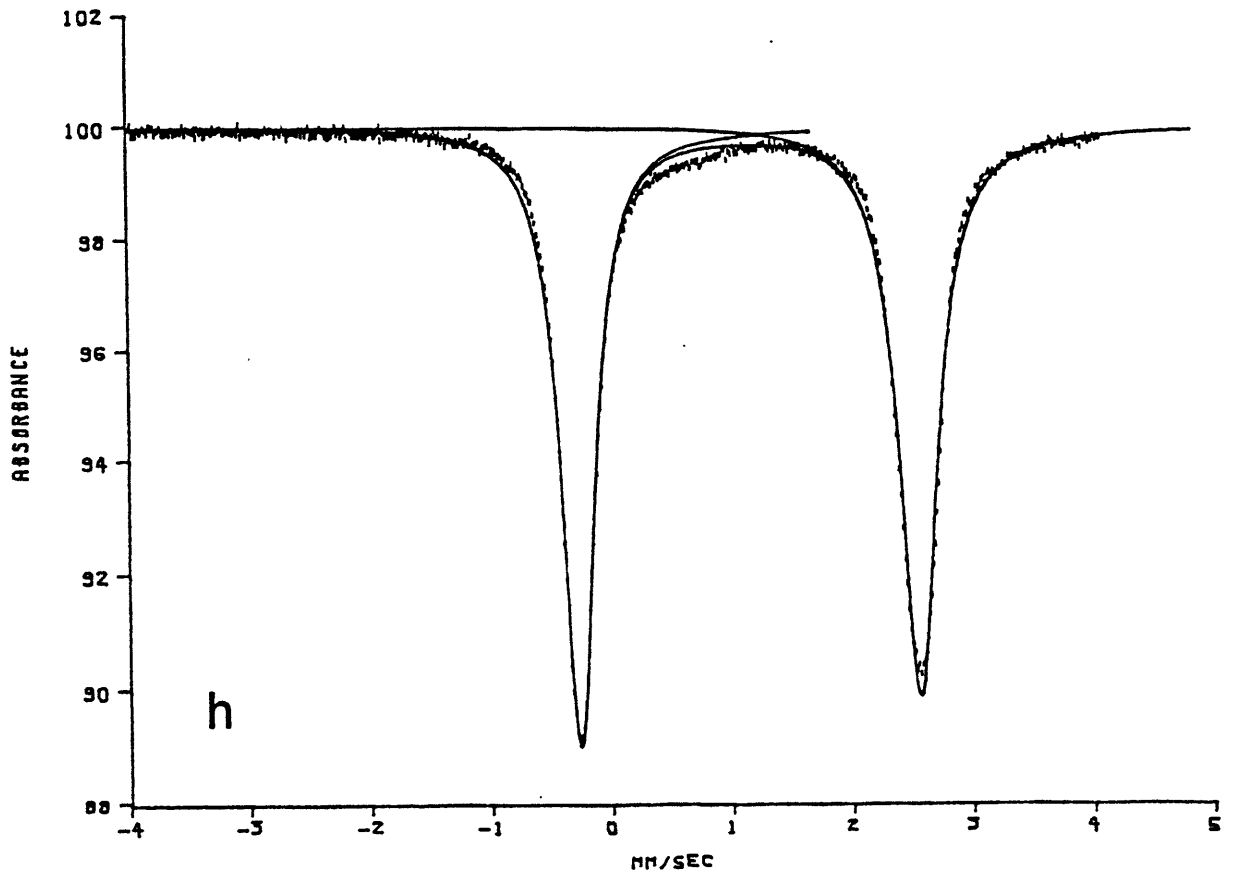
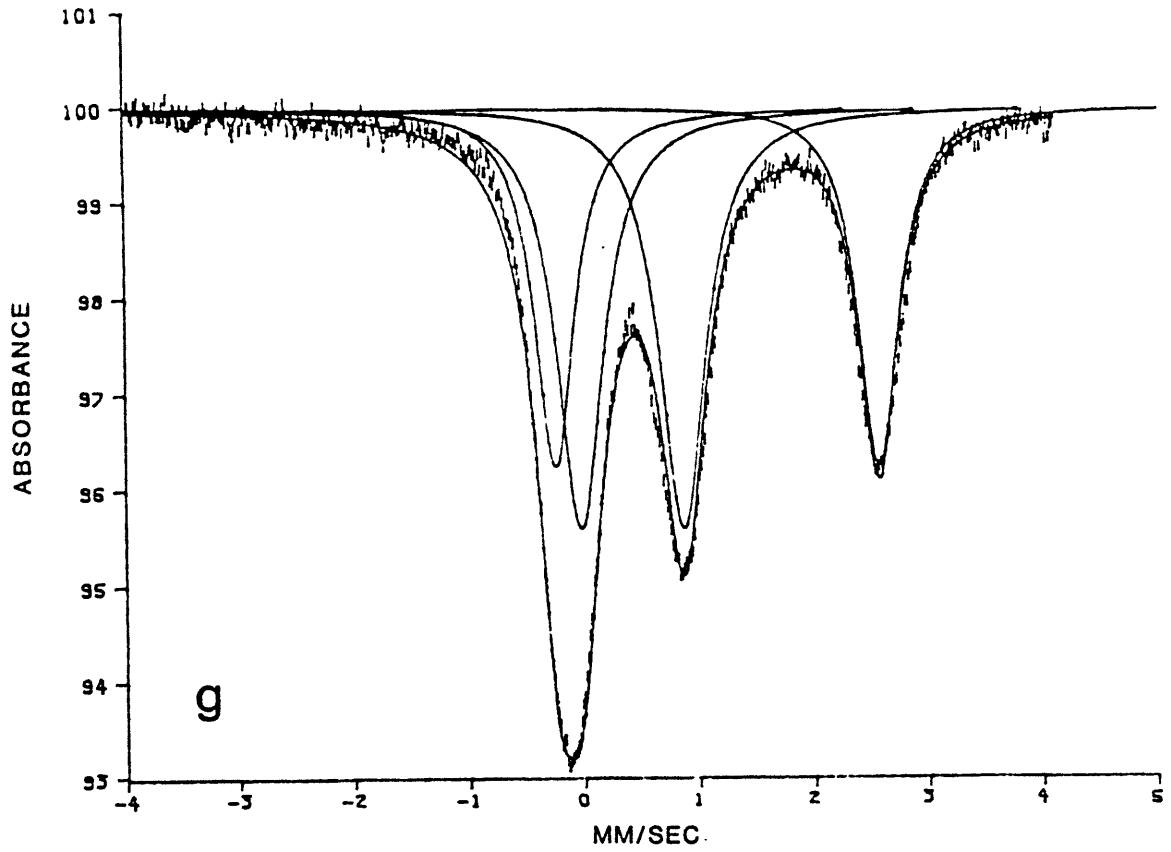


Figure 7a - 125 K Mössbauer spectrum of Rockport fayalite.

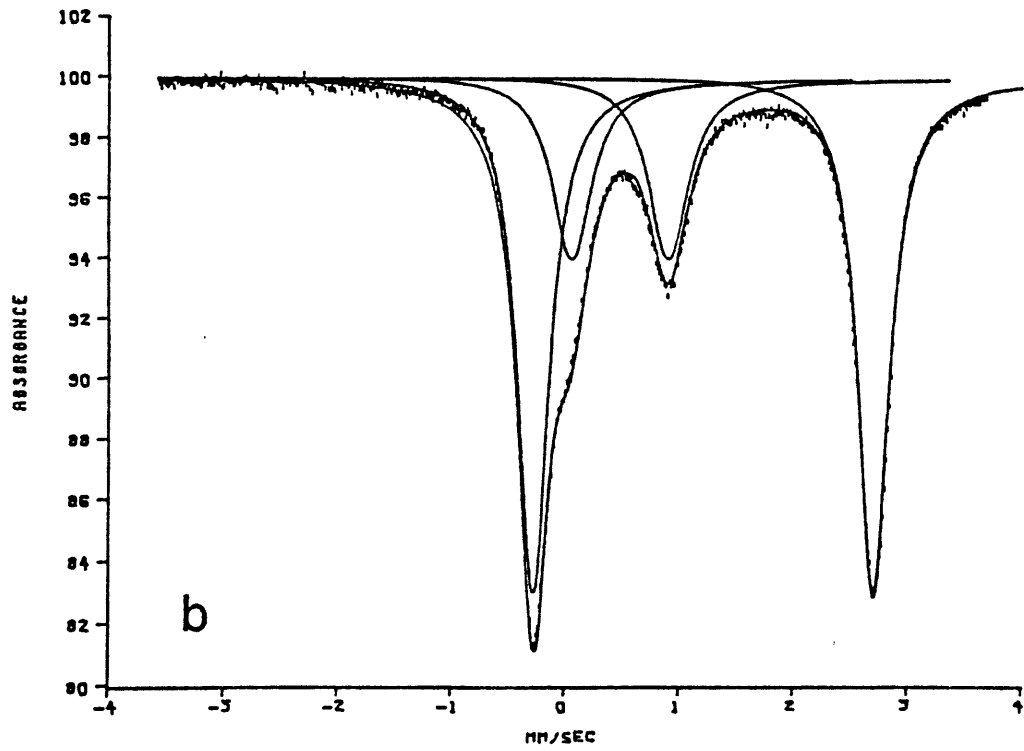
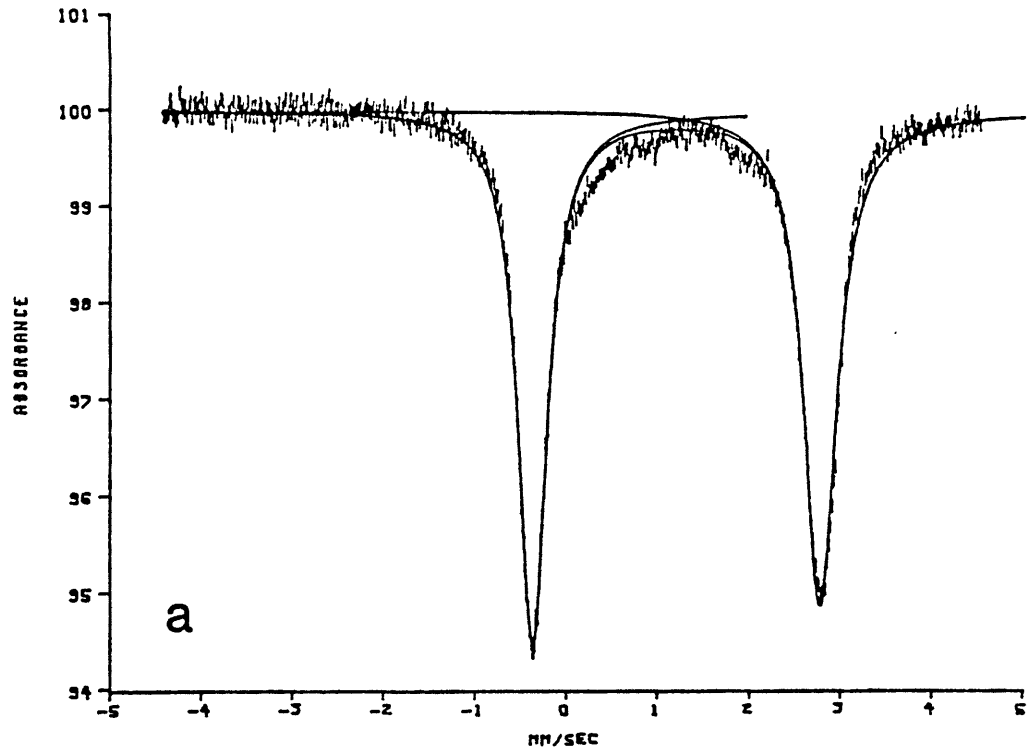
Figure 7b - 125 K Mössbauer spectrum of Mourne Mountains fayalite.

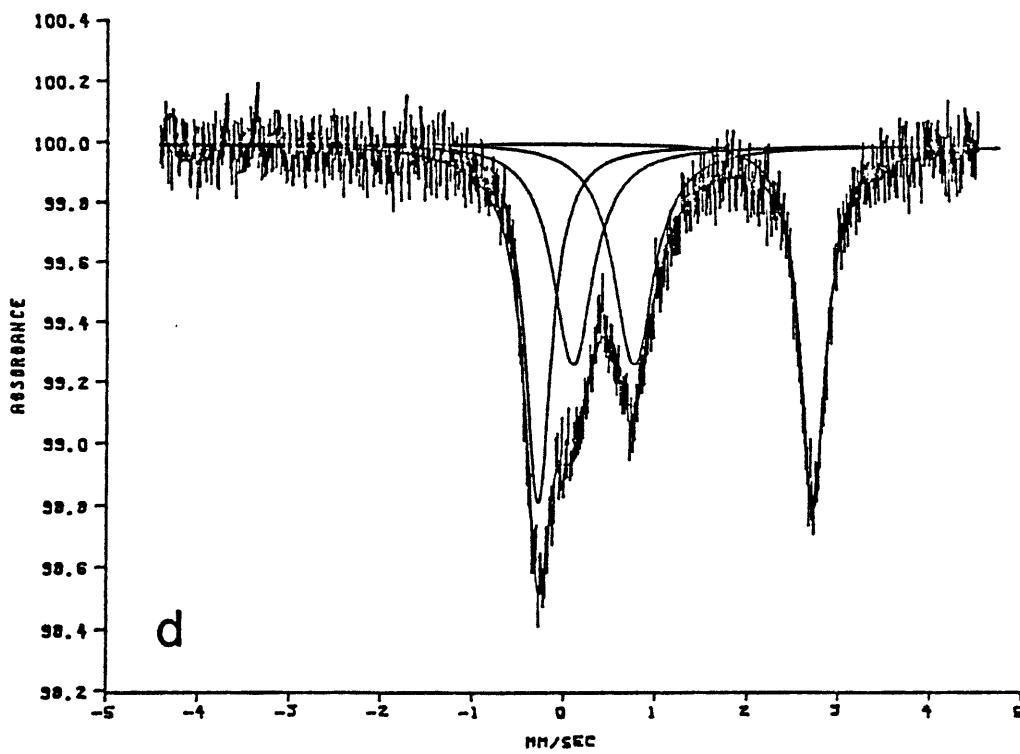
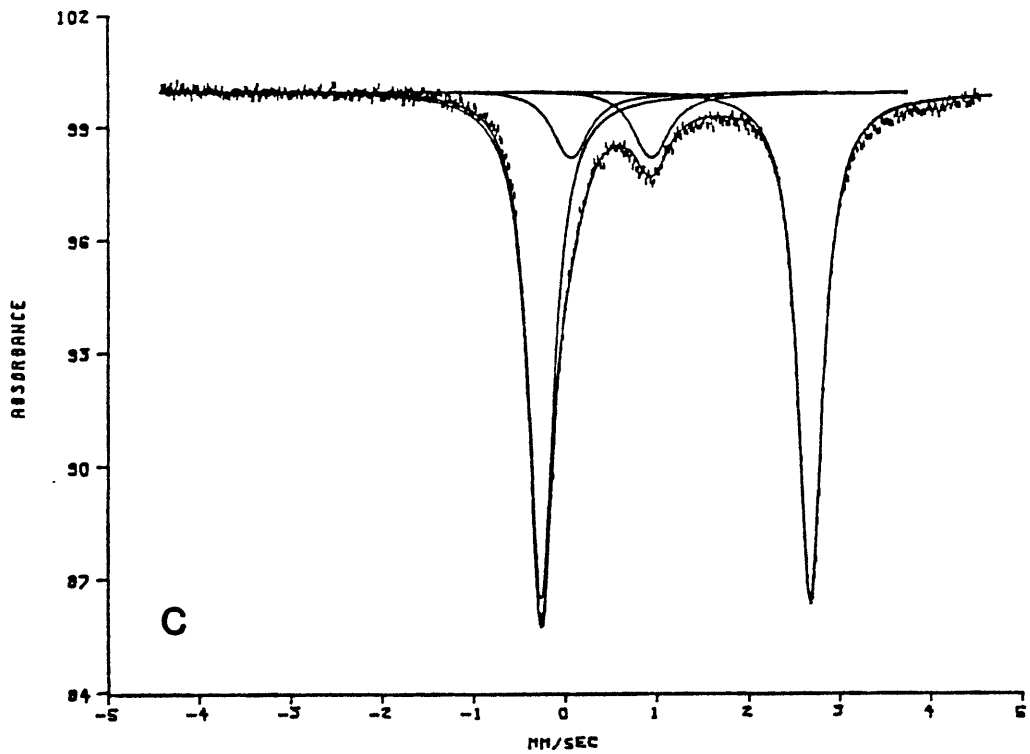
Figure 7c - 125 K Mössbauer spectrum of Pantelleria fayalite.

Figure 7d - 125 K Mössbauer spectrum of St. Peter's Dome fayalite.

Figure 7e - 125 K Mössbauer spectrum of Qianan County ferrifayalite.

These spectra were fit with the program described by Stone et al. (1971).





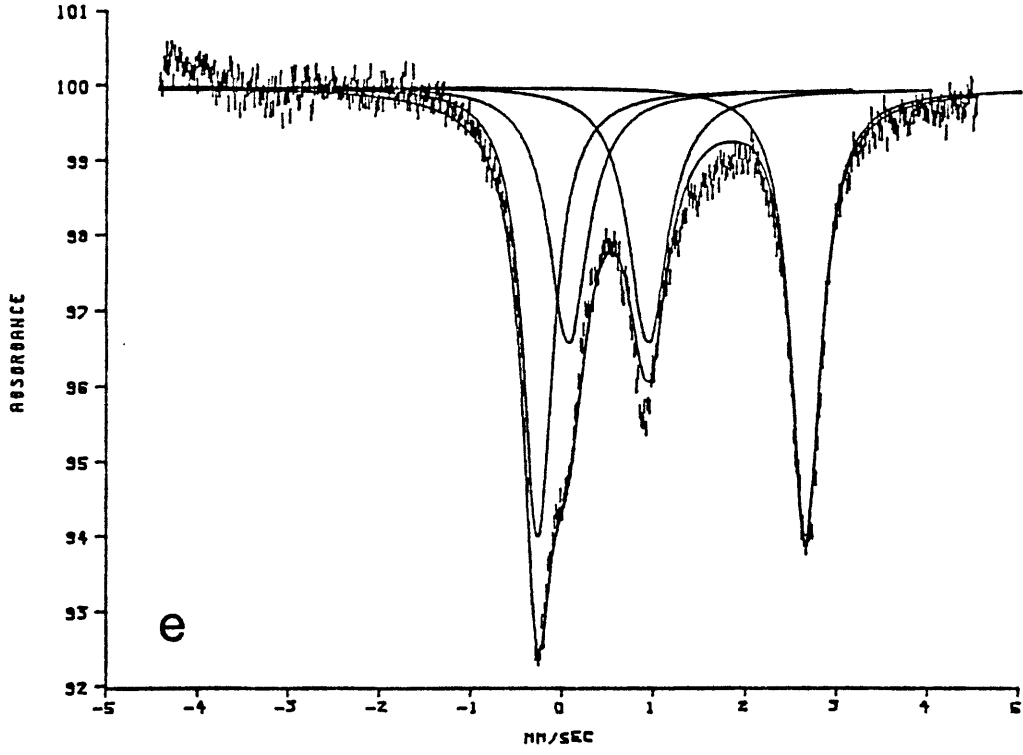


Table 10. X-ray powder diffraction spectra of my ferric-rich fayalites and Rockport fayalite

Rockport			Mourne Mountains			Pantelleria			St. Peter's Dome			Qianan County A			Qianan County B
d	I/I <sub>0</sub>	hkl	d	I/I <sub>0</sub>	hkl	hkl									
5.266	33	020	3.552	58	111	5.899	24		5.266	21	020	5.699	54		100
4.748	15		2.834	75	130	5.673	40		3.998	21	021	4.983	27	020	002
3.996	15	021	2.801	58		4.833	28		3.562	42	111	4.807	29		
3.562	52	111	2.629	33	022	3.037	28	002	2.844	100	130	3.455	100		111
3.389	48		2.560	58	131	2.814	52		2.651	46	022	2.885	73		200
3.301	19		2.504	100	112	2.629	16	022	2.632	67	040	2.785	77	130	013
3.091	26	002	2.454	50	200	2.573	12	131	2.576	67	131	2.615	27	022	
2.833	100	130	2.411	33	041	2.551	12		2.502	71	112	2.534	84	131	202
2.632	30	022	2.350	25	210	2.490	28	112	2.417	21	200	2.500	84		
<del>2.572</del>	<del>59</del>	<del>131</del>	<del>2.304</del>	<del>25</del>	<del>122</del>	<del>2.405</del>	<del>12</del>	<del>200</del>	<del>2.312</del>	<del>67</del>	<del>122</del>	<del>2.499</del>	<del>59</del>	112	113
2.498	89	112	2.280	42		2.305	20	122	1.774	58	222	2.347	23	210	104
2.408	19	200	2.246	25		2.080	12	132	1.677	25	061	2.246	41		014
2.309	26	122	2.189	25	211	1.778	16	222	1.517	58	004	2.207	16	211	022
2.190	15	211	2.129	33		1.706	8	241				1.752	41	222	024
1.779	56	222	1.778	67	222	1.697	8					1.653	36	133	124
1.705	11	241	1.760	33	240	1.610	8	043				1.581	18	310	304
1.680	30	061	1.673	33	061	1.526	100	004				1.456	50	330	401
1.627	19	152	1.541	50	311	1.516	24	062							
1.523	37	004				1.496	12	321							
1.516	44	062				1.434	48	331							

Qianan County A is indexed according to the Rockport indexing. Qianan County B is indexed according to ferrifayalite. Lines for which no indexing is given are of unknown source.

Table 11. Cell parameters of my ferric-rich fayalites and Rockport fayalite

	<u>Rockport</u>	<u>Mourne Mountains</u>	<u>Pantelleria</u>	<u>St. Peter's Dome</u>	<u>Qianan County A</u>	<u>Qianan County B</u>
a	4.81859 ± 0.00797	4.83446 ± 0.01128	4.85022 ± 0.0933	4.82933 ± 0.01337	4.81488 ± 0.01668	4.80690 ± 0.05755
b	10.49203 ± 0.01229	10.43096 ± 0.03238	10.49723 ± 0.03323	10.50028 ± 0.01998	10.21216 ± 0.11513	10.11957 ± 0.12114
c	6.10023 ± 0.00736	6.08356 ± 0.03230	6.09557 ± 0.01313	6.07552 ± 0.0975	6.11578 ± 0.04369	5.85423 ± 0.03985
γ	90	90	90	90	90	91.73983 ± 1.18701
v	308.4080 ± 0.5653	306.7820 ± 1.5506	310.3492 ± 0.9396	308.0854 ± 0.9580	300.7148 ± 2.7687	284.6403 ± 3.8359

69

examined by electron microprobe microanalysis, to obtain chemical compositions. Samples (powder or small crystal fragments) were mounted in epoxy in brass sample holders and carbon coated. Analysis of samples was performed on a rebuilt, semi-automated MAC Model 5 Series electron microprobe/scanning electron microscope with Canberra and Tracor/Northern peripherals. Data were analyzed by computer using a program based on the Bence-Albee data reduction method (Bence and Albee, 1968). Analyses are listed in Table 5.

Low temperature (down to 4.2 K) Mössbauer spectra were also taken of Rockport fayalite and the four ferric-rich specimens. These spectra were run at the Bitter National Magnet Lab on a Mössbauer spectrometer which uses a Ranger drive and multi-channel analyzer and Janis Corporation cryogenics. Samples were cooled by a spray of liquid nitrogen or liquid helium, depending on the temperature desired, and temperature was monitored by a thermocouple, which also supplied EMF to a controller used to supply signal to a heating element. The gamma ray source consisted of  $^{57}\text{Co}$  electroplated onto Rh, with an activity of about 100 mc. Spectra were calibrated against metallic Fe foil standards.

Rockport fayalite and the four ferric-rich fayalites were photographed by backscattered electrons under a scanning electron microscope (SEM). Samples mounted for the microprobe were used. The SEM used was an International Scientific Instruments Model DS130 with a Robinson backscattered electron detector.

In addition to the above work, one sample (St. Peter's Dome) was examined by transmission electron microscopy (TEM) for evidence of phases other than fayalite.

Chapter 6Room temperature Mössbauer spectra

Mössbauer spectra were run at room temperature of all fayalite samples to determine which contained ferric iron either as magnetite or hematite impurities, or as part of their crystal structure. A doublet produced by ferric iron in octahedral coordination was seen in the spectra of four samples: Qianan County ferrifayalite, and fayalites from Mourne Mountains, Pantelleria, and St. Peter's Dome. This doublet was superimposed on the doublet produced by ferrous iron in octahedral coordination, which is characteristic of ordinary fayalite. Spectra of ferric-rich fayalites, with Rockport fayalite for comparison, are seen in Figures 1 and 6. Ferric/ferrous ratios based on the ratios of the peak areas in these spectra (assuming equal recoil-free fractions for ferric and ferrous iron) are listed in Table 12. Observed center shifts and quadrupole splittings are listed for all samples in Table 13.

All ferrous center shifts range about the value of 1.167 mm/sec calculated for Rockport fayalite. Quadrupole splittings for the ferrous peaks of the ferric-rich fayalites are typically a bit higher than that for Rockport fayalite, perhaps indicating a greater octahedral site distortion. Ferric center shifts range between 0.374 and 0.431 mm/sec, and the ferric peaks are somewhat broader than the ferrous ones, particularly in the St. Peter's Dome spectrum. There is some variation in the ferric quadrupole splitting of the samples. Qianan County ferrifayalite and the fayalites from Mourne Mountains and Pantelleria have similar quadrupole splittings, while the quadrupole splitting for St.

Table 12.Ferric/ferrous ratios of samples, based on Mössbauer peak areas

<u>Sample locality</u>	<u>Ferric/ferrous ratio</u>
Rockport, MA	0
Qianan County, China	1.38
Mourne Mts, Ireland	0.46
Pantelleria, Italy	0.19
St. Peter's Dome, CO	0.85
N.Tunaberg, Sweden	0
artificial (from slag)	0
Hilläng, Sweden	0
Värmland, Sweden	0
Palmer Peninsula, Antarctica	0

Table 13.

Room temperature center shifts and quadrupole splittings  
of all samples (in mm/sec)

<u>Locality</u>	<u>Ferrous Peaks</u>				<u>Ferric Peaks</u>			
	<u>C.S.</u>	<u><math>\sigma</math></u>	<u>Q.S.</u>	<u><math>\sigma</math></u>	<u>C.S.</u>	<u><math>\sigma</math></u>	<u>Q.S.</u>	<u><math>\sigma</math></u>
Rockport	1.1667	0.0075	2.8077	0.0084	-----	-----	-----	-----
Qianan Co.	1.1687	0.0040	2.8129	0.0046	0.4312	0.0036	0.8893	0.0019
Mourne Mts.	1.1573	0.0021	2.8164	0.0026	0.4071	0.0025	0.8523	0.0032
Pantelleria	1.1541	0.0039	2.8202	0.0044	0.3843	0.0043	0.9123	0.0048
St. Peter's Dome	1.1657	0.0040	2.8349	0.0046	0.3740	0.0040	0.6785	0.0030
N. Tunaberg	1.1571	0.0040	2.7698	0.0048	-----	-----	-----	-----
	1.1519	0.0042	2.0676	0.0063	-----	-----	-----	-----
artificial	1.1656	0.0039	2.8240	0.0044	-----	-----	-----	-----
Hilläng	1.1507	0.0039	2.7910	0.0043	-----	-----	-----	-----
Värmland	1.1694	0.0075	2.7987	0.0083	-----	-----	-----	-----
Palmer Peninsula	1.1582	0.0039	2.8233	0.0044	-----	-----	-----	-----

Peter's Dome is significantly less: 0.678 as opposed to  $\sim 0.885$  mm/sec.

In addition to the normal and ferric-rich fayalites observed, one sample was found to have a very anomalous Mössbauer spectrum. This sample, fayalite from North Tunaberg, Sweden, was seen to have two ferrous doublets in its spectrum. This sample is probably not an olivine at all.

Low temperature ( $\sim 125$  K) spectra were also taken of the four ferric-rich fayalites and Rockport fayalite (Figure 7a-e). In the ferric-rich spectra, the ferric/ferrous ratio based on peak area ratios appeared to decrease at the lower temperature. This is an artifact brought on by two causes. First, the ferric-rich fayalites undergo a transition in the temperature range of about 100-150 K, in which the ferric doublet splits to form a hyperfine sextet. This transition will be more fully discussed in the section on low temperature spectra. Second, the 125 K spectra were taken at a velocity range of -4 to +5 mm/sec, at which setting it is difficult to observe the hyperfine sextet superimposed on the existing quadrupole spectrum.

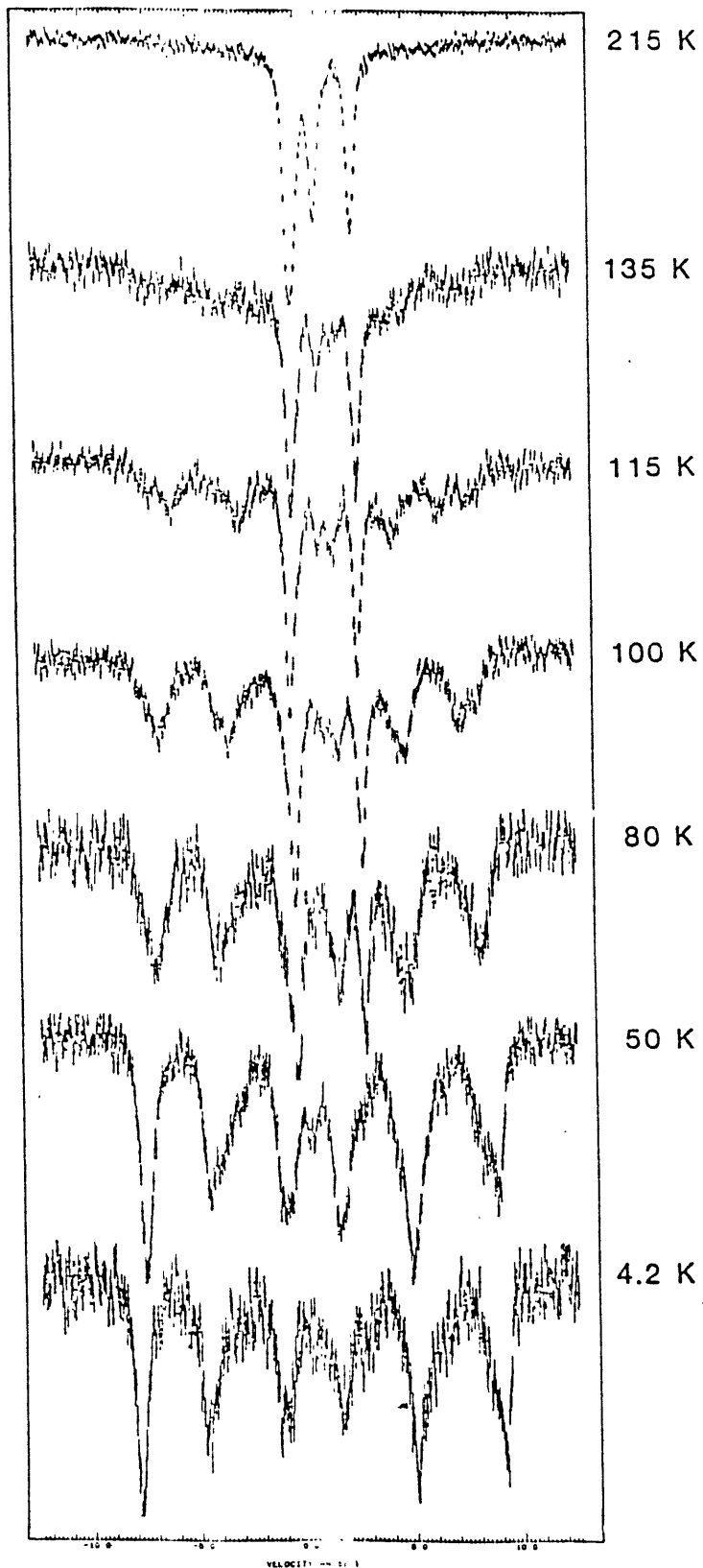
#### Low temperature Mössbauer spectra

Spectra were taken of Rockport fayalite and the four ferric-rich fayalites at temperatures ranging from 4.2 K to 215 K. Most attention was paid to the sample of ferrifayalite from Qianan County, which exhibited the highest ferric/ferrous ratio of the samples available. A plot of the variation of this spectrum with temperature is shown in Figure 8.

Two transitions are seen, one at about 100-150 K, and the other at about 50-80 K. Both of these transitions are very broad, and, due to the complexity of the low temperature spectrum, it is difficult to make

Figure 8 - Change in Qianan County ferrifayalite Mössbauer spectrum with temperature.

Qianan ferrifayalite



accurate estimates of the temperature ranges of the transitions. The resulting spectrum at very low temperatures bears almost no superficial resemblance to the traditional fayalite spectrum, having as its dominant characteristic a somewhat diffuse six-line pattern. In reality, this pattern is probably composed of a superposition of up to thirty-four lines! It was decided to be impossible to obtain a good computer fit to a spectrum of such complexity.

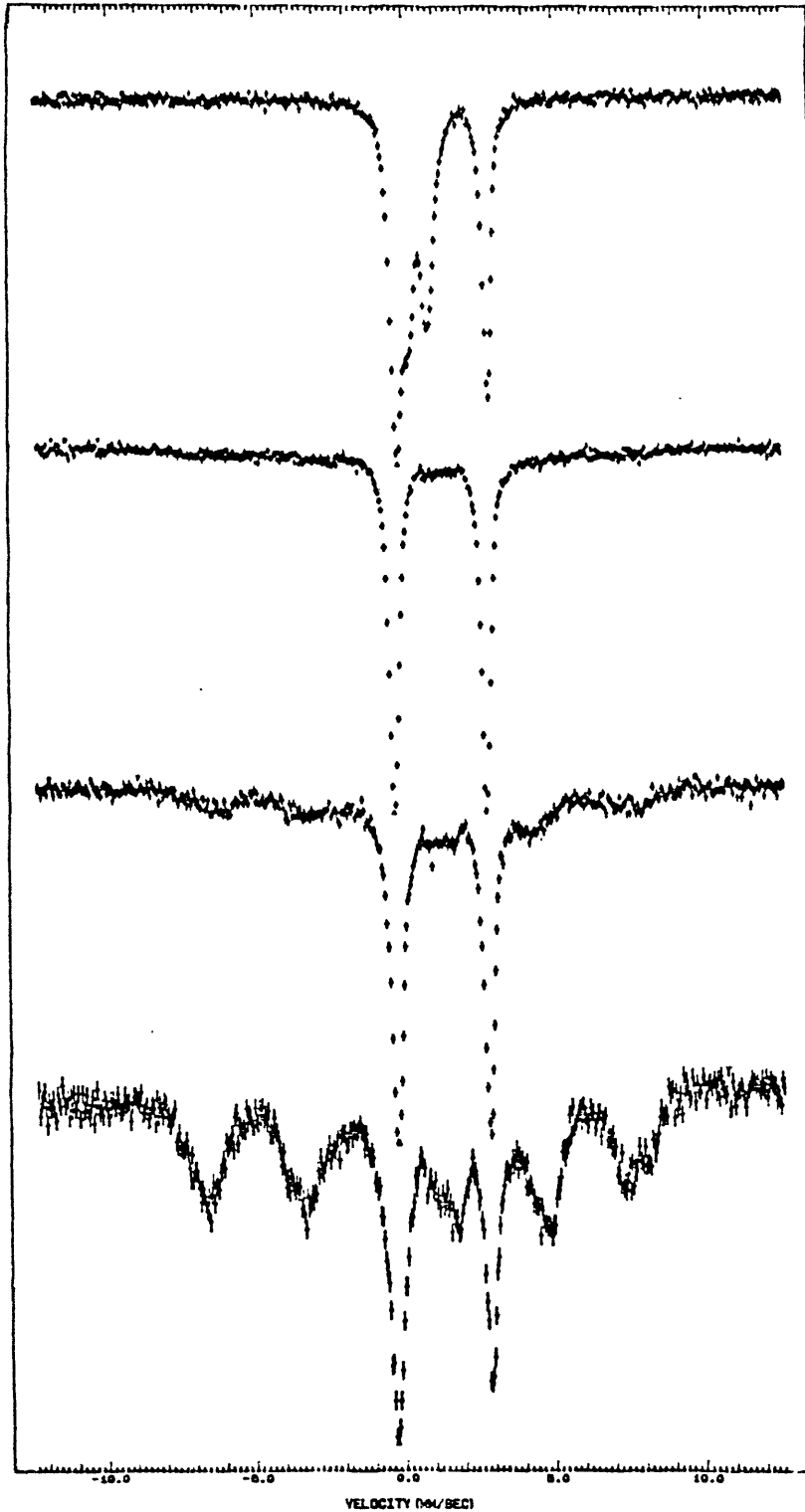
The high temperature transition appears to concern only the ferric doublet, and involves the gradual disappearance of this doublet, to be replaced by a hyperfine sextet, or perhaps two almost completely superimposed sextets, similar to the room temperature spectrum of magnetite. The lower temperature transition involves the gradual disappearance of the ferrous doublet as well, and its replacement by what appears to be yet another hyperfine sextet. In addition, it is possible to detect the appearance of the normal low temperature fayalite spectrum, mostly in the form of shoulders on the more prominent six-line pattern.

Spectra of Mourne Mountains fayalite and Pantelleria fayalite appear very similar to that of Qianan County ferrifayalite (Figures 9, 10 and 11). The chief difference seems to be merely the proportion of ferric to ferrous iron in the sample. The samples with less ferric iron show spectra in which the normal fayalite pattern is much more easily observed than in the Qianan ferrifayalite spectrum. Reference spectra of Rockport fayalite were taken, which were similar in appearance to previously published spectra (Kundig et al., 1967).

One sample, from St. Peter's Dome, was very different in appearance from Qianan County ferrifayalite at low temperatures, even though at room temperature it appeared more or less the same. No transition was observed

Figure 9 - Mössbauer spectra of ferric-rich fayalites at 100 K.

# 100 K



St. Peter's  
Dome

Pantelleria

Mourne Mts.

Qianan

VELOCITY (CM/SEC)

Figure 10 - Mössbauer spectra of ferric-rich fayalites and Rockport fayalite at 55 K.

# 55 K

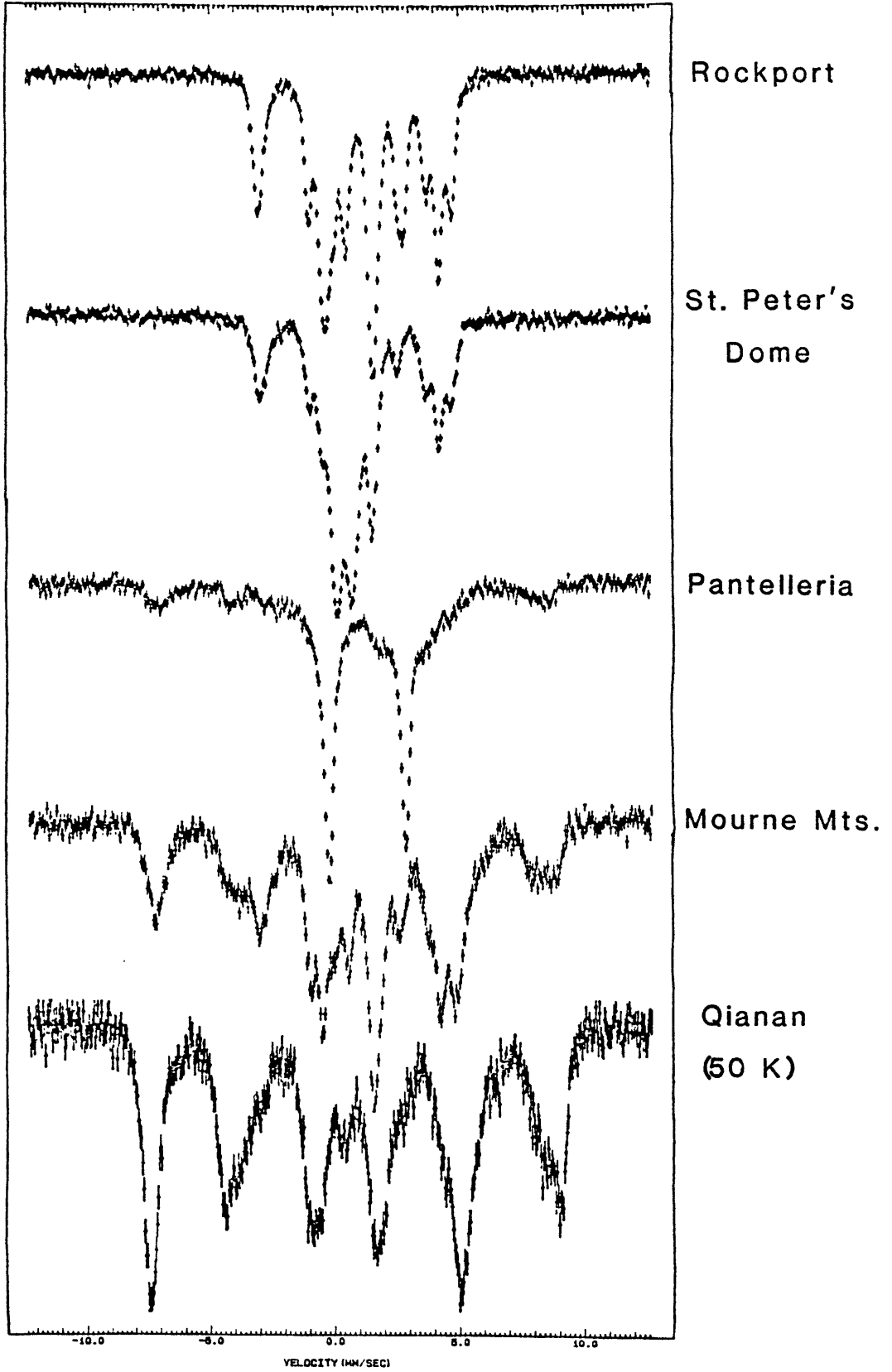
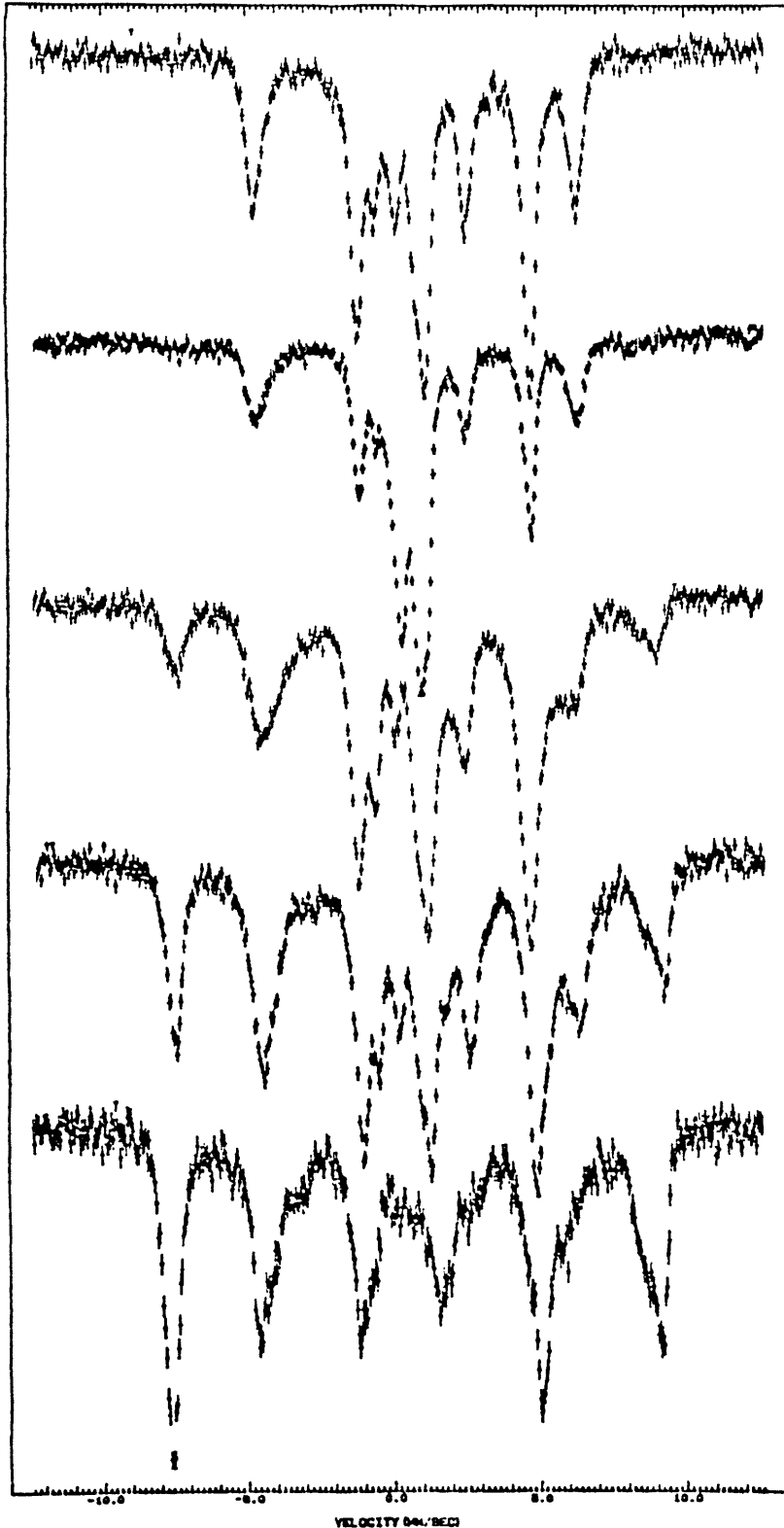


Figure 11 - Mössbauer spectra of ferric-rich fayalites and Rockport fayalite at 20 K.

# 20 K



Rockport

St. Peter's  
Dome

Pantelleria

Mourne Mts.

Qianan

in the 100-150 K temperature range, and the ferric doublet remained unsplit even down to 20 K. The ferrous doublet split between 100 and 55 K, probably at about 65 K, as does the normal fayalite ferrous doublet. This 65 K splitting in fayalite is not a splitting into a hyperfine sextet, but is caused by a magnetically ordered transition in the fayalite structure (Kundig et al., 1967), and such a transition can be presumed to be taking place in the normal fayalite components of all the ferric-rich fayalites as well.

Chapter 7Other Determinative Methods

The four ferric-rich fayalites, along with Rockport fayalite, were examined both by X-ray powder diffraction and by electron probe microanalysis (microprobe). The X-ray diffraction spectra were checked against the standard JCPDS Rockport fayalite spectrum, as well as against JCPDS cards for other likely components: magnetite, hematite, ferrosilite, and quartz. In addition, the Qianan County ferrifayalite spectrum was compared to the published spectrum of ferrifayalite (see Table 1). The only impurity identified was quartz, in the spectra of Rockport fayalite and Mourne Mountains fayalite. Most lines in the spectra were identified and indexed as belonging to fayalite (or in the case of Qianan County ferrifayalite, to ferrifayalite). There were some other lines present, which were not possible to identify or index. Spectra are tabulated in Table 10. It is noteworthy that the spectra of Rockport and St. Peter's Dome fayalite exhibited in general sharp lines, while the spectra of Pantelleria and Mourne Mountains fayalites exhibited diffuse lines. The spectrum of Qianan County ferrifayalite in particular exhibited very broad lines.

Cell parameters were determined from the X-ray diffraction spectra, and these were found to be very similar to the parameters for standard Rockport fayalite. Fitting with a monoclinic structure type was attempted for Mourne Mountains fayalite, and results were inconclusive. A  $\beta$  of  $90.44343 \pm 0.67924$  was determined. Cell parameters according to the orthorhombic system are listed in Table 11. The Qianan ferrifayalite

spectrum indexed with ferrifayalite reflections (monoclinic system) is included as Qianan County B. Monoclinic first setting was used in indexing in order to agree with the fayalite Pbnm orientation. It was impossible to determine which of the fits (by Rockport or ferrifayalite) for Qianan ferrifayalite was the better.

Electron probe analysis of samples indicated near end-member fayalite composition for all samples. Low oxide totals may be interpreted as resulting, in the most part, from the presence of ferric iron analyzed as FeO. When iron content is recalculated as  $\text{FeO} + \text{Fe}_2\text{O}_3$ , using ferric/ferrous ratios derived from Mössbauer data, the oxide totals of the analyses are brought up to a more respectable total. Analyses are listed in Table 5.

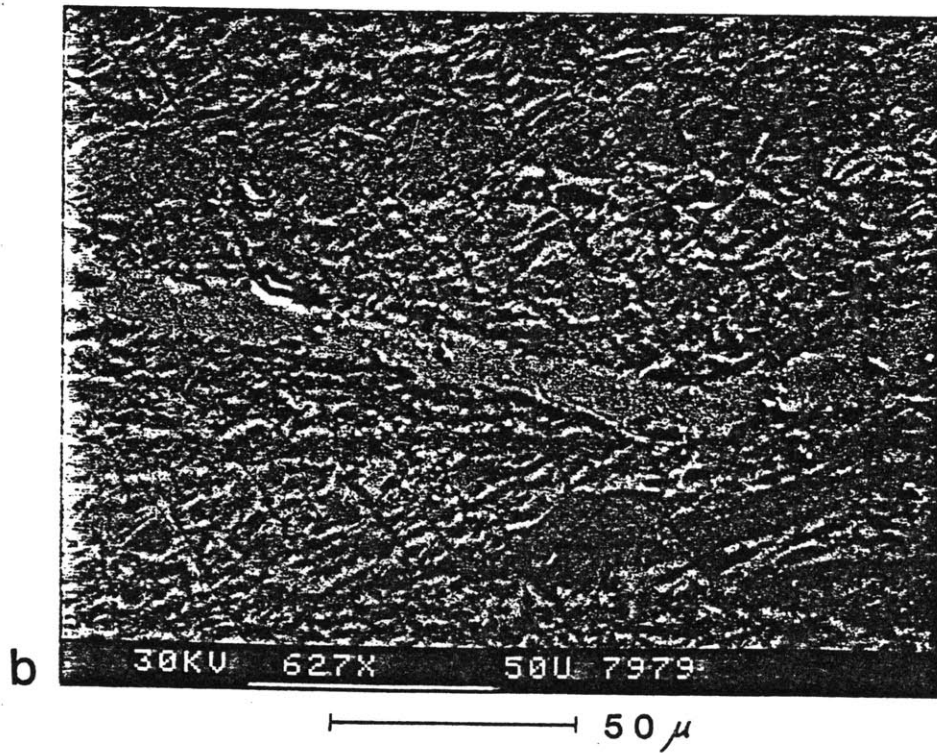
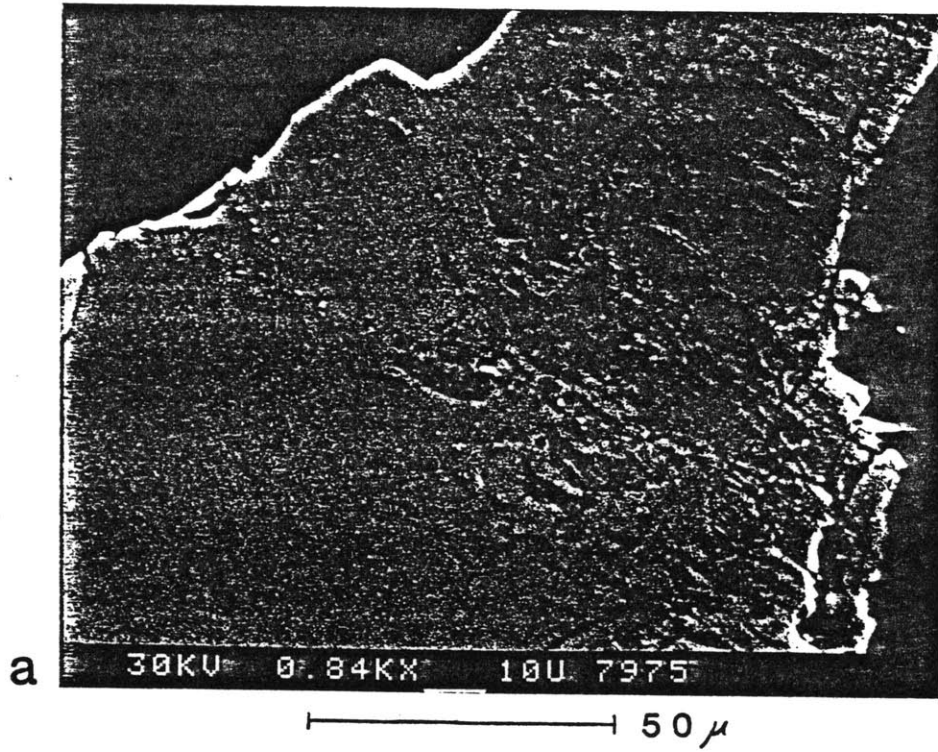
One sample, from St. Peter's Dome, was submitted to a cursory TEM analysis. The sample appeared crystalline and homogeneous, with the exception of some cracks along which alteration had occurred. The alteration product was not identified, but even if it was composed entirely of  $\text{Fe}_2\text{O}_3$ , the total volume of the observed cracks would not be sufficient to explain the observed ferric/ferrous ratio.

The four ferric-rich fayalites and Rockport fayalite were examined by SEM, primarily to check for the presence of imputites. No impurities (of size  $>3000\text{\AA}$ ) were found in sufficient quantity to be observed by Mössbauer spectroscopy or by X-ray diffraction. On the other hand, a very interesting structure was observed in two of the samples, those from Mourne Mountains and Qianan County. It was most pronounced in the Mourne Mountains fayalite, shown in Figure 12. Two intergrown phases were observed, both containing iron and silicon in reasonable proportions to identify them as fayalite. However, the lighter phase was found to

contain less oxygen than the darker phase, and to have a higher Fe/Si ratio, by about ten percent.

In Figure 12a, a primarily dark patch in a fragment of lighter material is seen. This dark patch is more extensively fractured than the lighter material. In Figure 12b, an intergrowth (possibly of exsolution origin) of the two phases is seen. A crack, filled with the lighter material, overlays the exsolution texture. These photographs will be discussed further in Chapter 8.

Figure 12 - SEM photographs of Mourne Mountains fayalite, showing two phase structure and exsolution texture. Scale as shown.



Chapter 8Discussion

Of the ten fayalite samples studied, four, including the Chinese ferrifayalite, were found to contain large amounts of ferric iron. All the fayalites were chosen for study primarily because of their color, which is dark to black. Of the four ferric-rich fayalites, one was very dark olive-green (Mourne Mountains), two were black (Pantelleria and Qianan ferrifayalite), and one was dark reddish-brown (St. Peter's Dome). None but the sample from Qianan showed metallic luster.

All ferric-rich fayalites were examined carefully for signs of exsolved magnetite or hematite, or any other significant impurity. None was visible under a petrographic microscope, in SEM pictures with resolution  $\sim 3000\text{\AA}$ , or, in the case of St. Peter's Dome, in TEM pictures as well. Expanded scale room temperature Mössbauer spectra showed no magnetically split ferric iron, and the low temperature Mössbauer spectra were not consistent with the presence of a superparamagnetic magnetite or hematite phase. No impurities other than quartz were seen on any X-ray powder diffraction spectra. Electron microprobe analysis produced results consistent both with the identification of the samples as fayalite and with the possibility that some of the iron was present in the ferric state.

Mössbauer spectroscopy indicates that two of the samples studied (Mourne Mountains and Pantelleria) are nearly identical with the Qianan ferrifayalite, and that the third sample (St. Peter's Dome) is closely related. Much work has been done by Fu et al. (1979,1982) on the crystal

structure of the mineral they call laihunite. Although the preliminary results on the crystal structure of laihunite indicated that the space group was  $Pb2_1m$  (implying that the  $Fe^{2+}$  cations were randomly distributed over approximately half of the M1 sites), later work implied that the space group was actually  $P2_1/b$  (which implies a strictly systematic alternation of occupation and absence with respect to the  $Fe^{2+}$  cations in the M1 sites).

Weissenberg photographs taken of laihunite single crystals by Fu et al. (1979,1982) show doubled spots for the (0kl), (00l), and most of the (h0l) diffractions, though not for the (h00) diffractions. This doubling of spots was observed in many different specimens. The reason behind this was thought by Fu et al. not to be due to inclusions of other minerals, cleavages in the crystals, or impurities, since the phenomenon exhibits certain structural characteristics: the double spots belong to two sets of lattices, combined according to a twin relation. This implies that there is a domain structure in laihunite. This domain twinning appears to follow an irregular periodicity. The twinning exists with (100) as the combination interface, but the size of the domains varies along the a axis.

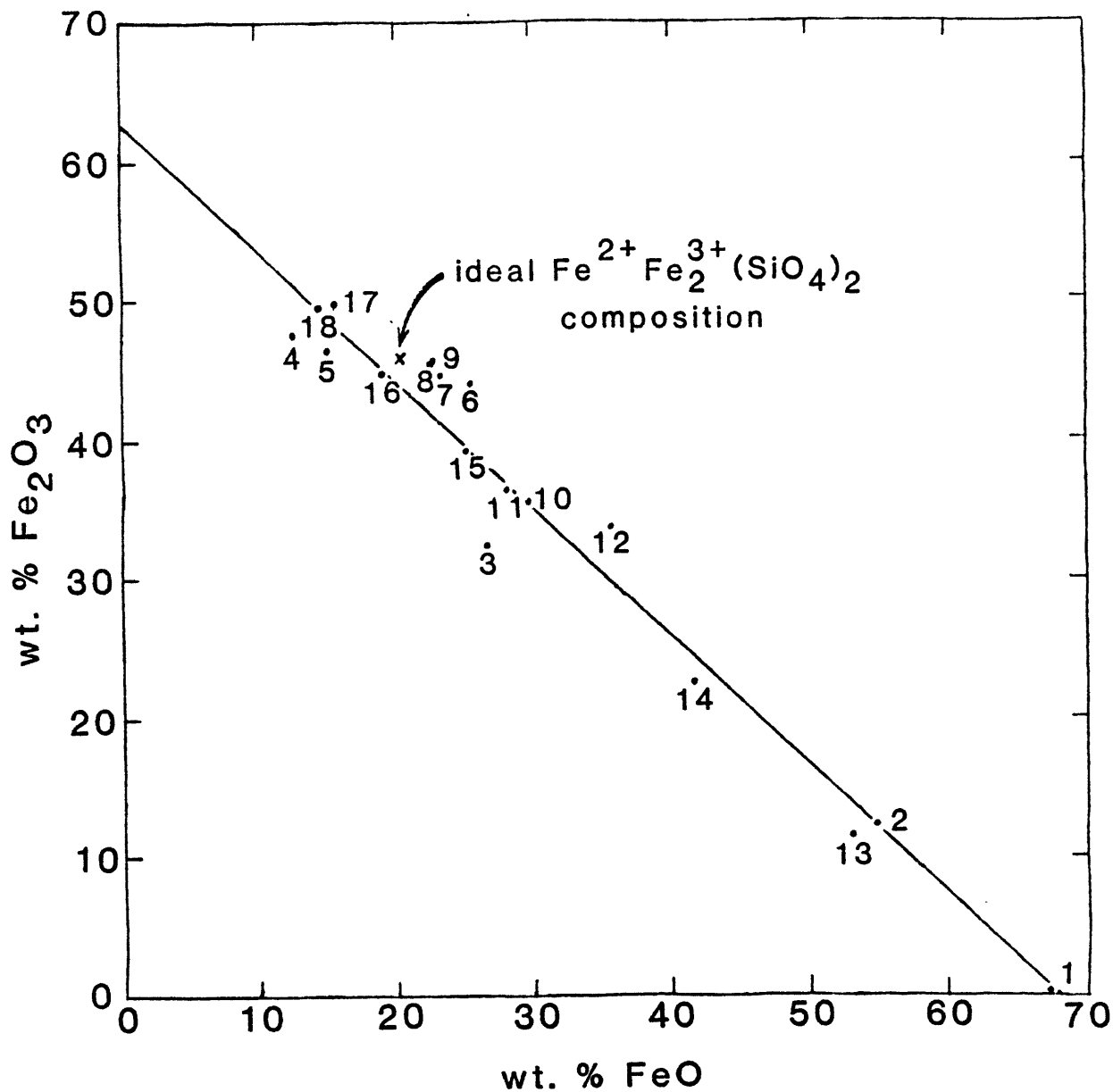
In this structure, if the crystal is taken as a whole, the ferric and ferrous ions are distributed inhomogeneously, and the size of the domains and the width of the boundary areas are not uniform. In the ferric- and vacancy-rich domains, the M2 sites are occupied by four  $Fe^{3+}$  ions, while the M1 sites are characterized by a strictly regular alternation of  $Fe^{2+}$  ions and vacancies. The proportion of ordered domains (as opposed to boundary areas) in the crystal is only 86%, and this disorder is reflected in the many diffuse lines (or spots) in the X-ray diffraction spectrum,

both as observed in the Weissenberg photographs taken by Fu et al., and in an X-ray powder diffraction spectrum taken by this author. Further support for this model comes from the coexistence of laihunite with fayalite, separated by a grey-black translucent transitional zone, indicating a close intergrowth of these minerals attributed to slight changes in oxidation conditions ( $fO_2$ ) during or after the formation of fayalite (Fu et al., 1979,1982).

Compositionally, the  $Fe^{3+}$  content can be thought of as increasing gradually from fayalite to laihunite, accompanied by a corresponding decrease in the number of Fe atoms per unit cell. Fu et al. proposed a model in which the decrease of total iron in the crystal can be imagined as a step by step loss of  $Fe^{2+}$  ions in the M1 sites, leaving more and more vacancies. Structurally, this change is manifested as the successive breaking down of the zig-zag chains of octahedrons typical of fayalite. The chains, as a result, become shorter and shorter. Initially, vacancies and  $Fe^{3+}$  ions are distributed randomly, but later local ordering must take place until straight chains, such as those present in laihunite, are built up. These chains are only three octahedra long and are separated from neighboring chains. Most of the data collected by this author support this domain model.

When a plot was made of weight percent  $Fe_2O_3$  vs. weight percent FeO for all samples of ferric-rich fayalite for which these data are known (Figure 13), two interesting results were noted. The first is that the points are linear. This could indicate that what we are seeing is a mixing line between ordinary ferrous fayalite and an extremely ferric-rich phase, possibly a form of solid solution between the two. The second result is a much more subtle one. When the x- and y-intercepts for the

Figure 13 - Weight percent  $\text{Fe}_2\text{O}_3$  vs.  $\text{FeO}$  for ferric-rich fayalites.  
Sample localities referenced in Tables 2, 7, and 9.



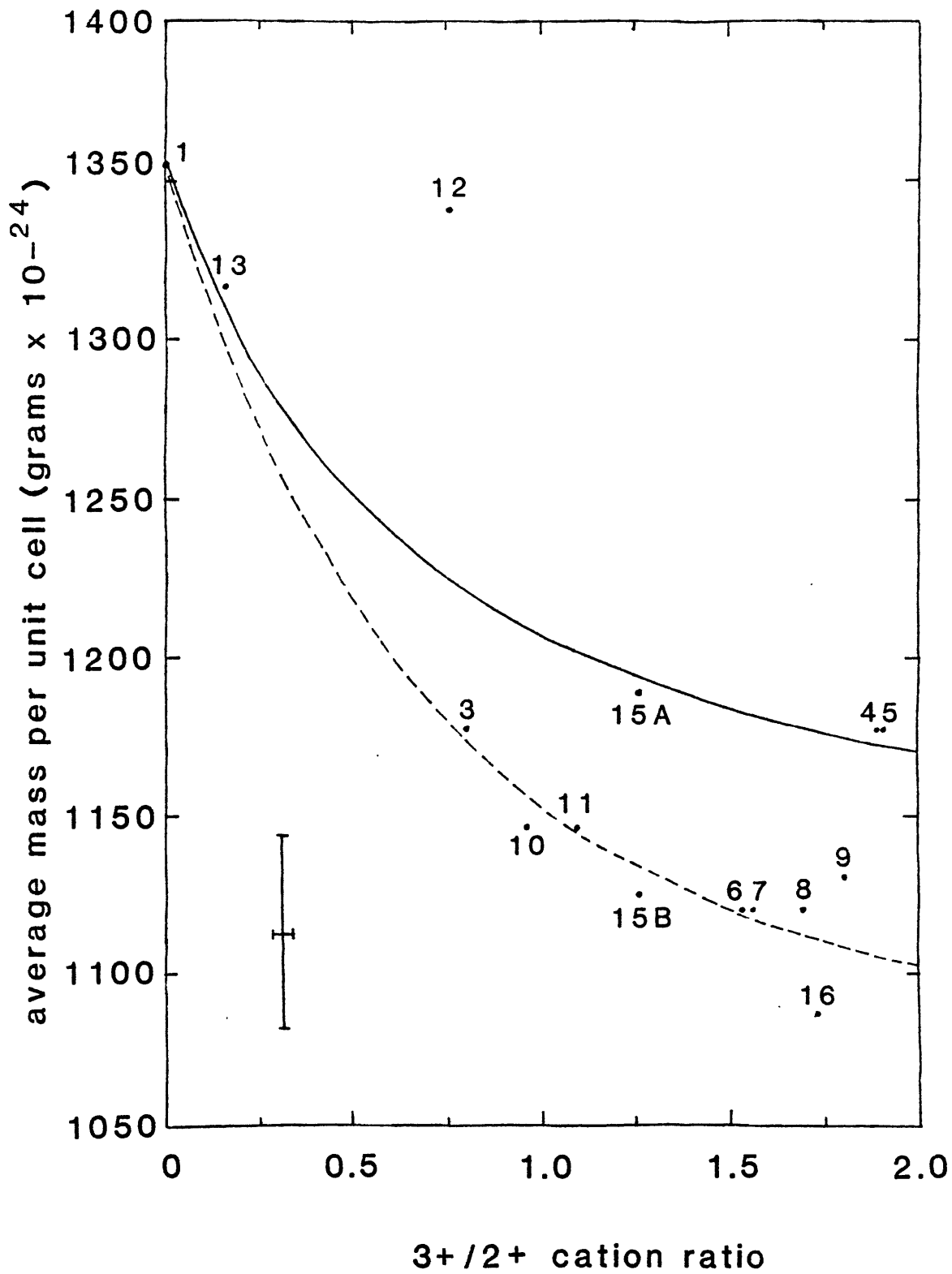
- |                             |                                |
|-----------------------------|--------------------------------|
| 1 Rockport fayalite         | 10 Chinese ferrifayalite (2)   |
| 2 Talasskite                | 11 Chinese ferrifayalite (3)   |
| 3 Russian ferrifayalite (1) | 12 St. Peter's Dome fayalite   |
| 4 Russian ferrifayalite (2) | 13 Pantelleria fayalite        |
| 5 Russian ferrifayalite (3) | 14 Mourne Mountains fayalite   |
| 6 Laihunite (1)             | 15 Qianan County ferrifayalite |
| 7 Laihunite (2)             | 16 Mexican laihunite (1)       |
| 8 Laihunite (3)             | 17 Mexican laihunite (2)       |
| 9 Chinese ferrifayalite (1) | 18 Mexican laihunite (3)       |

least-squares fit line to these points are calculated, they are found to be lower than would be expected, by about ten mole percent. In other words, each unit cell in ferric-rich fayalite seems to have an average of about ten percent fewer iron atoms than would be expected from the formula, even taking vacancies into account. The reason for this is that none of these samples is a pure end-member fayalite, but contains several percent of other cations,  $\text{Mn}^{2+}$ ,  $\text{Mg}^{2+}$ , and  $\text{Ca}^{2+}$ . These impurities have the additional effect of causing the ferric/ferrous ratios of some samples to be greater than 2. The value of 2 is a theoretical limit on the ferric/ferrous ratio required to insure charge balance of the crystal. The total  $3+/2+$  cation ratio of the samples do obey this limit.

A plot was also made relating the mass per unit cell (averaged over the crystal) to the  $3+/2+$  cation ratio  $[\text{Fe}^{3+}/(\text{Fe}^{2+} + \text{Mn}^{2+} + \text{Mg}^{2+} + \text{Ca}^{2+})]$  (Figure 14). A theoretical curve was plotted, as well as observed points for as many of the ferric-rich fayalites as possible. Average unit cell masses were calculated by multiplying the measured density of the mineral by the unit cell volume (from X-ray diffraction data), in the appropriate units. The value of  $\text{Fe}^{3+}/(\text{Fe}^{2+} + \text{Mn}^{2+} + \text{Mg}^{2+} + \text{Ca}^{2+})$  was used instead of simply  $\text{Fe}^{3+}/\text{Fe}^{2+}$  to correct for the effect noted in the last plot. The calculation of the theoretical curve is described in the Appendix.

From this graph, it appears that the observed points do not in general fall on the theoretical curve, but describe a different curve, with a lower density than would be expected. The discrepancy between the curves increases with increasing  $3+/2+$  cation ratio. This curious result may be explained by the action of several factors. First, measured densities of minerals are often observed to be lower than would be expected from unit cell mass and volume calculations, due either to errors in the

Figure 14 - Mass per unit cell vs.  $3+/2+$  cation ratio for ferric-rich fayalites and Rockport fayalite. Numbers refer to the same samples as in Figure 12. In addition, 15A refers to Qianan County ferrifayalite indexed with Rockport indexing, and 15B to Qianan County ferrifayalite indexed with ferrifayalite indexing. The solid line refers to the theoretical model, while the dashed line is an approximate fit to the observed data. An approximate worst case error bar for the observed data is shown. Most of the error is assumed to be in the measurement of the density.



experimental determination of the density or to defects present in the crystal (Azároff, 1968, p. 71). This discrepancy has been noted to be as high as 2 percent, in the case of tourmaline (Buerger, 1970, p. 190). Second, a deficiency of oxygen would act to lower the apparent mass of the unit cell, since a value of four oxygens per formula weight was assumed in its calculation.

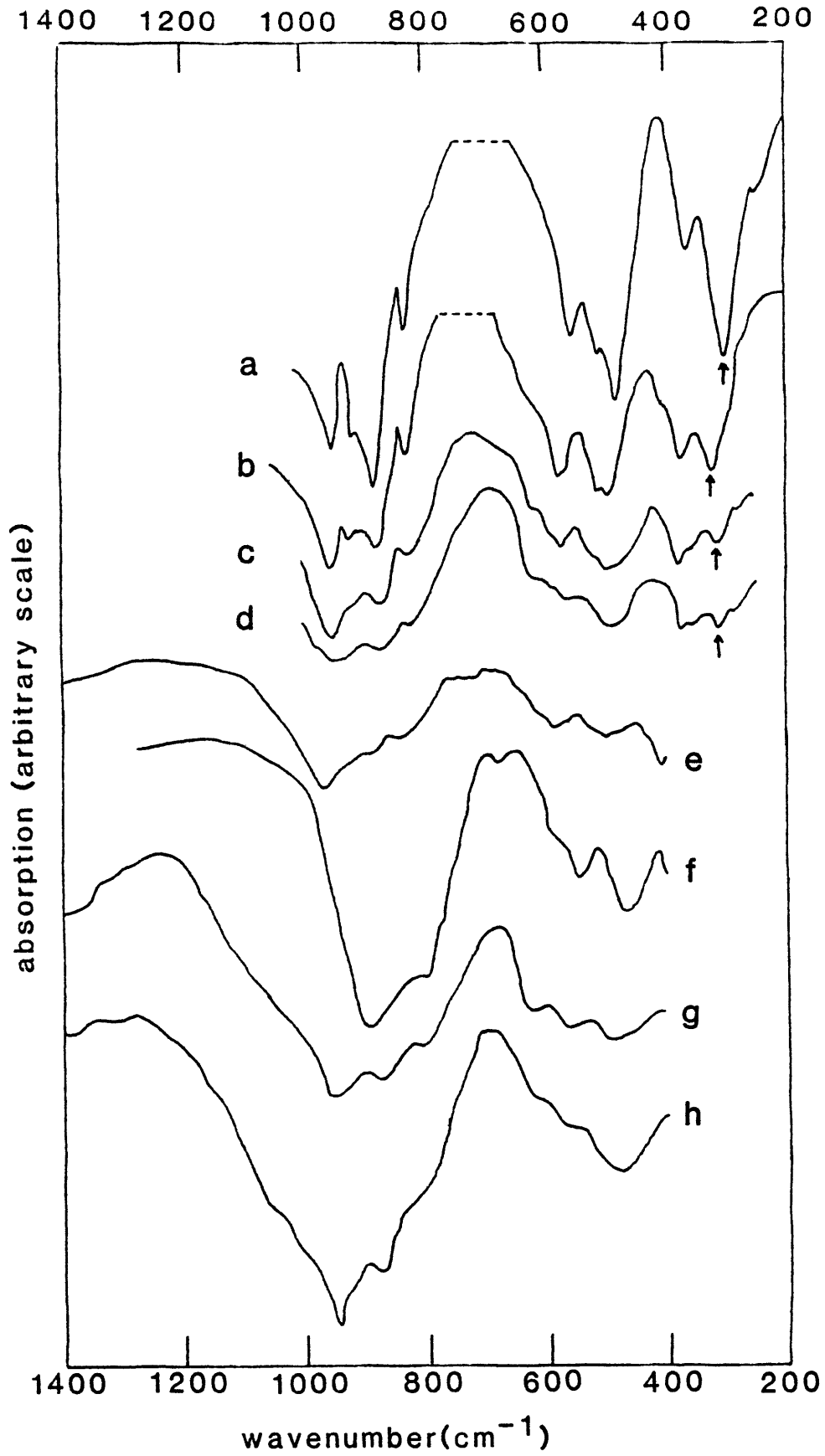
The dominant process here is probably the lowering of measured density due to defects in the crystal. These minerals commonly exhibit X-ray diffraction spectra with broadened peaks, another indication of inhomogeneity, or of many defects, in the crystal. This effect is most notable in samples having a high  $3+/2+$  cation ratio. An increase in  $3+/2+$  cation ratio would very likely act to increase the extent of the boundary regions between the ferrous fayalite and the ferric-rich fayalite domains in the crystal, by increasing the number of the latter. The net effect would be an increased disorder in the crystal, which can be seen in the X-ray spectra and in the graph under discussion.

Another interesting point about this graph is that the most anomalous point on the graph is the point for St. Peter's Dome fayalite, which shows anomalous behavior in its low temperature Mössbauer spectrum as well.

Several authors have proposed that  $Fe^{3+}$  prefers the M2 site (Fu et al., 1979, 1982; Shinno, 1981), one has proposed that it prefers M1 (Zeira and Hafner, 1974), and one that  $Fe^{3+}$  has no site preference in olivine (Weeks et al., 1974). Infrared spectra of ferric-rich fayalites have been taken by many authors (Huggins, 1970; Zhang et al., 1981; Ginzburg et al., 1962; Laihunite Research Group, 1976, 1982; Ferrifayalite Research Group, 1976). They are shown in Figure 15. Of these spectra, four cover the

Figure 15 - Infrared spectra of some ferric-rich fayalites and Rockport fayalite.

- a - Rockport fayalite (Huggins, 1970).
- b - Mourne Mountains fayalite (Huggins, 1970).
- c - Chinese ferrifayalite L<sub>5-1</sub> (Zhang et al., 1981)
- d - Chinese ferrifayalite 79L<sub>3-4</sub> (Zhang et al., 1981).
- e - Russian ferrifayalite - thin layer (Ginzburg et al., 1962)
- f - Russian ferrifayalite - thich layer (Ginzburg et al., 1962).
- g - Laihunite (Laihunite Research Group, 1976,1982).
- h - Chinese ferrifayalite (Ferrifayalite Research Group, 1976).



region below  $400\text{ cm}^{-1}$  (spectra a - d).

The vibrational spectra of minerals with the olivine structure show two distinct regions. The higher frequency ( $>450\text{ cm}^{-1}$ ) region shows only variations in positions of vibrational peak maxima with changing cation content. Features in this region are probably due to vibrations of the isolated  $[\text{SiO}_4]^{4-}$  tetrahedra within the olivine structure (Huggins, 1973). The lower frequency ( $<450\text{ cm}^{-1}$ ) region shows variations in intensity and shape of peaks as well as variations in peak positions with changing cation content. The strength of the band marked in spectra a - d is related to iron or manganese content in the M1 site (Huggins, 1970). This marked band is much less intense in the spectrum of Mourne Mountains fayalite than in the Rockport fayalite spectrum, and still smaller in the two spectra of the Chinese ferrifayalites, even though all four of these samples are near end member fayalites, with much the same proportions of iron to other cations. Since there is a near constant total iron content for these four samples, but there is less iron in the M1 site of the ferric-rich fayalites, it would appear first of all that vacancies are ordered into the M1 sites. Also, since this band in the spectrum is presumably caused by  $\text{Fe}^{2+}$  in the M1 sites, there is support for placing  $\text{Fe}^{3+}$  preferentially in the M2 sites. This seems a reasonable placement in light of the fact that  $\text{Fe}^{2+}$  frequently prefers the M1 site in other olivines, such as tephroite.

There are other data supporting the ordering of  $\text{Fe}^{3+}$  into M2 and vacancies into M1 as well. Plots were made of average metal-oxygen distance vs. cation radius (Figure 16a and b), average oxygen-oxygen distance vs. cation radius (Figure 17a and b), and average oxygen-oxygen distance vs. average metal-oxygen distance (Figure 18a and b) for the M1

Figure 16a - Average metal - oxygen distance vs. cation radius for the M1 site in olivine (after Brown, 1970).

Figure 16b - Average metal - oxygen distance vs. cation radius for the M2 site in olivine (after Brown, 1970).

Fo - forsterite

Ho - hortonolite

Fa - fayalite

Kn - knebelite

FF - ferrifayalite

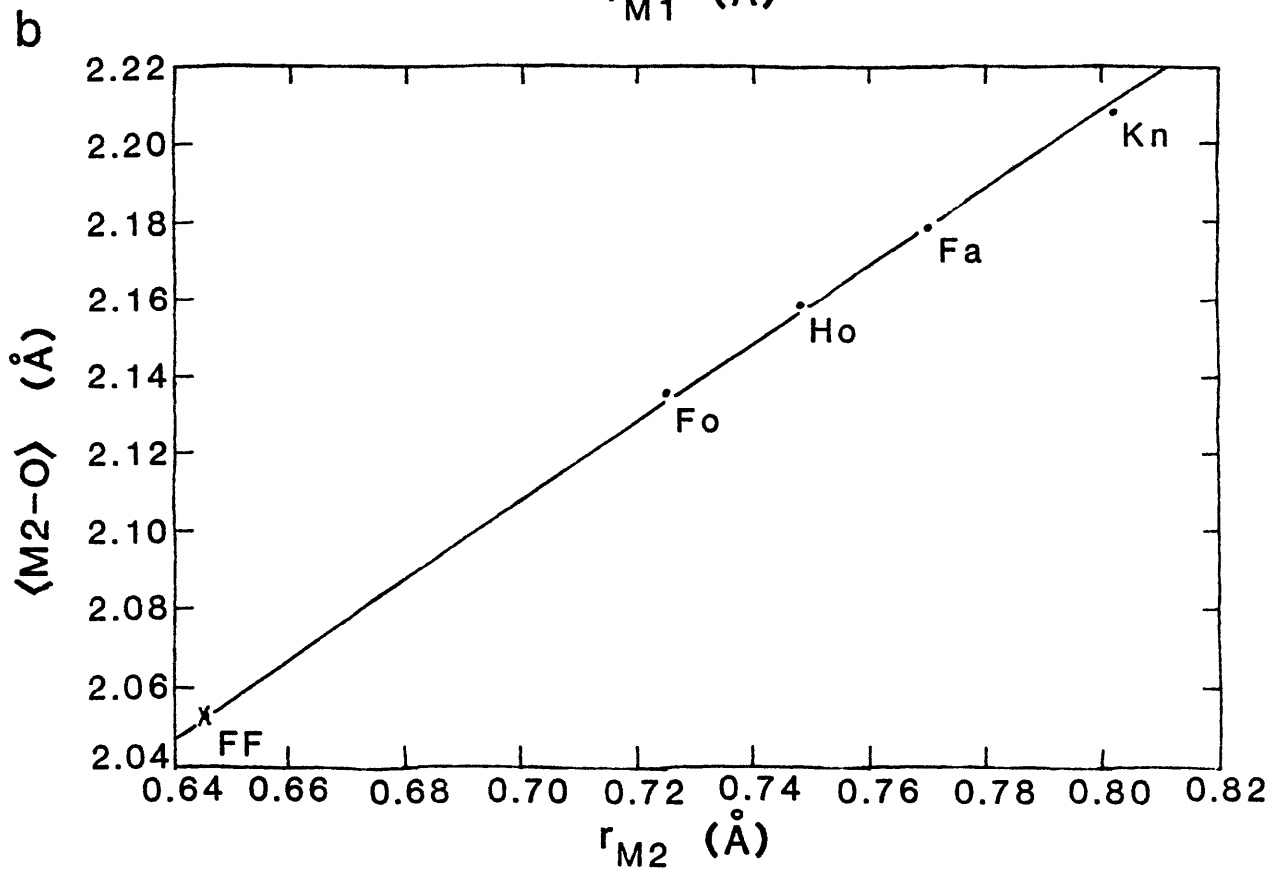
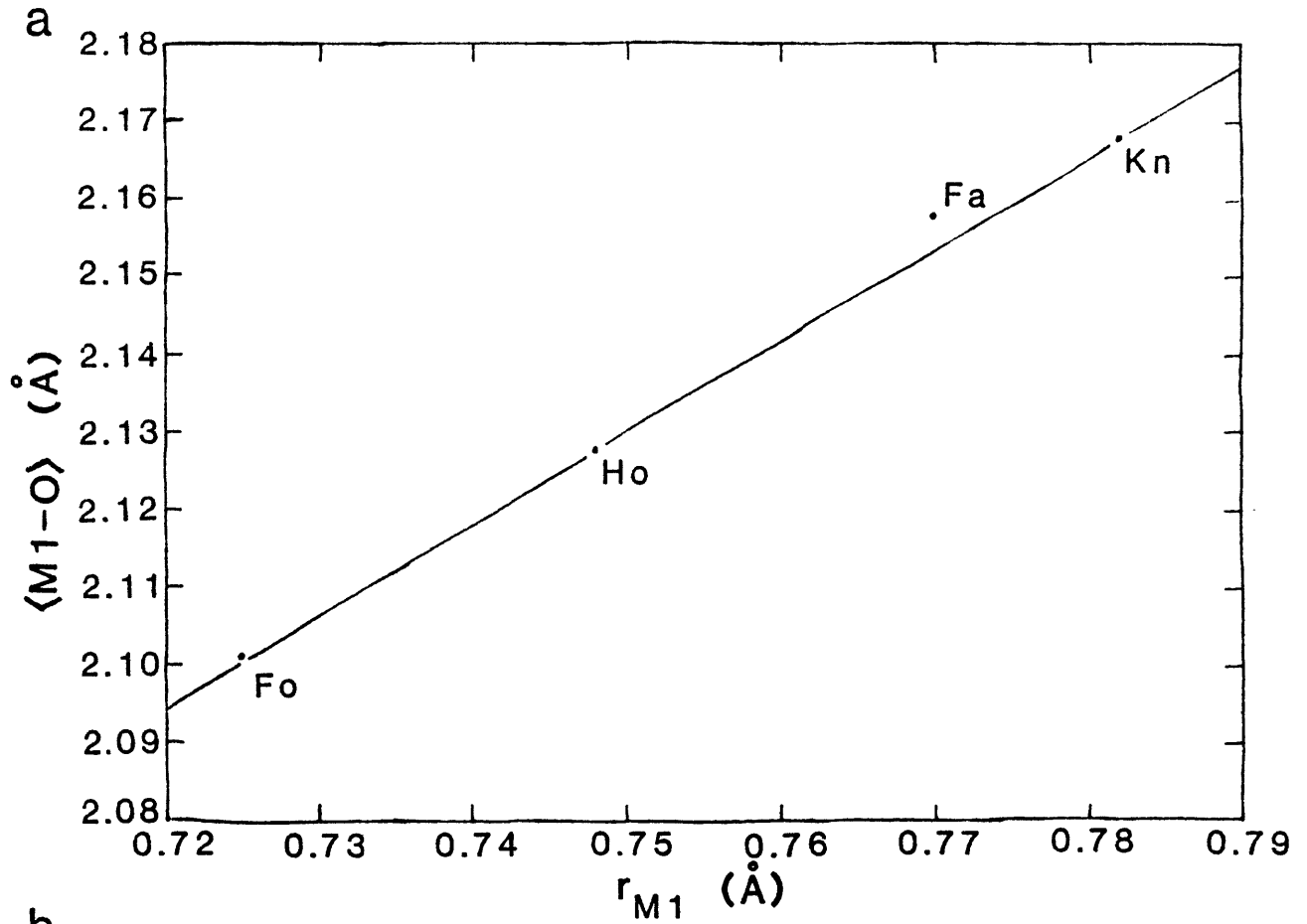


Figure 17a - Average oxygen - oxygen distance vs. cation radius for the M1 site in olivine (after Brown, 1970).

Figure 17b - Average oxygen - oxygen distance vs. cation radius for the M2 site in olivine (after Brown, 1970).

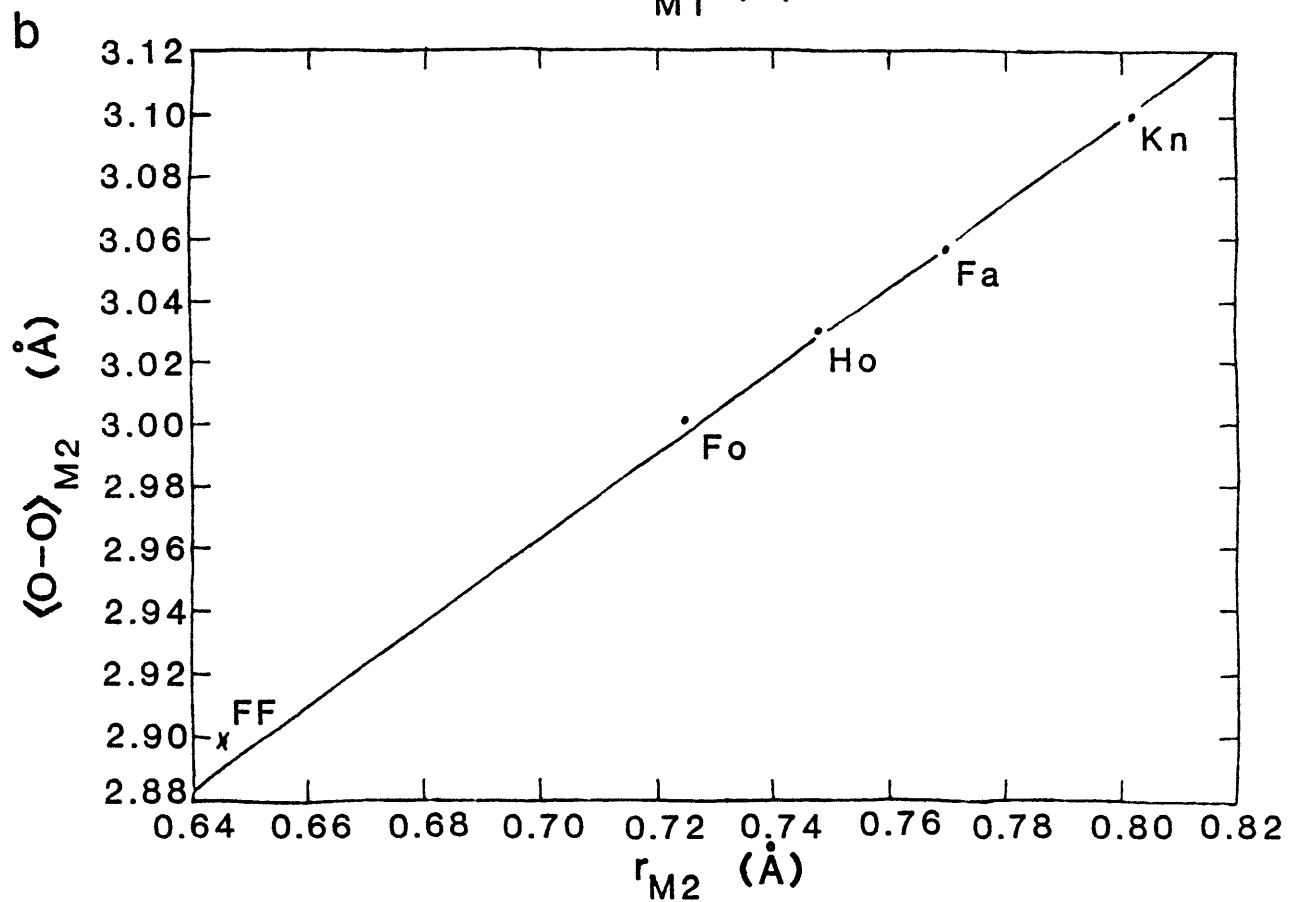
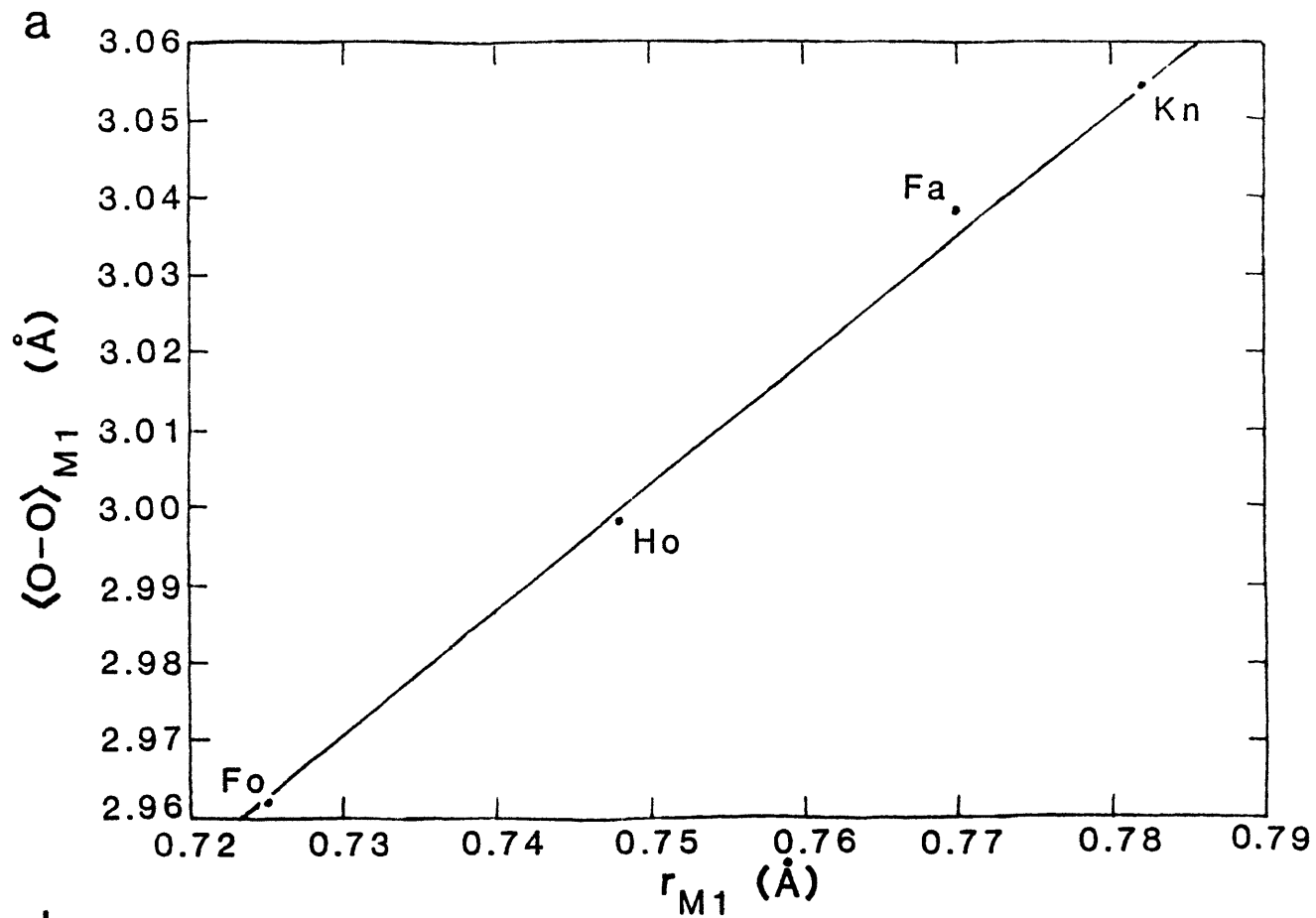
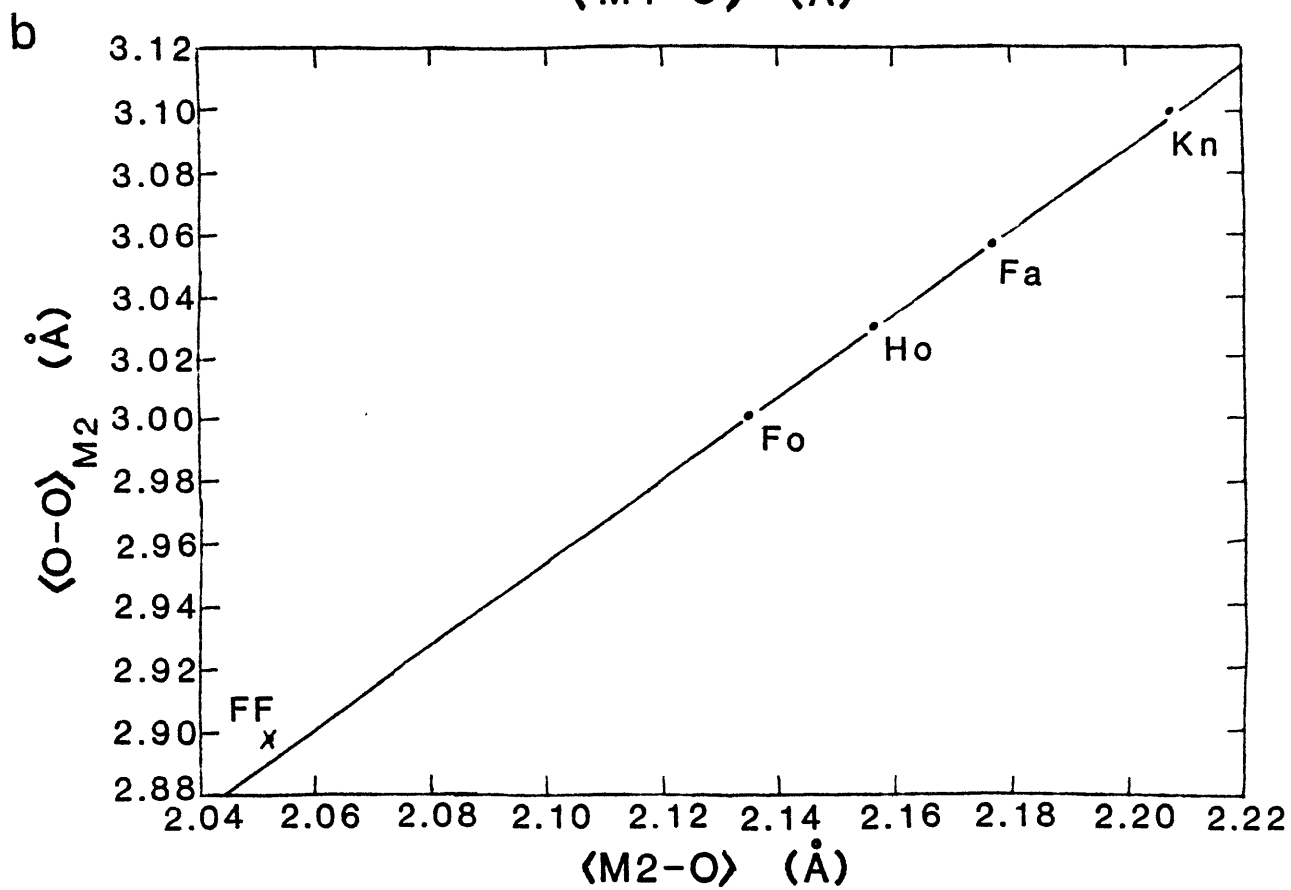
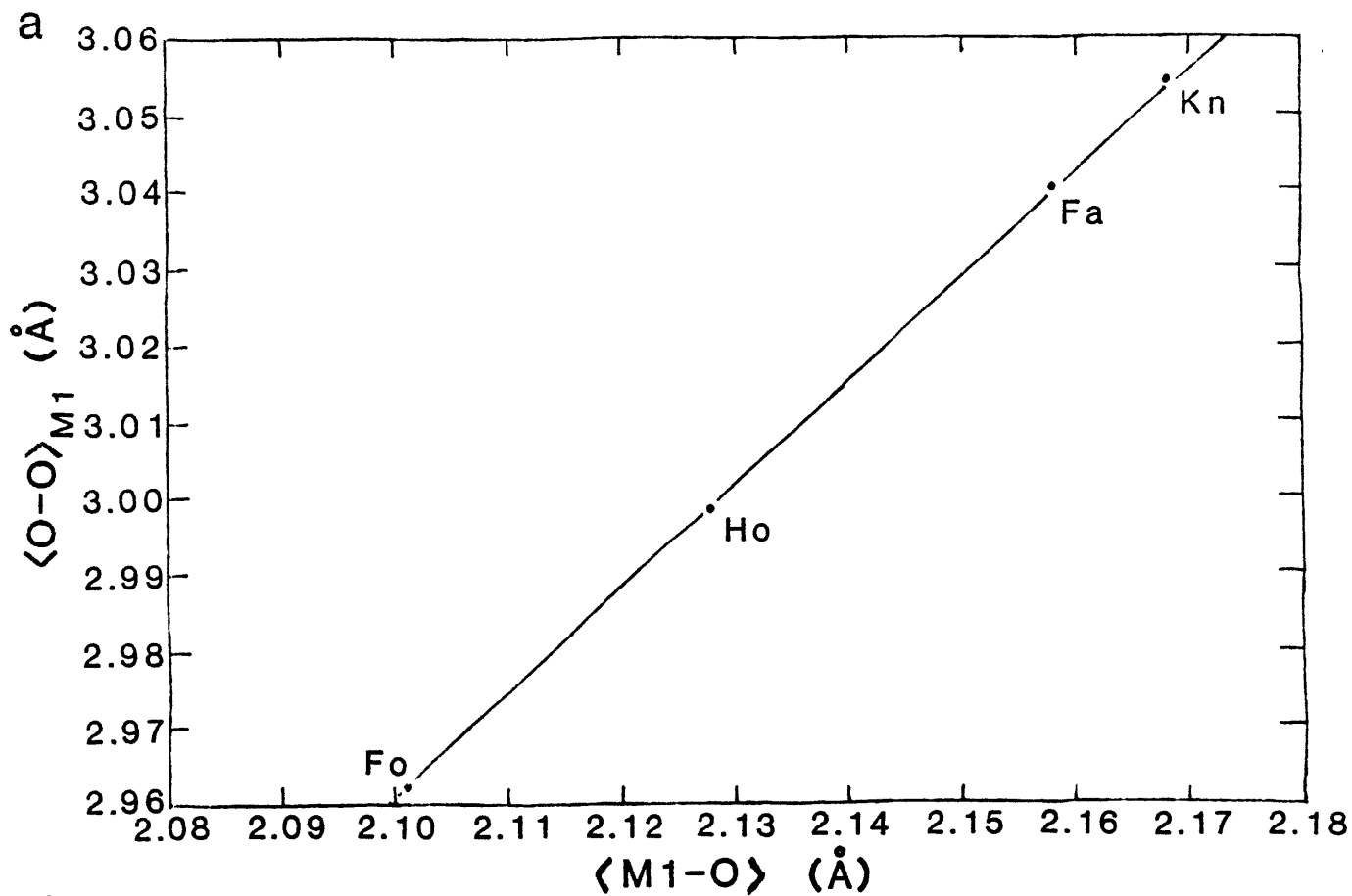


Figure 18a - Average oxygen - oxygen distance vs. average metal - oxygen distance for the M1 site in olivine (after Brown, 1970).

Figure 18b - Average oxygen - oxygen distance vs. average metal - oxygen distance for the M2 site in olivine (after Brown, 1970).



and M2 octahedra (modified after Brown, 1970). When an average metal-oxygen distance calculated from data given by Fu et al. (1979,1982) is plotted and a linear variation of the parameters (determined by Brown, 1970) assumed, a cation radius of 0.645 Å may be determined from the graph for the M2 site. This is the same as the cation radius for Fe<sup>3+</sup> given in Shannon and Prewitt's (1969) table of cation radii.

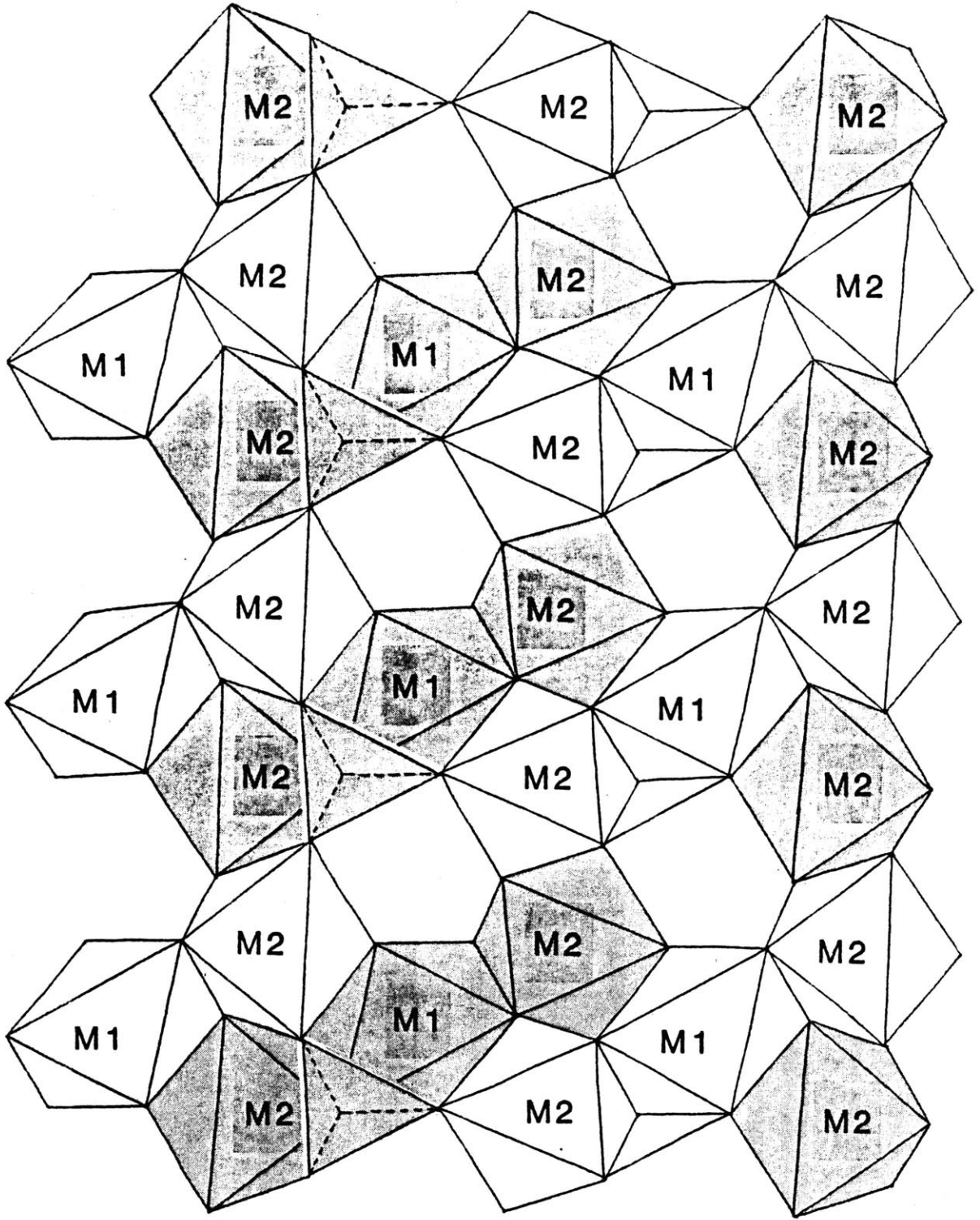
It was not possible to plot similar information about the M1 site for ferrifayalite, since there are insufficient data on the size and shape of the vacancy sites. Using values for only occupied M1 sites in ferrifayalite take from Fu et al. (1979,1982) and Shannon and Prewitt's (1969) value for the cation radius of Fe<sup>2+</sup>, disagreement with Brown's (1970) linear relationship is found. This supports the idea of vacancies concentrated in the M1 sites, distorting the average of the M1 sites and changing its size.

A possible structure for ferrifayalite is shown in Figure 19. This model agrees with that of Fu et al.'s (1979,1982) calculated structure, as well as my own determinations. It shows a basic olivine framework, similar to that shown in Figure 2b for forsterite, with ordered vacancies in the M1 sublattice. In this structure, Fe<sup>2+</sup> is ordered into M1 as well, and Fe<sup>3+</sup> into M2.

There is one major problem with this structural model. In this model, Fe<sup>2+</sup> and Fe<sup>3+</sup> ions are in quite close contact with each other, and should interact strongly. But, the behavior of the Mössbauer spectra at low temperature would seem to indicate that there is no coupling at all between Fe<sup>2+</sup> and Fe<sup>3+</sup> ions, which would imply perhaps that they are separated somehow in the structure.

The Mössbauer spectra of the Mourne Mountains and Pantelleria

Figure 19 - A possible structure for ferrifayalite.



fayalites and Qianan ferrifayalite are all basically similar at low temperatures. They all show an ordinary ferrous fayalite spectrum superimposed on another pattern which can be described generally as a sextet. The spectrum of St. Peter's Dome fayalite, on the other hand, shows a normal ferrous fayalite spectrum superimposed on an unsplit ferric doublet. In both cases the ferric and ferrous doublets seen in the spectra of the ferric-rich fayalites split at very different temperatures. This indicates that the  $\text{Fe}^{3+}$  and  $\text{Fe}^{2+}$  ions in the crystal are completely uncoupled. If the minerals are assumed to contain domains of ferrous fayalite and domains of ferric-rich fayalite, this uncoupling of ferric and ferrous ions becomes less of a problem. The fayalite domains will produce normal fayalite Mössbauer spectra, and the ferric-rich domains will produce the other pattern seen.

The alternative possibility, that the ferric ions are inserted into the normal olivine structure in such a way as to interact very little with the ferrous ions, is unsatisfactory. The previously discussed model, with ferrous ions and vacancies ordered on the M1 sites, and ferric ions occupying the M2 sites, would not produce the desired spectrum. The presence of the normal low temperature Mössbauer spectrum as part of the observed pattern would imply that ferrous ions are present in equal proportions on both the M1 and M2 sites, according to the magnetic ordering model proposed by Santoro et al. (1966) to explain the low temperature fayalite spectrum. Also, it is difficult to imagine how to arrange the ferric and ferrous ions in the olivine structure in such a way as to prevent any significant interaction between them. This would imply that there are essentially no shared edges between the coordination octahedra of the ferric and ferrous ions in the crystal, a configuration

difficult to obtain given the restrictions of the olivine structure.

The SEM photographs support the existence of a two domain system. In photographs of Qianan County ferrifayalite and especially Mourne Mountains fayalite two phases were seen. The composition of these phases was semi-quantitatively determined to be that of fayalite, but with differing proportions of iron and oxygen (to silicon). Two sorts of textures were seen (Figure 12b): one was an exsolution-type texture, which would indicate that possibly at higher temperatures a true solid solution existed between ferric-rich and normal fayalite, which separated into two phases as the system cooled; the other appeared to be the filling of a crack by the lighter-colored phase, normal fayalite. It is noticeable in Figure 12a that the dark, ferric-rich area is much more extensively fractured than the lighter area. This is supportive of the idea derived from the density data, that the existence of ferric-regions increases the total disorder of the crystal.

Only one phase was observable in the fayaltes from St. Peter's Dome and Pantelleria. It is quite possible that higher-resolution SEM photographs would be able to distinguish exsolution lamellae of a smaller scale than at present.

In view of the great confusion in nomenclature of these minerals in the literature (particularly the Chinese literature) today, I would like to propose a nomenclature for this system. The extremely ferric-rich end member of the series should be known as laihunite, while the ferric-poor end member remains fayalite. The series itself, whether thought of as a true solid solution (which it may be at high temperature), or as a mixture of two phases (similar to plagioclase feldspar), should be known as ferrifayalite.

Getting back to the low temperature Mössbauer spectra, one possibility, very difficult to confirm due to the extreme complexity of the spectra, is that the sextet spectrum is not due exclusively to the ferric ions, but is due to a magnetic interaction between the ferrous and ferric ions in the ferric-rich domains. It is interesting to note that the splitting of the ferric doublet in the spectra of these ferric-rich fayalites does take place at approximately the same temperature as the magnetic ordering temperature of magnetite (the Verwey temperature), another mineral containing both ferric and ferrous iron.

If this spectrum is due to ferric and ferrous ions interacting in a manner similar to the way sub-Verwey temperature ferric and ferrous ions interact in magnetite, it would provide a theoretical basis for the possibility that below 125 K, the ferric-rich fayalite domain spectrum contains not one, but two magnetic sextets. One could belong to the  $\text{Fe}^{3+}$  ions in the M2 sites and the other, less intense pattern, to the  $\text{Fe}^{2+}$  ions in the M1 sites. It would appear that this transition is not completely analogous to the Verwey transition, however, since the ferric-rich fayalite is not magnetically split at all above the transition region.

The width of the transition temperature region probably merely indicates inhomogeneity in the sample, although it is possible for a polymorphic transition to take place over an appreciable range of temperature. The likelihood of inhomogeneity is supported, in the case of the samples from Mourne Mountains, Pantelleria, and Qianan County, by the broadening of the lines observed in the X-ray diffraction spectra. The X-ray diffraction lines were not broadened in the spectra of Rockport or St. Peter's Dome fayalites, the two specimens which do not show broad Mössbauer transitions.

The transition seen for the ferrous fayalite domains of the

ferric-rich fayalites is quite sharp, as it is for Rockport fayalite. It is difficult to tell if the transition seen at 65 K is caused merely by this normal fayalite transition, or if the ferric-rich domains are undergoing a transition as well. It would be possible to produce arguments for either possibility, based on the spectra presently available.

Summary

It has long been believed by geologists and mineralogists that the olivine structure is not capable of accommodating ferric iron. There now exists sufficient evidence to show that this is not strictly true. Ferric iron can be accommodated in the fayalite crystal structure, with charge balance for the crystal being accomplished by the presence of vacancies in the octahedral cation sites. These vacancies, which exist in the proportion of 1 vacancy to every 2 ferric cations, alternate with the remaining ferrous cations in the M1 site. The ferric cations prefer the M2 site.

The gross crystal structure of the ferric-rich fayalites may be described as a domain structure, with domains of ferrous fayalite and domains of ferric-rich fayalite coexisting. The ferric-rich fayalite domains contain 2 vacancies per unit cell; perhaps some proportion exist with only 1 vacancy per unit cell, but this cannot be determined conclusively with the data available at present.

This domain structure is observed in the low temperature Mössbauer spectra of the ferric-rich fayalites and in SEM photographs of some samples. The low temperature spectra show a superposition of the normal fayalite spectrum and an unfamiliar pattern. There is also evidence from X-ray crystallography and density calculations that there are increasing disorder and defects in this mineral with increasing ferric iron present.

There appears to be a sort of solid solution between normal ferrous fayalite and ferric-rich fayalite, similar to that seen in the plagioclase

feldspars. I would like to propose a nomenclature for this new series of the olivine group. The extremely ferric-rich ( $3+/2+$  cation ratio = 2) end member of the series should be known as laihunite, after the location of its first discovery (Laihunite Research Group, 1976,1982). The series between laihunite ( $\text{Fe}^{2+}\text{Fe}^{3+}_2(\text{SiO}_4)_2$ ) and fayalite ( $\text{Fe}^{2+}_2\text{SiO}_4$ ) should be known as ferrifayalite, after the Russian and Chinese discoveries of that name (Ginzburg et al., 1962; Ferrifayalite Research Group, 1976).

#### Suggestions for Further Study

This study has clearly only scratched the surface of a fascinating topic. Several specific research problems on the ferrifayalite series spring to mind. First, high resolution TEM photographs should be taken of as many ferrifayalite samples as possible, especially those near the midpoint of the series. Such photographs may show evidence of the proposed domain structure of this mineral. Photographs of the laihunite end member may even be capable of showing evidence of ordered vacancies in the crystal.

Second, low temperature magnetic studies should be done on laihunite, in an attempt to interpret in more detail the low temperature Mössbauer spectra. Such studies might include neutron diffraction analysis, Mössbauer spectra with an external applied magnetic field, magnetization vs. temperature curves, and specific heat vs. temperature curves.

Third, thermal and electrical conductivity measurements should be taken of the entire series. It has been observed that the specific conductivity of fayalite equilibrated with  $\text{SiO}_2$  and  $\text{Fe}_3\text{O}_4$  may be more than one order of magnitude greater than that of fayalite

equilibrated with  $\text{SiO}_2$  and metallic iron (Will et al., 1979). This effect is thought to be caused by the presence of small numbers of ferric cations and defect vacancies in the metal sites (Söckel, 1974; Duba et al., 1973). If small  $\text{Fe}^{3+}$  and vacancy concentrations can have such severe effects on conductivity, what effect might large concentrations have? This effect could be of extreme importance to the study of heat flow in the mantle.

Fourth, high temperature Mössbauer spectra ( $>500$  K) may offer conclusive evidence as to cation ordering in ferrifayalite. Since the quadrupole doublets produced by ferrous iron in the M1 and M2 sites are resolved at high temperatures, site preferences can be determined with great ease.

Fifth, attempts should be made to synthesize ferrifayalite. Formation conditions of 600–700°C temperature,  $>15$  kb pressure, and high  $f_{\text{O}_2}$  have been proposed by Wang (1980), but these conditions have not as yet been confirmed experimentally. In addition, it would be interesting to determine if there is a high pressure spinel polymorph of ferrifayalite, as there is of fayalite.

Sixth, optical spectra should be taken of members of the ferrifayalite series. This may prove challenging in the case of laihunite-rich samples, as those tend towards opacity, but it is those samples which should prove most interesting. Black color and metallic luster often indicate the presence of intervalence charge transfer in minerals, particularly mixed-valence minerals. There is no evidence as yet that  $\text{Fe}^{2+} \rightarrow \text{Fe}^{3+}$  charge transfer does take place in the ferrifayalite series minerals, but such spectra might determine whether this is the case.

Lastly, though I have no concrete suggestions other than those

outlined above as to specific procedures, I would like to see more studies made of the St. Peter's Dome fayalite. This sample, which proved anomalous in so many ways, seems particularly intriguing and worthy of study.

Appendix

For a crystal containing domains with different populations of  $\text{Fe}^{3+}$ ,  $\text{Fe}^{2+}$ ,  $\text{Mn}^{2+}$ ,  $\text{Mg}^{2+}$ , and  $\text{Ca}^{2+}$  ions, and also containing vacancies (required by charge balance), we want to determine the mass per unit cell (averaged over the crystal) as a function of  $R$ , the  $\text{Fe}^{3+}/(\text{Fe}^{2+} + \text{Mn}^{2+} + \text{Mg}^{2+} + \text{Ca}^{2+})$  ratio. The divalent cations can be summed together since there is complete solid solution between these cations in olivine. The average mass per unit cell is determined by adding up the masses of the individual anions and cations in an average unit cell. The number of cations per unit cell (containing four formula units) in normal ferrous fayalite is 8, so the number of cations in fayalite containing  $N_v$  vacancies should be  $(8 - N_v)$ . For simplicity, we shall assume that the average mass of the divalent cations is the same as the mass of Fe, since we are dealing with a system in which  $\text{Fe}^{2+}$  is by far the dominant divalent cation, and the other divalent cations are of much smaller (and variable) concentration. We now wish to calculate the number of vacancies,  $N_v$ , as function of  $R$ .

The average mass per unit cell of the crystal,

$$\langle M \rangle = N_{\text{O}}m_{\text{O}} + N_{\text{Si}}m_{\text{Si}} + N_{\text{M}}m_{\text{Fe}},$$

where  $N_{\text{M}} = N_{\text{Fe}} + N_{\text{Mn}} + N_{\text{Mg}} + N_{\text{Ca}} = N_{\text{Fe}} + N_v$ .

By definition,  $N_{\text{Fe}} = N_{\text{Fe}^{2+}} + N_{\text{Fe}^{3+}}$ .

By charge balance,  $N_v = \frac{1}{2}N_{\text{Fe}^{3+}}$ .

Given  $N_{\text{M}}$  sites in an average unit cell, and  $N_v$  vacancies, the probability that a given site contains a vacancy is  $P$ , and that it contains no vacancy is  $(1 - P)$ . From charge balance considerations, the maximum number of vacancies in a unit cell is restricted to 2. Therefore,

$$P = N_v/2.$$

Let the probability that the two independent sites in the unit cell contain zero vacancies equal  $P_0$ , that they contain one vacancy equal  $P_1$ , and that they contain two vacancies equal  $P_2$ .

$$\begin{aligned} P_0 &= (1 - P)(1 - P) &= 1 - 2P + P^2 &= 1 - N_v + N_v^2/4 \\ P_1 &= (1 - P)P + P(1 - P) &= 2P - 2P^2 &= N_v - N_v^2/2 \\ P_2 &= PP &= P^2 &= N_v^2/4 \end{aligned}$$

Note that  $P_0 + P_1 + P_2 = 1$ .

Now let's look at these cases:

	<u>Fe<sub>3</sub><sup>+</sup></u>	<u>Fe<sup>2+</sup> + M<sup>2+</sup></u>	<u>V</u>	<u>N<sub>M</sub></u>
Case 0:	0	8	0	8
Case 1:	2	5	1	7
Case 2:	4	2	2	6

The average total number of cations,  $N_M = N_0P_0 + N_1P_1 + N_2P_2$ , where  $N_0$  is the number of cations from the case 0 unit cells,  $N_1$  is the number of cations from the case 1 unit cells, and  $N_2$  is the number of cations from the case 2 unit cells.

$$N_0 = 8,$$

$$N_1 = 7,$$

$$N_2 = 6.$$

$$\begin{aligned} N_M &= 8P_0 + 7P_1 + 6P_2 \\ &= 8[1 - N_v + N_v^2/4] + 7[N_v - N_v^2/2] + 6[N_v^2/4] \\ &= 8 - N_v, \text{ as expected.} \end{aligned}$$

$$\begin{aligned} N_M &= N_{Fe^{2+}} + N_N + N_{Fe^{3+}} \\ &= (N_N + N_{Fe^{2+}})(1 + R) \\ 8 &= N_{Fe^{2+}} + N_N + N_{Fe^{3+}} + N_v \\ &= (N_{Fe^{2+}} + N_N)(1 + R + N_v/(N_{Fe^{2+}} + N_N)) \\ N_M/8 &= (1 + R)/(1 + R + N_v/(N_{Fe^{2+}} + N_N)), \end{aligned}$$

and  $N_V = N_{Fe}^{3+}/2$ , so

$$N_M/8 = (1 + R)/(1 + R + \frac{1}{2}R) = (1 + R)/(1 + 3R/2).$$

$$N_M = 8[(1 + R)/(1 + 3R/2)]$$

$$N_V = 8 - N_M = 8 - 8[(1 + R)/(1 + 3R/2)]$$

$$= 8[1 - (1 + R)/(1 + 3R/2)]$$

$$= 8[(1 + 3R/2 - 1 - R)/(1 + 3R/2)]$$

$$= 8[\frac{1}{2}R/(1 + 3R/2)]$$

$$= 4R/(1 + 3R/2)$$

$$N_M = 8 - 4R/(1 + 3R/2)$$

$$\text{Average mass per unit cell} = N_{O}m_O + N_{Si}m_{Si} + N_M m_{Fe}$$

$$= 16(15.9994) + 4(28.086) + N_M(55.847)$$

$$= 368.334 + N_M(55.847)$$

This value can then be multiplied by  $1.661 \times 10^{-24}$  gm/amu to obtain the average mass per unit cell in grams.

References

Azáróff, L.V. (1968) Elements of X-Ray Crystallography, McGraw-Hill, New York, 610 pp.

Bancroft, G.M. (1973) Mössbauer spectroscopy, an Introduction for Inorganic Chemists and Geochemists, McGraw-Hill, London, 252 pp.

Bence, A.E., Albee, A.L. (1968) Empirical correction factors for the electron microanalysis of silicates and oxides, J. Geol. 76, 382-402

Brown, G.E., Jr. (1970) Crystal chemistry of the olivines, Ph.D. thesis, Virginia Polytechnic Institute, Blacksburg, Virginia

Buerger, M.J. (1970) Contemporary Crystallography, McGraw-Hill, New York, 364 pp.

Burnham, C.W. (1962) Lattice constant refinement, Carnegie Inst. Of Washington Year Book 61, 132-135

Burns, R.G. (1970) Mineralogical Applications of Crystal Field Theory, Cambridge University Press, Cambridge, 224 pp.

Carmichael, I. (1982) private communication

Deer, W.A., Howie, R.A., Zussman, J. (1962) Rock-Forming Minerals, v.1, Ortho- and Ring Silicates, Longmans, Green, and Co., Ltd., 333 pp.

Duba, A., Ito, J., Jamieson, J.C. (1973) The effect of ferric iron of the electrical conductivity of olivine, Earth and Planet. Sci. Lett. 18, 279-284

Eckel, E.B. (1961) Minerals of Colorado, a 100-Year Record, USGS Bullitin 1114, U.S. Government Printing Office, Washington, 399 pp.

Ferrifayalite Research Group [Dept. of Geology of the Peking University, Institute of Geology and Mineral Resources of the Chinese Academy of Geological Sciences] (1976) Ferrifayalite and its crystal structure, Acta Geol. Sinica 2, 160-175 (in Chinese )

- Fu, P., Kong, Y., Zhang, L. (1979) Domain twinning of laihunite and refinement of its crystal structure, *Geochimica* 6, 103-119 (in Chinese)
- Fu, P., Fong, Y., Zhang, L. (1982) Domain twinning of laihunite and refinement of its crystal structure, *Geochemistry* 1, 115-133
- Ghose, S., Wan, C., McCallum, I.S. (1976) Fe<sup>2+</sup> - Mg<sup>2+</sup> order in an olivine from the lunar anorthosite 67075 and the significance of cation order in lunar and terrestrial olivines, *Indian J. Earth Sci.* 3, 1-8
- Ginzburg, I.V., Lisitsina, G.A., Sadikova, A.T., Sidorenko, G.A. (1962) Fayalite of granite rocks and the products of its alteration (Kuraminskii Range, Central Asia), *Akad. Nauk CCCP, Trudy Mineralog. Museya* 13, 16-42 (in Russian)
- Gross, E.B., Heinrich, E.W., (1965) Petrology and mineralogy of the Mount Rosa area, El Paso and Teller counties, Colorado, I. The granites, *Amer. Min.* 50, 1273-1295
- Gross, E.B., Heinrich, E.W., (1966) Petrology and mineralogy of the Mount Rosa area, El Paso and Teller counties, Colorado, II. Pegmatites, *Amer. Min.* 51, 299-323
- Harris, J. (1983) private communication
- Hidden, W.E. (1885) Mineralogical notes, *Amer. J. Sci.*, 3<sup>rd</sup> series 29, 249-251
- Hidden, W.E., Mackintosh, J.B. (1891) Mineralogical notes, *Amer. J. Sci.*, 3<sup>rd</sup> series 41, 438-439
- Huggins, F.E. (1970) Infra-red study of some orthosilicate minerals, B.A. thesis, Oxford University, Oxford, 136 pp.
- Huggins, F.E. (1973) Cation order in olivines: evidence from vibrational spectra, *Chemical Geology* 11, 99-109
- Kundig, W., Cape, J.A., Lindquist, R.H., Constabaris, G. (1967) Some magnetic properties of Fe<sub>2</sub>SiO<sub>4</sub> from 4° K to 300° K, *J. Appl. Phys.* 38, 947-948

Laihunite Research Group, Guiyang Institute of Geochemistry, Academia Sinica, and 101 Geological Team of Liaoning Metallurgical and Geological Prospecting Company (1976) Laihunite - a new iron silicate mineral, *Geochemica* 6, 95-103 (in Chinese)

Laihunite Research Group, Institute of Geochemistry, Academia Sinica, and Geological Team No. 101 of Liaoning Metallurgical and Geological Prospecting Company (1982) Laihunite - a new iron silicate mineral, *Geochemistry* 1, 105-114

Lumpkin, G.R., Ribbe, P.H. (1983) Composition, order-disorder and lattice parameters of olivines: relationships in silicate, germanate, beryllate, phosphate and borate olivines, *Am. Min.* 68, 164-176

Mahood, G.A. (1980) The geological and chemical evolution of a late Pleistocene rhyolitic center: the Sierra La Primavera, Jalisco, Mexico, Ph.D. thesis, University of California, Berkeley, California

*Mineraly Uzbekistana* 3 (1975-1977) Silicates, Nesosilicates with Isolated Tetrahedrons, 44-46 (in Russian)

Mossman, D.J., Pawson, D.J. (1976) X-ray and optical characterization of the forsterite-fayalite, tephroite series with comments on knebelite from Bluebell mine, British Columbia, *Can. Mineralogist* 14, 479-486

Nikitin, V.D. (1934) A new variety of mineral of the olivine group, *Zap. Vseros. Min. ob-va, seriya 2, ch. 65, vip. 1-2*, 281-288 (in Russian)

Nockolds, S.R., Richey, J.E. (1939) Replacement veins in the Mourne Mountains granites, N. Ireland, *Amer. J. Sci.* 237, 27-47

Palache, C. (1950) Fayalite at Rockport, Massachusetts, *Amer. Min.* 35, 877-881

Richey, J.E. (1927) The structural relations of the Mourne granites (Northern Ireland), *Geol. Soc. London Quart. Journ.* 83, 653-688

Santoro, R.P., Newnham, R.E., Nomura, S. (1966) Magnetic properties of  $Mn_2SiO_4$  and  $Fe_2SiO_4$ , *J. Phys. Chem. Solids* 27, 655-666

Shannon, R.D., Prewitt, C.T. (1969) Effective ionic radii in oxides and fluorides, *Acta. Cryst.* B25, 925-946

Shinno, I. (1981) A Mössbauer study of ferric iron in olivine, *Phys. Chem. Minerals* 7, 91-95

Socket, H.G. (1974) Defect structure and electrical conductivity of crystalline ferrous silicate, in: *Defects and Transport in Oxides*, Schmelzer, N.S., Jaffe, R.J. (eds.), Plenum Press, New York, 341-355

Soellner, J. (1911) Über Fayalit von der Insel Pantelleria, *Z. Kryst.* 49, 138-151 (in German)

Stebbins, J. (1983) private communication

Stone, A.J., Augard, H.J., Fenger, J. (1971) MOSSPEC Program for resolving Mössbauer spectra, Riscoe Rep., Danish Atomic Energy Comm., R150-M-1348, 42pp.

Wang, S. (1980) The stability of laihunite - a thermodynamic analysis, *Geochimica* 3, 31-42 (in Chinese)

Washington, H.S. (1913) The volcanoes and rocks of Pantelleria, Part I., *J. Geol.* 21, 653-670

Weeks, R.A., Pigg, J.C., Finch C.B. (1974) Charge-transfer spectra of  $\text{Fe}^{3+}$  and  $\text{Mn}^{2+}$  in synthetic forsterite ( $\text{Mg}_2\text{SiO}_4$ ), *Am. Min.* 59, 1259-1266

Will, G., Cemic, L., Hinze, E., Seifert, K.-F., Voigt, R. (1979) Electrical conductivity measurements on olivines and pyroxenes under defined thermodynamic activities as function of temperature and pressure, *Phys. Chem. Minerals* 4, 189-197

Yoder, H.S., Sahama, Th.G. (1957) Olivine X-ray determination curve, *Am. Min.* 42, 475-495

Zeira, S. Hafner, S.S. (1974) The location of  $\text{Fe}^{3+}$  ions in forsterite ( $\text{Mg}_2\text{SiO}_4$ ), *Earth and Planet. Sci. Lett.* 21, 201-208

Zhang, R., Cong, B., Ying, Y., Li, J. (1981) Ferrifayalite-bearing eulysite from Archaean granulites in Qianan County, Hebei, North China, *TMPM Tschermaks Min. Petr. Min.* 28, 167-187